STUDIES ON HEAT TRANSFER CHARACTERISTICS OF SCREEN MESH WICK HEAT PIPE USING NANOFLUIDS

THESIS SUBMITTED TO THE PONDICHERRY UNIVERSITY FOR THE AWARD OF THE DEGREE OF

DOCTOR OF PHILOSOPHY

IN

MECHANICAL ENGINEERING

by

R.MANIMARAN

Under the Supervision of

Dr.K.PALANIRADJA
(Research Supervisor)

DEPARTMENT OF MECHANICAL ENGINEERING

PONDICHERRY ENGINEERING COLLEGE

PUDUCHERRY – 605 014, INDIA

JUNE 2013

Dr.K.PALANIRADJA
Associate Professor
Department of Mechanical Engineering
Pondicherry Engineering College
Puducherry- 605 014
India

BONAFIDE CERTIFICATE

Certified that the thesis entitled **"STUDIES ON HEAT TRANSFER CHARACTERISTICS OF SCREEN MESH WICK HEAT PIPE USING NANOFLUIDS"** submitted by **Mr.R.MANIMARAN** in partial fulfilment of the requirements for the award of the degree of **Doctor of Philosophy** in the **Mechanical Engineering**, is the candidate's own work carried out by him under my supervision and guidance. The matter presented in this thesis has not been submitted for the award of any other degree of this or any other University/Institute.

K.PALANIRADJA
(Research Supervisor)

Place: Puducherry

Date:

DECLARATION

I hereby declare that the work presented in the thesis entitled "**STUDIES ON HEAT TRANSFER CHARACTERISTICS OF SCREEN MESH WICK HEAT PIPE USING NANOFLUIDS"** submitted to Pondicherry University for the award of Degree of Philosophy is a record of original and independent research work carried out under the supervision of **Dr.K.PALANIRADJA**, Associate Professor, Department of Mechanical Engineering, Pondicherry Engineering College, Puducherry.I hereby assure that this work has not been presented in this or a similar form for the award of any Degree or Diploma and Fellowship or other similar titles to any candidate of any university.

R.MANIMARAN

Place: Puducherry

Date:

ACKNOWLEDGEMENT

I take the opportunity to express my heartfelt adulation and gratitude to my beloved guru and supervisor, **Dr. K.Palaniradja**, Associate Professor, Mechanical Engineering Department, Pondicherry Engineering College, Puducherry for his unreserved guidance, constructive suggestions, thought provoking discussions and inspiration in nurturing this research work. I am deeply indebted to my guide for giving me the opportunity to pursue my research work under his guidance.

I am indebted to **Dr. D.Govindarajulu**, Principal, Pondicherry Engineering College, Puducherry for providing me the necessary facilities to carry out the research work.I am thankful to Doctoral committee members **Dr.N. Satyanarayana**, Professor, Department of Physics, Pondicherry University, Puducherry and **Dr.N.Alagumurthi**, Professor, Department of Mechanical Engineering, Pondicherry Engineering College, Puducherry, for his timely guidance, support and encouragement during the course of my work.

I am grateful to **Dr.R.Arokiadass**, Professor, Department of Mechanical Engineering, Vedantha Institute of Technology, Ulundurpet. I wish to thank **Dr.K.Velmurugan**, Professor, Department of Mechanical Engineering, Sri Manakula Vinayagar Engineering College, Puducherry. I am particularly thankful to **Dr.R.Senthilkumar**, Assistant Professor, Annamalai University, Chidambaram for providing technical assistance during the experimental work.

I am thankful to **Mr.D.Sendilkumar**, Assistant Professor, Department of Mechanical Engineering, Ganesh College of Engineering, Puducherry for providing technical assistance during the experimental work. It is my pleasure to thank all my colleagues and friends for giving me all kinds of support and encouragement throughout the tenure of the work.

R.MANIMARAN

ABSTRACT

The heat pipe is a device of very high thermal conductance. With the development of thermal equipments the demand for efficient heat pipe are growing. Since the heat pipe uses phase change of working fluid to transfer heat, importance should be given to the selection of working fluids in order to enhance the thermal performance of heat pipe. At present the working fluid used in the heat pipe is of very low thermal conductivity and the heat transfer is limited due to its thermo physical properties.

The performance of heat pipe is affected by parameters such as heat input, angle of inclination and filling ratio. The problem of arriving at the optimum levels of the operating parameters has attracted the attention of the researchers and practicing engineers for a very long time. The literature survey has revealed that a little research has been conducted to obtain the optimal levels of operating parameters.

The heat transfer enhancement of the heat pipe is done by using nanofluids, which exhibits higher thermal conductivity when compared to the traditional working fluids. The objective of the present work is aimed at improving the heat transfer characteristics of conventional screen mesh wick heat pipe using TiO_2 and CuO nanofluids and comparing the results with heat pipe using DI Water. In addition the preparation of TiO_2 and CuO nanofluids are carried out along with characterization.

The size of the nanoparticle used in this study is of 20 nm.Experimental results show that the nanoparticles have a significant effect on the heat transfer enhancement. The response surface methodology (RSM) in conjunction with Box-Behnken design has been used to develop the empirical models for response thermal resistance and overall heat transfer coefficient of heat pipe. Desirability functions have been used for simultaneous optimization of performance measures. Also, confirmation experiments are further conducted to validate the results.

TABLE OF CONTENTS

LIST OF TABLES

LIST OF FIGURES

NOMENCLATURE

SYMBOL	DESCRIPTION
ANOVA	Analysis of variance
b_{is}	Linear coefficients
b_{iis}	Quadratic coefficients
b_{ijs}	Interaction coefficients
b_0	Constant coefficient
^0C	Centigrade
CuO	Copper Oxide
DI	De-ionized
EDXS	Energy dispersive X-ray spectroscopy
FPHP	Flat plate heat pipe
K	Kelvin
LHP	Loop heat pipe
RSM	Response surface method
SEM	Scanning electron microscope
TiO_2	Titanium di-oxide
X_i & X_j	Coded values of the independent variables
XRD	X-ray diffractometer

CHAPTER-1

INTRODUCTION

1.1 Heat pipes

Heat pipe is a device which transfers heat from one location to another location over a small temperature gradient and they are also referred as superconductors of heat as they possess an extraordinary heat transfer capacity and with almost no heat loss. Of various means of heat transport heat pipe is found to be most satisfactory in all means. Angier March Perkins developed the heat pipe originally in 1839 and introduced the concept of working fluid in a single phase system (also he had a patent on the hermetic tube boiler which works on this principle).Later Jacob Perkins patented the Perkins Tube in 1936 and it has been widely used in locomotive boilers and baking ovens.

The Perkins Tube is a system in which a long and twisted tube passed over an evaporator and a condenser, which caused the working fluid (water) present within the tube to operate in two phases, was later called as thermosyphon which mostly relied on the gravity force to return the liquid to the evaporator. It was R.S. Gaugler of the General Motors Corporation putforth the concept of the modern heat pipe, which relied on a wicking system to transport the liquid against the gravity and up to the condenser. According to his patent in 1944, Gaugler described how his heat pipe would be applied to refrigeration systems. The serious development of heat pipe took place when it was reinvented by Grover in 1960 (Faghri, 1995)

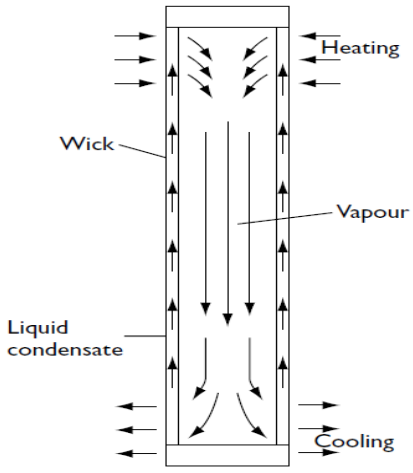

Figure 1.1 Schematic diagram of heat pipe

The heat pipe is a closed tube or chamber of different shapes whose inner surfaces are lined with a porous capillary wick. One end of pipe is known as heating end (evaporator) where heat is absorbed & the other end is known as cooling end (condenser) where heat is given out. The working fluid is placed inside and it is highly evacuated. Because of that the working fluid is virtually in a state of liquid-vapour equilibrium (Figure1.1). The wick is saturated with the liquid phase of the working fluid and the remaining volume of the tube contains the vapour phase. Consequently, a slight increase in temperature will cause it to boil &evaporate (Chi 1976).The central portion of the heat pipe is heavily insulated on the outside to prevent the heat loss.

1.2 Theory of operation

A heat pipe is an evacuated tube sealed hermitically, which contains sintered powder wick or mesh wick filled with a working fluid in both liquid and vapour phase. When one end of the heat pipe is heated, the liquid present inside the tube gets evaporated and turns to vapour by absorbing the latent of vaporization. Thus the generated vapour flows to the colder part of the heat pipe where it is condensed by releasing its latent heat and the vapour is converted into water droplets. The re-condensed liquid flows back then to the hot end of the heat pipe by capillary action in case of wick heat pipe and it is moved by gravity in case of vertically-oriented heat pipes.

As the latent heat of evaporation is very large, more amount of heat can be transported from one end of the heat pipe to the other end with a very small temperature difference. Also the pressure drop of the vapour between the evaporator and condenser is very small and hence the boiling and condensing becomes an isothermal process. Hence a proper design can be made by minimizing the heat loss between the heat source and the vapour and between the vapour and the heat sink. The special feature of the heat pipe is that it can be designed to transport heat between the heat source and the heat sink with very small temperature losses.

An interesting property of heat pipes is the temperature over which they are effective. The effectiveness of heat pipes is greatly enhanced due to the evaporation

and condensation of the working fluid. The heat of vaporization greatly exceeds the sensible heat capacity. The thermal performance of heat pipe is expressed in terms of equivalent thermal conductivity and it can be illustrated as follows. A heat pipe of tubular section using water as the working fluid and operated at 150 ºC which has a thermal conductivity several hundred times that of a copper bar of the same dimensions.

Heat pipes can be manufactured at temperature ranging from - 269 ºC to 2300 ºC by suitable choice of container materials and working fluid. When making heat pipes, there is no need to create a vacuum in the pipe. One simply boils the working fluid in the heat pipe until the resulting vapour has purged the non condensing gases from the pipe and ends are sealed.

1.3 Heat pipe material

The outer envelope of the heat pipe is made with different types of materials such as metals, glass and ceramic materials. The metal copper is usually used as a container material due to its high thermal conductance and also it offers the flexibility to change its shape and the overview of the material selection is given by Groll et. al. (1998).
The metal copper has an advantage in its compatibility with water as working fluid as well as with other low temperature working fluids. Also the metal aluminium with its low density and low weight offers compatibility with ammonia working fluid which suits well for the satellite thermal control application in addition different shapes of heat pipe can be obtained by extrusion process.

Reay and Kew (2006) pointed out the function of the container is to isolate the working fluid from the outside environment. It has therefore, to be leak-proof, to maintain the pressure differential across its walls and to enable the transfer of heat from the working fluid. Selection of the container material depends on several factors. They are

(i) Compatibility (both with working fluid and the external environment)
(ii) Strength-to-weight ratio
(iii) Thermal conductivity
(iv) Ease of fabrication, including weldability, machineability and ductility

(v) Porosity and

(vi) Wettability

The use of titanium as a container material for a heat pipe with water as the working fluid was proposed by Hwang et.al. (2007).The advantage of using titanium was its higher structural strength, and its capability to operate the water heat pipe at higher temperatures when compared to copper material thus using heat transfer properties of water as a better working fluid. Rosenfeld (2006) also investigated the use of magnesium and its alloys as a container material for heat pipe manufacturing. The advantage of using magnesium as higher structural strength and low density which makes suitable for the applications of aerospace and electronics industry and the drawback is difficulty in sealing process.

1.4 Wick structure

The purpose of the wick structure is to generate capillary pressure to transport the working fluid from the condenser to the evaporator and also to distribute the liquid around the evaporator section to any areas where heat is likely to be received by the heat pipe. The selection of the wick for a heat pipe depends on many factors, several of which are closely linked to the properties of the working fluid. The wick along with the container material is exposed to the working fluid and therefore compatibility between wall and wick, as well as wick and working fluid needs to be ensured. From the literature we can find three main types of wicks such as screen mesh, sintered powder and grooved. Reay and Kew (2006) stated that meshes can be manufactured from a range of materials including stainless steel, nickel, copper and aluminum as well as alloys of the above.

1.4.1 Sintered powder wick

The advantage of sintered copper wicks is that it contains smaller pores when compared to wire mesh and provides better controllability of porosity and pore size to optimize heat pipe performance. A larger capillary pumping pressure is developed at the liquid -vapour interface, but such small pores often cause a larger pressure drop in

the liquid-flow passage. It also provides high power handling, high capillary forces and low temperature gradients for anti-gravity applications.

1.4.2 Grooved wick structure

These kinds of wick can be satisfactorily used for cryogenic, moderate temperature and liquid metal heat pipes. It generates smaller capillary driving force which is well suitable for low power heat pipes when operated horizontally or with gravity. However the available manufacturing techniques limit the separate control of pores for capillary pressure development and liquid flow.

1.4.3 Screen mesh wick

Screen mesh wick is used in the majority of the products and provides readily variable characteristics in terms of power transport and orientation sensitivity, according to the number of layers and mesh counts used.

1.5 Working fluid

For a heat pipe to operate, its wick structure must remain saturated with the liquid phase of a working fluid. Identification of suitable working fluid in the operating vapour temperature range should be considered as an initial stage. Several working fluids exist in various temperature band and many characteristics should be considered for the application purpose and the basic requirements are compatibility with wick and wall materials, good thermal stability, wettability of wick and wall materials, vapour pressure which is not too high or low over the operating temperature range, high latent heat, high thermal conductivity, low liquid and vapour viscosities, high surface tension, acceptable freezing or pour point.

Thermodynamic considerations should be followed in selection of the working fluid, which are concerned with the various limitations to heat flow occurring within the heat pipe like, viscous limit, sonic limit, capillary limit, entrainment limit and nucleate boiling limit. The working fluids should have high value of surface tension which corresponds to large capillary pumping capabilities, a large heat of vaporization

corresponds to more efficient heat transport and a large thermal conductivity corresponds to small temperature drops across the wick at both evaporator and the condenser region. In addition to high surface tension, it is necessary for the working fluid to wet the wick and the container material i.e. contact angle should be zero or very small. The melting point, boiling point and useful temperature range of different working fluids are given in the Table 1.1.

Table 1.1 Temperature ranges of different working fluids

Working Fluid	Melting point, K at 1atm	Boiling point, K at 1 atm	Useful temperature Range, K
Helium	1.0	4.21	2-4
Hydrogen	13.8	20.38	14-31
Neon	24.4	27.09	27-37
Nitrogen	63.1	77.35	70-103
Argon	83.9	87.29	84-116
Methane	90.6	111.4	91-150
Ethane	89.9	184.6	150-240
Ammonia	195.5	239.9	213-373
Pentane	143.1	309.2	253-393
Acetone	180.0	329.4	273-393
Methanol	175.1	337.8	283-403
Ethanol	158.7	351.5	273-403
Heptane	182.5	371.5	273-423
Water	275.1	373.1	303-473
Toluene	178.1	383.7	323-473
Mercury	234.2	630.1	523-923
Sulphur	385.9	717.8	530-947
Potassium	336.4	1032	773-1273
Sodium	371.0	1151	873-1473
Lithium	453.7	1615	1273-2073
Calcium	1112	1762	1400-2100
Lead	600.6	2013	1670-220
Silver	1234	2485	2073-2573

1.6 Performance limits

The circulation of working fluid is an important heat pipe factor. The maximum possible circulation is required to obtain the maximum heat transport capability of the heat pipe. The limitation on the heat transport capability pumping ability (capillary limitation), choking of vapour flow (sonic limitation),tearing of liquid off the liquid-vapour interface by vapour flowing at high velocity (entrainment limitation), disruption of the liquid flow by nucleate boiling in the wick (boiling limitation) and viscous limitation (Figure 1.2). Additional factors that affect heat pipe performance

include the temperature characteristics of the heat pipe, the interface condition between the heat pipe and the external source and sink and the effects of various heat pipe control techniques. A very brief description is provided for each limitation and more details can be found in the source itself whilst only the brief ones are cited here.

1.6.1 Capillary limitation

During steady state operation of a heat pipe the working fluid in the vapour phase flows continuously from evaporator section to the condenser section and returns to the evaporator section in the liquid phase. As the vapour flows from evaporator to condenser, there exists a liquid pressure gradient along the vapour flow passage. There also exists a liquid pressure gradient as the condensed liquid flows back from the condenser to the evaporator. This pressure difference between the two sides of the liquid-vapour interface is called the capillary pressure. If a heat pipe is to operate continuously without drying out the wick, then the required capillary pressure will not exceed the maximum possible capillary pressure at any point along the heat pipe.

1.6.2 Boiling limitation

The liquid in the evaporator wick boils and the wall temperature will become excessively high if the radial heat flux in the evaporator section becomes too high thus affecting the circulation of the working fluid and if this boiling is severe it dries out the wick in the evaporator region and it is said to be the boiling limit.

1.6.3 Sonic limitation

In a heat pipe of constant vapour core diameter, the vapour stream accelerates and decelerates because of the vapour addition in the evaporator section and the vapour removal in the condenser section. Velocity variations in a converging-diverging nozzle result from a constant mass flow through a variable area, whereas in a heat pipe velocity variations result from a variable mass flow through constant area. During start up or steady state operation the vapour velocity may reach sonic or supersonic values and this choked working condition is called the sonic limit.

1.6.4 Entrainment limitation

If the vapour velocity in the heat pipe is too high, then the shear force present at the liquid - vapour interface which may tear the liquid from the wick surface and entrain it into the vapour flow stream. If the entrained becomes too high, dry out phenomena will occur at the evaporator region. The heat transfer rate at which this occurs is called the entrainment limit and it is often associated with low or moderate temperature heat pipe with small diameter. Entrainment can be detected by sounds made by droplets striking the condenser end of the heat pipe.

1.6.5 Viscous limit

When the viscous forces dominate the vapour flow, as for a liquid-metal heat pipe, the vapour pressure at the condenser end may reduce to zero. Under this condition the heat transport of the heat pipe may be limited. A heat pipe which is operating at temperatures below its normal operating range can encounter this limit, which is also known as the vapour pressure limit.

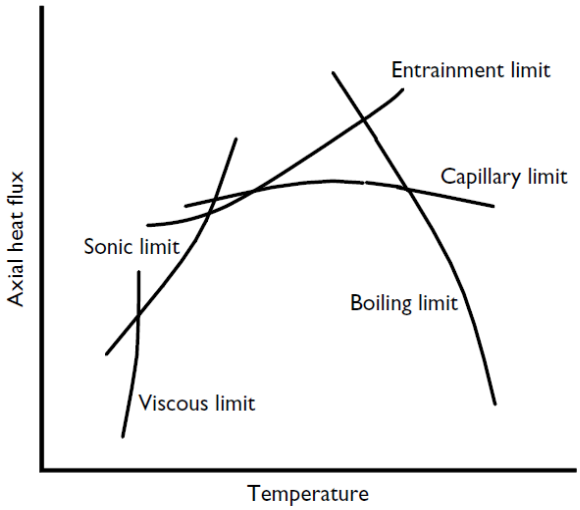

Figure 1.2 Heat transport limitations in a heat pipe

1.7 Types of heat pipes

Heat pipes have been designed and built with different cross-sectional areas such as micro heat pipe (0.6×0.6) mm and 25mm in length, and also length of 100 m. All

heat pipes have an evaporator and condenser sections. Almost all heat pipes have three different sections namely evaporator section, adiabatic section and condenser section. Each and every section will have different dimensions and has designed to satisfy the limitations of the heat pipe and application. The wick inside the heat pipe is used for circulation of the working fluid by capillary forces.

Based on the applications many configurations of heat pipe can be designed. Many such configurations are shown in Figures 1.3 to 1.10. Heat pipe containers are manufactured in the shape of circular, rectangular (flat heat pipe), conical (rotating heat pipe) and nose cap (rotating heat pipe).In general heat pipes in cylindrical shapes are used for its simplicity in design and manufacturing.

1.7.1 Two-phase closed thermosyphon

A two-phase closed thermosyphon works on gravity under the absence of wick structure is shown in Figure1.3.The condensate is returned by gravity and the condenser section is located above the evaporator section. The working of the thermosyphon is limited by sonic and vapour pressure limits when compared to the operation of capillary-driven heat pipes. Due to free liquid surface in thermosyphon the entrainment limit is found to be higher than in capillary driven heat pipes. Due to the flooding limit, a sudden increase in wall temperature and pressure occurs in thermosyphon.The working of the thermosyphon is more sensitive to filling ratio and maximum heat transfer rate increases up to a certain value without wick.

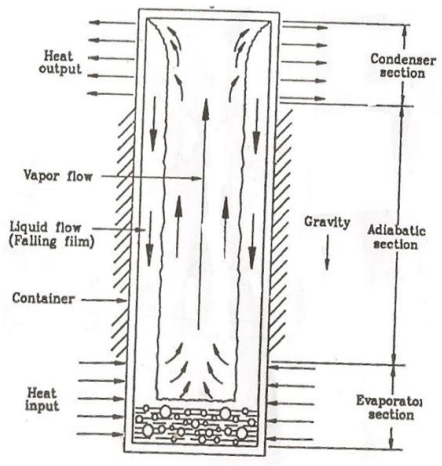

Figure 1.3 Two phase closed thermosyphon

Since gravity acts a major driving force for the condensate return, the capillary limit is generally of no concern in the operation of the thermosyphon.

1.7.2 Capillary-driven heat pipe

Capillary-driven heat pipes are lined with a wick structure on the inner radius of the heat pipe and the containers are sealed one (Figure 1.4). The function of the wick is to provide a capillary driven force for the return of condensate from condenser section to the evaporator section. To saturate the wick inside the heat pipe sufficient working fluids are filled inside the heat pipe. In this heat pipe, heat input is given at the evaporator section and the liquid presents inside evaporates and the vapour moves to the condenser section due to the pressure difference between the evaporator and condenser section. The vapour at the condenser section gets condensed by releasing its latent heat of vapourization.The condensed vapour is then pumped back to the evaporator section by the capillary force generated in the wick structure. Since the heat pipe works under two phase phenomenon, it is ideal for transferring heat for a long distance with a very small temperature drop. The performance of capillary drive heat pipe is affected by capillary limitation. This occurs when the wick cannot return enough condensate to the evaporate section to keep it saturated with liquid.

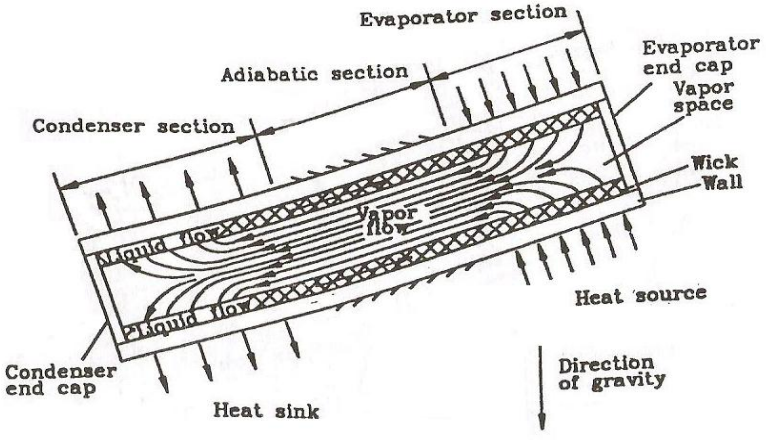

Figure 1.4 Capillary driven heat pipe

At this point, the evaporator wall experiences sudden and continuous increase in temperature. The capillary operated heat pipe finds application in aerospace industry.

1.7.3 Annular heat pipe

The vapour space in annular heat pipe is in annular shape instead of circular shape as in conventional capillary-driven heat pipe (Figure 1.5). Hence the surface area for heat input and output can be increased significantly without increasing the outer diameter of the heat pipe by placing wick material both on the inside of the outer pipe and on the outside of the inner pipe.Therefore, the capillary limit of the annular heat pipe is greater than that of a conventional heat pipe having the same outer dimension.

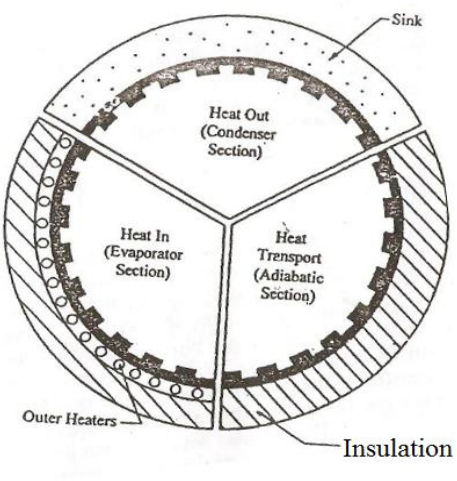

Figure 1.5 Annular heat pipe

1.7.4 Flat-plate heat pipe

The flat-plate heat pipe is of rectangalar shape and capillary-driven with a small aspect ratio, as shown in Figure 1.6.When the condenser is below the evaporator section the wick present between the evaporator and the condenser aid in condensate return and if the condenser is above the evaporator, there is no need to have a wick in the condenser section, since the condensate on the upper part of the heat pipe will flow back to the evaporator.The flat plate heat pipe is an excellent device for use in electronic cooling applications. Small semiconductors or transistor packages can be mounted in arrays on the flat heat pipe for cooling and temperature flattening.

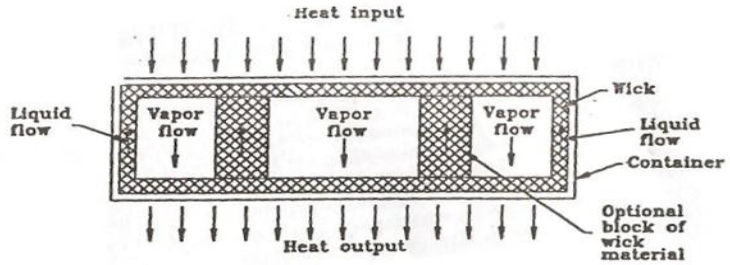

Figure 1.6 Flat plate heat pipe

1.7.5 Rotating heat pipe

Rotating heat pipe is of two types one is in the shape of circular cylinder with or without an axial taper.which rotates either about its own axis of symmetry and the other is available in the shape of disk where the vapour space is formed by joining two parallel disk together at the outer and inner radii (Figure 1.7). The working principle of cylindrical rotating heat pipes is similar to conventional cylindrical heat pipes except internal tapers which are used for returning the condensate to the evaporator with the help of centrifugal force,whereas in case of disk-shaped heat pipes, heat input is given at the outer radii and removed at the inner radii, which allows the condensate to be driven back to the evaporator by centrifugal force with the aid of an internal taper. Hence wicks are not used in rotating heat pipes. To cool the rotating armatures of electric motors and metal-cutting tools such as drill bits and end mills cylindrical rotating heat pipes have been used and disk-shaped heat pipes are used to cool turbine components and automobile brakes.

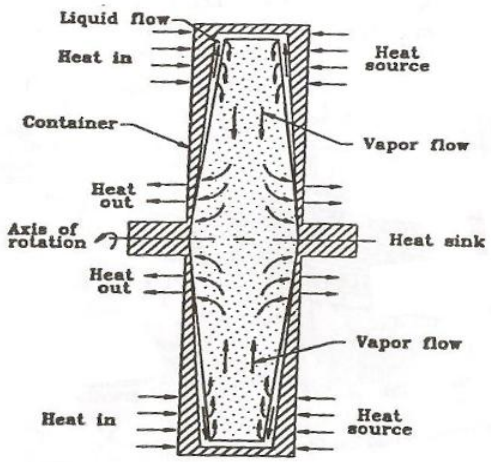

Figure 1.7 Rotating heat pipe

1.7.6 Leading edge heat pipe

Since the leading edge heat pipe faces higher heat fluxes and temperatures, the design and manufacturing impose challenges on the heat pipe engineers.These kind of heat pipes are proposed to cool the leading edges of future hypersonic aircraft (Figure 1.8). The heat pipes are used for cooling the leading edges of the wings and engine nacelles, where the aerodynamic heating is much higher and the absorbed heat is transported from evaporator section to condenser section, where it will be rejected by radiation and/or convection.

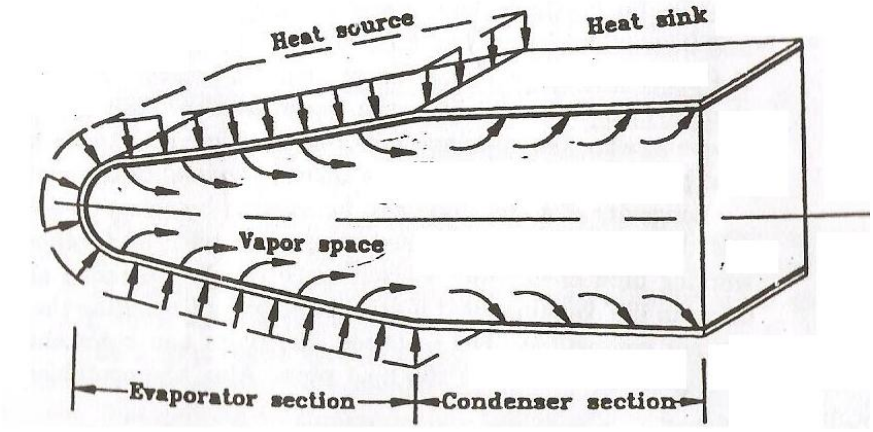

Figure 1.8 Leading edge heat pipe

1.7.7 Gas-loaded heat pipe

The gas-loaded heat pipe has a unique feature that makes it different from other types of heat pipe and has the ability to maintain a device mounted at the evaporator at constant temperature, independent of the amount of power being generated by the device (Figure 1.9).

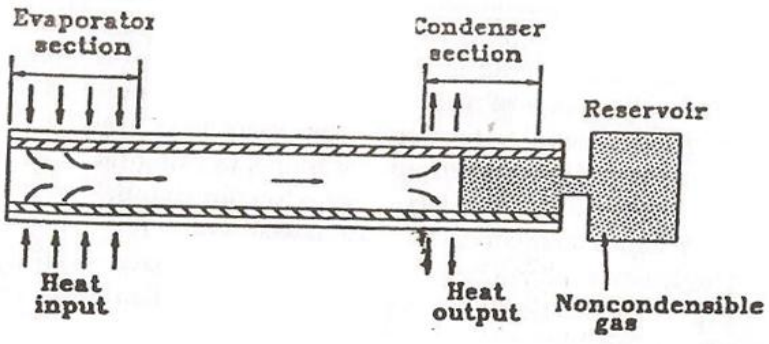

Figure 1.9 Gas loaded heat pipe

During the operation of a heat pipe, vapour flows from the evaporator to condenser section.As a consequence any non condensing gas which present in the vapour is swept along and since such gas does not condense, it accumulates at the condenser blocking a portion of the condenser.A decrease in heat load for these heat pipes causes a small drop in vapour temperature which produces a large drop in vapour pressure by virtue of the rapid change of vapour pressure with respect to its temperature.This drop in vapour pressure causes non condensing gas from the gas reservoir to in activate a portion of the condenser (i.e) decreasing heat load causes conductance to decrease which in turn minimizes the tendency for the heat pipe temperature to change.The applications include thermal control of components and systems on satellites and conventional electronics temperature control.

1.7.8 Loop heat pipe

The loop heat pipe (LHP), illustrated in Figure 1.10 comprises an evaporator and a condenser as in conventional heat pipes, but differs in having separate vapour and liquid lines, rather like the layout of the single-phase heat exchanger system used in buildings for heat recovery, the run-around coil. Those who recall the technical efforts made to overcome liquid–vapour entrainment in heat pipes and, more importantly, in thermosyphons will know that isolation of the liquid path from the vapour flow

(normally counter current) is beneficial. In the LHP, these flows are co-current in different parts of the tubing. A unique feature of the LHP is the use of a compensation chamber. This two-phase reservoir helps to establish the LHP pressure and temperature, as well as maintain the inventory of the working fluid within the operating system. The LHP can achieve very high pumping powers, allowing heat to be transported over distances of several meters. This overcomes some of the limitations of other active pumped systems that require external power sources.

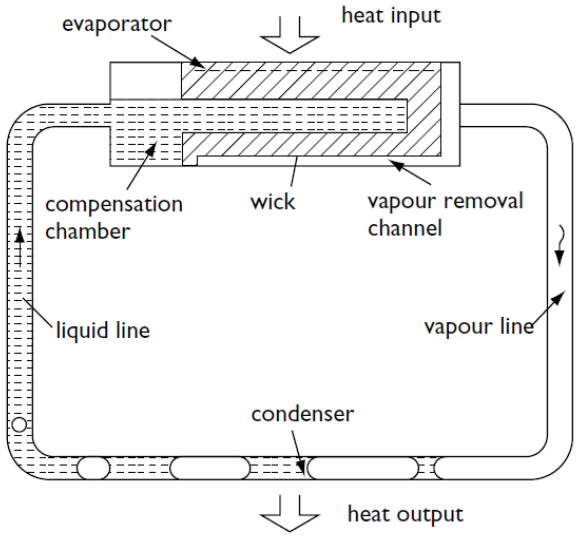

Figure 1.10 Loop heat pipe

1.8 Applications of heat pipe

Electronics cooling - small high performance components cause high heat fluxes and high heat dissipation demands. It is used to cool transistors and high density semiconductors.

Aerospace - cool satellite solar array, as well as shuttle leading edge during re-entry.

Heat exchangers - power industries use heat pipe heat exchangers as air heaters on boilers.

Other applications - production tools, medicine and human body temperature control, engines and automotive industry.

1.9 Advantages of heat pipe

1. Rate of heat transfer is very high than the solid material.
2. It has no moving parts hence maintenance is not required.
3. It can transmit heat over the appreciable distance without loss of the heat (i.e isothermal) and thus permitting separation of the heat source and sink.
4. It requires no power source to accomplish this function.
5. It can transfer the heat where a very low temperature difference is available in between source and sink.
6. It is ideal device for removing the heat from a concentrated heat source such as thermo core.
7. It is rugged like any piece of pipe or tube and has no wearing part hence it has long life.
8. The absence of the gravity does not affect the operation of the heat pipe determinately liquid flow does not depend on gravity.

1.10 Design of experiments

A methodology for designing experiments was proposed by Ronald A. Fisher, in his innovative books, the arrangement of Field Experiments (1926) and the Design of Experiments (1935). The conventional method of optimization involves varying one parameter at a time and keeping others constant. This does not often bring about the effect of interaction of various parameters as compared to factorial design (Box and Draper 1987). But the experiments conducted using the factorial designs, enable all factors to vary simultaneously. This helps in quantifying linear, square and interactive effects of the test variables. Another important advantage is that, the experimental designs could be changed progressively until a fitted model is found to describe the studied phenomenon (Mason et.al. 1989).

1.10.1 Response surface methodology

Response surface methodology is an empirical statistical technique employed for multiple regression analysis of quantitative data which obtained from statistically designed experiments by solving the multivariate equations simultaneously. The graphical representation of these equations are called as response surfaces which could be used to describe the individual and cumulative effect of the test variables on the response and to determine the mutual interaction between the test variables and their subsequent effect on the response Khuri and Cornell (1987) and Montgomery (1991).

Box and Draper (1987) developed RSM to model experimental responses and then the concept was migrated to modeling of numerical experiments. The difference is in the type of error generated by the response. In physical experiments, inaccuracy can be due, for example, to measurement errors while, in computer experiments, numerical noise is a result of incomplete convergence of iterative processes, round-off errors or the discrete representation of continuous physical phenomena (Giunta et al. 1994). In RSM, the errors are assumed to be random and the application of RSM to design optimization is aimed at reducing the cost of expensive analysis methods (e.g. finite element method or CFD analysis) and their associated numerical noise (Cochran and Cox 1962).

1.10.2 Box-Behnken design

Box-Behnken design is defined as a set of experimental designs for response surface methodology that has points at center and the midpoint of each side. Devised by George E. P. Box and Donald Behnken in 1960, these are designed to achieve goals such as: a) each factor, or independent variable, is placed at one of three equally spaced values, b) the design should be sufficient to fit a quadratic model, that is, one containing squared terms and products of two factors, c) the ratio of the number of experimental points to the number of coefficients in the quadratic model should be reasonable and d) the estimation variance should more or less depend only on the distance from the centre, and should not vary too much inside the smallest (hyper) cube containing the experimental points.

The Box-Behnken design is an independent quadratic design which does not contain an embedded factorial or fractional factorial design. In this design the treatment combinations are at the midpoints of edges of the process space and at the center. These designs are rotatable (or near rotatable) and require 3 levels of each factor. The designs have limited capability for orthogonal blocking compared to the central composite designs. They are very useful in the same setting as the central composite designs.

It is used to further study the quadratic effect of factors after identifying the significant factors using screening factorial experiments.Box-Behnken designs do not contain any points at the vertices of the experimental region. This can be advantageous when the points on the corners of the cube represent factor-level combinations that are prohibitively expensive or impossible to test because of physical process constraints.

1.11 Work involved in this research

Work presented in this thesis contains six different technical parts, of which some are broken down into two or more sub-sections.

Part 1: The first part of the work discusses about the introduction of heat pipe and topics related to heat pipes. Also it includes theory of operation, heat pipe material, wick structure, working fluid, performance limits, types of heat pipes, applications of heat pipes and advantages of heat pipes. The introduction part provides sufficient information about the heat pipes and paves way for new innovative thoughts for this research work.

Part 2: The second part of this work is presented in chapter 2, where a detailed literature review is carried out. In this chapter many sub sections are included to a cover a detailed work done on the heat pipe. Existing literature works have been reviewed carefully and the following sub sections are discussed i) Introduction to heat pipes and thermosyphon,ii) Types of heat pipes using nanofluids,iii) Conventional heat pipe using different working fluids,iv) Applications of heat pipe, v) Introduction

to nanofluids, vi) Techniques used in synthesis of nanofluids,vii) Synthesis of nanofluids using two step method, viii) Synthesis of nanofluids using single step method, ix) Conventional heat pipe using nanofluids and x) Modeling and parameter optimization.

Part 3: The third part of this work is introduced in chapter 3.This chapter contains design part, specifications of conventional screen mesh wick heat pipe and properties of working fluid. The knowledge gained from the literature review is used in designing of heat pipe and for choosing the working fluid. Also the synthesis and characterization of TiO_2 and CuO nanofluids are carried out. The experimental procedures carried out with the above working fluids, the components and instrumentation used in the experimental part are discussed elaborately.

Part 4: The fourth part of this research is presented in chapter 4 which contains the result and discussions of this thesis work. In this section the behavior of working fluids such as DI Water, TiO_2 nanofluid and CuO nanofluid under various experimental conditions are discussed elaborately. This work is aimed at identifying the optimized value of thermal resistance and overall heat transfer coefficient for all the three working fluids and also evaluating the best working fluid in terms of heat transfer characteristics. The statistical analysis and modeling of heat transfer characteristics of heat pipe for all the three working fluids are discussed. With the help of Minitab 16 statistical software the design matrix is obtained. The regression equation for thermal resistance and overall heat transfer coefficient of all the working fluids is obtained. The fitness and adequacy of the models are verified with the help of ANOVA table along with normal probability plot

Part 5: In this part the responses are optimized for the heat pipe using DI Water, TiO_2 nanofluid and CuO nanofluid by response surface method. The optimal charts are presented for the responses. A validation test is conducted and the results are compared and tabulated.

Part 6: Finally the results of the entire chapter are concluded in this part of work. The novelty and the benefits obtained from the results of this research are presented in a summarized form. In addition the scope for future work is also introduced. All the

work carried out in this research has been aimed to give the conventional screen mesh wick heat pipe, its position among other wick structure and other heat pipes they deserve. In addition to that a newer working fluid has been proposed to suit its applications when applied correctly.

CHAPTER - 2

LITERATURE SURVEY

A detailed literature review has been carried out in this section which includes the heat pipe applications, heat pipe using nanofluids, synthesis and characterization of nanofluids and the concept of parameter optimization.

2.1 Introduction

Han et.al. (2002) studied the heat transfer performance of closed thermosyphon under low temperature conditions on the plain copper tubes and tubes having 50, 60,70,80,90 internal grooves by choosing three different working fluids such as distilled water, methanol and ethanol. The parameters included are volumetric filling ratio 10 to 40 % and an inclination angle of zero to 90 degree in order to compare the heat transfer performance of thermosyphon.The results shows that working fluids, liquid fill charge ratio, number of grooves and inclination angle are very important factors for the operation of thermosyphon. A higher heat transfer rate is achieved when the thermosyphon is operated with internal grooves when compared to plain tubes and found that the optimum filling ratio lies between 25 to 30% and the angle of inclination is 20^0 to 30^0.

Wong and Lin (2011) experimentally studied the effects of copper surface wettability on the evaporation performance of a copper mesh wick in a flat-plate heat pipe by using three different working fluids such as water, methanol and acetone at same volumetric liquid charge. The results concluded that with increasing heat load, the evaporative resistance decreased with liquid film recession until a critical heat load showing the minimum evaporative resistance. Afterwards, partial dry out began from the front end of the evaporator. With decreasing wettability, the evaporating water film receded faster with increasing heat load and the critical heat loads were significantly reduced. In contrast, the critical heat loads for methanol and acetone seemed hardly affected by different wettability conditions. The minimum evaporative resistances, however, remained unaffected by surface wettability for all the three working fluids.

Wang et.al. (2011) conducted series of experiments to investigate the effect of evaporation and condensation length on thermal performance of flat plate heat pipes. In the experiments, the FPHP had heat transfer length of 255 mm and width of 25 mm, and pure water was used as the working fluid. The results showed that both the evaporation section length and condenser section length had a significant effect on thermal performance of FPHP.However when the condensation section length approached to evaporation section length, the FPHP had better overall performance, therefore, the condensation section length should be consistent with evaporation section length in applications. Lefevre et.al. (2012) investigated experimentally two different flat plate heat pipes of the capillary structure in which first flat plate heat pipe is made of one or two screen mesh layers and the second flat plate heat pipe uses screen mesh covered grooves and tested the heat pipe with methanol as the working fluid in different configurations i.e. with various locations of heat sinks and heat sources, numbers and natures of the heat sinks and orientation. Good thermal performance is also observed in various tilted positions when two heat sinks are used at each extremity of the flat plate heat pipe.

Zhang (2001) has suggested an innovation of heat pipe system by using new working fluids, which have a positive gradient of surface tension with temperature, to improve the performance of capillary-pumping heat pipe systems and their operative stability and concluded that water can be replaced by a dilute aqueous solution of long-chain alcohols and ammonia can be replaced by amino-group fluids that developed by adding an ionic surfactant into ammonia. Because of the unusual characteristics of surface-tension gradient with temperature of the new working fluids, the capillary limit and the boiling limit of the heat pipe systems are increased significantly.

Sarmasti Emami et.al. (2008) investigated the effect of the aspect ratio and filling ratio on the thermal performance of an inclined two-phase closed thermosyphon under normal operating conditions experimentally. The experiments were carried out for a filling ratio in the range of 20-60% and aspect ratios of 15, 20, and 30 for an inclination angle range of 15°- 90°. The thermosyphon was manufactured using a copper tube with an inside and outside diameter of 14 and 16 mm respectively, and a 1000 mm length. Distilled water was used as the working fluid. The results showed

that the maximum thermal performance of the thermosyphon occurred at 60° for all three aspect ratios and several filling ratios. The thermal performance of the inclined thermosyphon with an inclination angle of 60° was better for a filling ratio of 45%. It was also found that a higher condensation heat transfer coefficient for all three aspect ratios took place between 30 and 45 degrees.

Zhang et.al. (2008) investigated the characteristics of phase change heat transfer experimentally on two-phase thermosyphon with different working fluids by considering different heat fluxes. The experimental results show that the two-phase thermosyphon with water as working fluid has a better performance when compared with ethanol as working fluid throughout the tested heat flux range in experiments. Also the thermal resistances of the evaporation and condensation surfaces are the main factors that influence the two-phase thermosyphon performance; ensuring that the working fluid at the evaporation surface is fully at boiling state which is vital to the two-phase thermosyphon enhancing this boiling heat transfer is the most efficient way to improve its performance.

Mozumder et.al. (2010) made **a**n attempt to design, fabricate and test a miniature heat pipe with 5 mm diameter and 150 mm length with a thermal capacity of 10 W and conducted experiments with and without working fluid for different thermal loads to assess the performance of heat pipe by considering the working fluids such as water, methanol and acetone. The performance of the heat pipe was quantified in terms of thermal resistance and overall heat transfer coefficient. The amount of liquid filled varied and the variation of the performance parameters for varying liquid inventory was observed. Finally, optimum liquid fill ratio was identified in terms of lower temperature difference and thermal resistance and higher heat transfer coefficient. Overall heat transfer coefficient of the miniature heat pipe found to be the maximum for the Acetone as working fluid. In general, fill ratios of working fluid greater than 85% of volume of evaporator showed better results in terms of increased heat transfer coefficient, decreased thermal resistance and reduced temperature difference across the evaporator and condenser.

Anwarul Hasan et.al. (2003) performed experimental investigation on gravity assisted heat pipe of diameter 12.5 mm and length 0.50 m using water as working

fluid at various inclination angles and different heat flux input at the evaporator section. The parameters covered in this study are the inclination angle from 0 to 60^{o}, heat input from 25 to 40 W and a fill charge ratio of 0.20.The best performance of heat pipe is achieved at its vertical position where gravity serves to assist return of condensate from condenser to evaporator. The thermal resistance increases with the increase of inclination angle. Overall heat transfer coefficient is found to be proportional to the heat flux at the evaporator and inversely proportional to the inclination angle. Also at a particular heat input, the wall temperature of the evaporator section is the lowest when the heat pipe is placed vertically.

Charoensawan and Terdtoon (2008) experimentally investigated the thermal performance of a horizontal closed- loop oscillating heat pipe (HCLOHP) at normal operating condition. The HCLOHPs were made of copper capillary tubes with various inner diameters, evaporator lengths and number of turns. Distilled water and absolute ethanol were used as the working fluids within the HCLOHPs and were added into the tubes to various filling ratios. The thermal performance of a HCLOHP improved by increasing the evaporator temperature and decreasing the evaporator/effective length. The best performance of all the HCLOHPs occurred at the maximum number of 26 turns. The proper filling ratio for a HCLOHP with a 150 mm Le is 30% and for a 50 mm Le is both 30% and 50%. Mirshahi and Rahimi (2009) reported a study on the effect of the cooling water flow rate, fill ratio, heat flux, and extra volume on the overall performance of a partially vacuumed thermosyphon. A 1 m copper tube with an inner and outer diameter of 17.5 and 19 mm was used as a test rig. The length of the evaporator, the adiabatic section and the condenser are 40, 20 and 40 cm, respectively. It was observed from the experimental results that change in heat flux, fill ratio and employing different extra volumes, has a significant effect on its performance.

2.2 Types of heat pipe using nanofluids

Chen et.al. (2008) carried out experimental investigation on a flat heat pipe using silver nano-fluid to study the effect of various concentrations on flat heat pipe thermal performance by air-cooling testing equipment. The silver nano particle used in this study was 35nm in size and the base working fluid was pure-water. In this

experiment, the thickness and length of the heat pipe are 3 mm and 200 cm, respectively. The results show that at the same charge volume, the thermal resistance and temperature difference of the heat pipe filled with nano-fluid was lower than that of DI water because of increasing effective liquid conductance and the effective thermal conductivity of the wick structure in heat pipes.

Shafahi et.al. (2010) investigated the thermal performance of rectangular and disk-shaped heat pipes using Al_2O_3, CuO and TiO_2 nanofluids with analytical models. The authors used nanofluid as the working fluid for the heat pipe and obtained liquid pressure, liquid velocity profile, temperature distribution of the heat pipe wall, temperature gradient along with the heat pipe, thermal resistance and maximum heat load. Compared to the regular fluid the thermal performance of flat-shaped heat pipe using nanofluid is enhanced and the nanoparticles present in the working fluid reduces thermal resistance and increases the maximum heat load capacity.

Do and Jang (2010) investigated the thermal performance of a flat micro-heat pipe with a rectangular grooved wick using water-based Al_2O_3 nanofluids as working fluid. For solving one dimensional equation for the wall, the axial variations of the wall temperature, the evaporation and condensation rates are considered. The phase change process is studied by Young-Laplace equation. In particular, consideration has been given to the thermo physical properties of nanofluids as well as the surface characteristics formed by nanoparticles such as a thin porous coating. The authors has made a comparison of the thermal performance of heat pipe using both DI water and nanofluids and found that the thin porous coating layer formed by nanoparticles suspended in nanofluids is a key effect of the heat transfer enhancement for the heat pipe using nanofluids.In addition the effects of the volume fraction and the size of nanoparticles on the thermal performance are studied. The thermal performance of the nanofluid heat pipe is enhanced up to 100% by adding nanoparticles less than 1.0 Vol% into the base fluid.

Chien et.al. (2003) analyzed the effect of suspended nanoparticles such as gold and carbon in base fluids, called nanofluids, on the thermal resistance of a disk-shaped miniature heat pipe with the help of experimental setup.From the experimental results it is found that the thermal resistance of disk-shaped miniature heat pipe varies

with the charge volume and the type of working medium. A reduction in thermal resistance of disk-shaped miniature heat pipe is obtained at same charge volume if nanofluid is used as the working fluid instead of DI water. Ma et.al. (2006) developed an ultrahigh performance cooling device, called the nanofluid oscillating heat pipe with thermally excited oscillating motion. Result from the experiments show that the heat transport capability increases when the heat pipe is charged with nanofluid. For example, at 80W, input power the diamond nanofluid can reduce the temperature difference between the evaporator and the condenser from 40.9 to 24.3 °C.

Naphon et.al. (2009) studied the performance of heat pipe using refrigerant (R11) as a base working fluid and titanium nanoparticles of diameter 21nm is used in this study. The heat pipe is fabricated from copper tube of outer diameter 15mm and length 600mm.The parameters such as heat pipe tilt angle, charge amount of working fluid on the efficiency of heat pipe are considered. The heat pipe at the tilt angle of 60^0, working fluid charge amount of 50% gives the highest efficiency when pure refrigerant is used as working fluid. However at the optimum conditions, the heat pipe with 0.1% nanoparticles concentration in pure refrigerant gives efficiency 1.40 times higher than that of the heat pipe with pure refrigerant.

Moraveji and Razvarz (2012) investigated the heat pipe thermal efficiency enhancement using aluminum oxide nanofluid and pure water. The size of the nanoparticle is 35nm in diameter. The heat pipe was made of a straight copper tube with an outer diameter and length of 8 mm and 190 mm and a 1 mm wick-thickness sintered circular heat pipe. In the heat pipe tube, there is a 90° curve between the evaporator and condenser sections. The concentration of nanofluid used in this study are 0%, 1% and 3%wt. Experimental results show that thermal performance is enhanced by reducing the thermal resistance and wall temperature difference by charging the nanofluid to the heat pipe. Hung et.al. (2013**)** studied the effect of Al_2O_3/water nanofluid on the enhancement of the thermal performance of heat pipe charged with nanofluid and the concentrations of Al_2O_3/water nanofluid used in heat pipes are 0.5, 1.0, and 3.0 wt. %. The heat pipe in this study is a straight copper tube with an outer diameter of 9.52 mm and different lengths of 0.3 m, 0.45 m, and 0.6 m. To evaluate the thermal performance of heat pipe the effects of charged volume ratio, tilt angle, heat pipe length, heating power and weight fraction of nanoparticles are

considered. Experimental results show that at 40W heat input power the optimal thermal performance for Al_2O_3/water nanofluid heat pipes measured for 0.3 m, 0.45 m, and 0.6 m was 22.7%, 56.3%, and 35.1%, respectively which is better than heat pipes using distilled water as the working fluid.

Liu et. al. (2011) studied the heat transfer performance of a cylindrically micro-grooved heat pipe using aqueous nanofluids as the working fluids experimentally and the base fluid is distilled water. Five kinds of nanofluids are used in this study. The particles are Cu with two mean diameters of 40 nm and 20 nm, CuO with two mean diameters of 50 nm and 20 nm and SiO with a mean diameter of 30 nm were added respectively into the base liquid to compose different kinds of nanofluids.. Experimental results show that adding Cu and CuO nanoparticles into the base fluid can apparently improve the thermal performance of the heat pipe. However, adding SiO nanoparticles into the base fluid will contrarily deteriorate the heat transfer performance. The main reason that causes these differences in the heat transfer performance results from the surface structure of the coating layer formed by sediment of nanoparticles on the heated surface.

Paramatthanuwat et.al. (2010) has carried out investigation on heat transfer characteristics of a two-phase closed thermosyphon using silver nanofluid (De Ionize water mixed with silver nano particles of size less than 100 nm). The thermosyphon is made of copper tube with different inner diameters such as 7.5, 11.1 and 25.4 mm. The filling ratios of 30, 50 and 80% by evaporator length and aspect ratios of 5, 10, and 20 (Le/di) with vertical position. A comparison has been made between pure water and DI water mixed with silver nanofluid. The working temperatures were 40^0, 50^0 and 60^0C. From the results the working temperature had an effect on the heat transfer rate of the two-phase closed thermosyphon, and the heat transfer rate using silver nanofluids for all filling ratio were better than with pure water.

2.3 Conventional heat pipes using different working fluids

Vikas kumar et.al. (2007) developed a test rig to study the thermal performance of wire screen heat pipe. Based on the thermal resistance network method, the overall heat transfer coefficient is computed in which the evaporator section of the heat pipe

is subjected to forced convective heating and the condenser section to natural convective cooling in air. The model also computes thermal resistances at the external surface of the evaporator and condenser as well as inside the heat pipe. The effects of operating parameters such as tilt angle of the heat pipe and heating fluid inlet temperature at the evaporator have been experimentally studied. Experimental results have been used to compare the analytical model. The heat transfer coefficients are predicted by the model at the external surface of the evaporator and condenser are reasonably in agreement with experimental results.

Nemec et.al. (2011) constructed a heat pipe device working on two phase change of working fluid to identify thermal performance at various working positions. From the experimental results, it has been found that the heat pipe can operate on maximum thermal performance and maximum mass flow rate when it is operated in a vertical position. Anwarul Hasan et.al. (2003) discussed experimental investigation on gravity assisted heat pipe of diameter 12.5 mm and length 0.50 m using water as working fluid. Experiment has been performed on the heat pipe at various inclination angles and different heat flux input at the evaporator section to study the thermal performance. The study covers the range of inclination angle from 0 to 60^{o}, heat input from 25 to 40 W and a fill charge ratio of 0.20. The best performance of heat pipe is achieved at its vertical position where gravity serves to assist return of condensate from condenser to evaporator.

Wong and Kao (2008) presented visualization of the evaporation process and thermal measurements of operating horizontal transparent heat pipes which consisted of a two-layered copper mesh wick consisting of 100 and 200 mesh screens, a glass tube and water as the working fluid. Experimental results indicated that nucleate boiling was prompted for a wick having a fine 200-mesh bottom layer. Optimal thermal characteristics with smallest thermal resistances across the evaporator and lowest overall temperature distributions were found for such a wick/charge combination. Partial dry-out was observed in the evaporator region when the heat pipe was used with smaller charge whereas under a larger charged working fluid, liquid recession with increasing heat load was limited and bubbles grew and burst violently at high heat loads.

Senthilkumar et.al. (2011) performed a comparative study of conventional heat pipe performance using the aqueous solution of n-Pentanol with water at various angle of inclinations. The orientation of the heat pipe plays the significant role in its performance and also directly related to the wick structure. An Aqueous solution of n-Pentanol having a positive surface tension gradient with temperature is suggested as a working medium for heat pipe to improve the performance of capillary limit and operating stability. From the analysis, it has been found that the aqueous solution of n-Pentanol gives the better results than the water because that the aqueous solutions have a positive surface tension gradient with temperature.

Ahmad and Rajab (2010) designed and manufactured an experimental test rig to investigate the performance of a stainless steel heat pipe lined with a three-layer stainless steel mesh wick. Different experimental parameters such as power input, filling charge of the working fluid (water) represented by a volumetric ratio with respect to evaporator volume and the inclination angle with a horizontal line are considered. All tests were carried out at a pressure around the atmospheric pressure during steady state conditions. The experimental results showed that the conductivity was about 2060 times that of the solid piece of the stainless steel (the material of the heat pipe).The results from the present work showed a good agreement with empirical and theoretical correlations of other researchers.

Mozumder et.al.(2011) experimentally investigated the heat pipe which is 5mm in diameter and 150mm long with a thermal capacity of 10W for dry condition and with three different liquids such as acetone, methanol, and water having four fill ratios, for each liquid. The experimental study revealed that the dominating parameters for the heat transfer coefficient are evaporator surface temperature, saturated boiling temperature of working fluid, latent heat of vaporization, and fill ratio. In addition, the investigation also showed that an optimum value of heat transfer coefficient is obtained at 85% fill ratio.

Hossain et. al. (2010**)** designed and fabricated a micro heat pipe having inner diameter 1.8 mm and length 150 mm.By experimental investigations, the heat transfer characteristics of a micro heat pipe is carried out with different experimental parameters which include inclination angles, coolant flow rate, working fluid and heat

input. Inclination angle is varied from 30^0 to 90^0, whereas coolant flow rate and heat input is varied from 0.3 to 1.0 lit/min and 0.612 W to 8.71W respectively. Working fluids such as acetone, ethanol and methanol are used in the experiments. From the experimental results it is found that the inclination angle, coolant flow rate, and heat input have significant impact on the performance of the micro heat pipe and also inferred that overall heat transfer coefficient is higher for higher heat input.

Savino et.al. (2007) experimentally tested the performance of heat pipes filled with a self-rewetting fluid (alcohol aqueous solutions) and commercial water both in normal and low gravity conditions. The results have confirmed improved capability of the considered heat pipes with respect to traditional heat pipes filled with water. The experimental results reveal that the difference of the average evaporator and condenser temperatures, which are proportional to the thermal resistance are smaller for the heat pipe filled with the aqueous alcohol solution than the heat pipe filled with pure water. Shukla et.al. (2012) fabricated conventional cylindrical heat pipe of 19.5 mm outer diameter and 400 mm length and tested two different working fluids such as DI-water and copper nanofluids. Experiments were performed to study the heat transfer characteristics in the evaporator and condenser section of the heat pipe. The overall heat transfer coefficient of the system increases gradually with increase in heat flux. Hence there is a quantitative improvement in the heat transfer coefficient when the nanoparticles are suspended in the working medium.

2.4 Heat pipe applications

Azad (2008) designed and constructed a heat pipe solar collector at IROST to analyze the thermal behavior both theoretically and experimentally. A theoretical model based on effectiveness-NTU method was developed for evaluating the thermal efficiency of the collector, the inlet, outlet water temperatures and heat pipe temperature. Optimum value of evaporator length to condenser length ratio is also determined. From the investigation the results suggested an optimum heated length-cooled length ratio to absorb more heat and increase the overall amount of useful heat. Azad (2009) investigated both experimentally and theoretically about the performance of the heat pipe solar collector which employs wick-assisted heat pipe for the heat transfer from the absorber (evaporator) to a heat exchanger (condenser). The heat pipe

is made with a copper tube and the evaporator section is finned with aluminium plate. The experimental results obtained are in good agreement with the developed theoretical model.

Gurses and Cannistraro (1991) investigated the performance of inclined water filled heat pipes using theoretical and experimental method for solar energy applications. From the results it is observed that the effectiveness of the heat transfer rate depend strongly on the inclination angle. The maximum heat transfer rate is achieved when the heat pipe is operated in vertical position whereas the minimum heat transfer rate is achieved when the heat pipe is in horizontal position. In addition, it is concluded that both the capillary limit and entrainment limit become effective on the heat transfer rate at higher inclination angle. Park (1997) optimized the heat distribution of satellite equipment using heat pipe of length 0.45 m with two heat sources along with the experimental setup. The experimental results show that temperature profile at the outer wall can be controlled by the optimum distribution of heat sources.

Possamai et. al. (2009) studied the heat transfer and temperature distribution of a hermetic reciprocating refrigeration compressor using miniature heat pipe as a two phase thermal control system both analytically and experimentally. The aim of the investigation is to reduce the temperature of the refrigerant and to increase its density in the compressor piston. The results showed a reduction in temperature is achieved between the parts of the compressor. Kerrigan et.al. (2011) fabricated and tested high thermal output heat pipe based radiator using simulation driven design technique. The prototype heat pipe based double convector radiator has proven the concept that using heat pipes as heat spreaders for effective heat dissipation in domestic applications has many advantage over conventional wet panel radiators, including a doubling of the power density and significantly reduced thermal mass for improved controllability.

Kim et.al. (2003) developed both top heating and bottom heating type heat pipe cooling module which implements RHE through application of heat pipe to desktop PC cooling system and the performance result showed that heat pipe cooling module shows excellent thermal performance. Noie-Baghban and Majideian (2000) designed and constructed a heat pipe heat exchanger for heat recovery to hospital and

laboratories using a single heat pipe with three different types of wick and three working fluids. From the developed computer simulation the heat transfer rate obtained at the evaporator section which is very close to the experimental results of the constructed heat pipe.

Jouhara et. al. (2009) developed a new concept based on heat pipe technology for nuclear desalination system aimed at reducing the tritium level. In addition the authors showed that Heat pipes has the potential for reducing environmental impacts of nuclear desalination plants as they improve the overall thermodynamics of the desalination process. Jen et.al. (2002) performed numerical and experimental study to analyze the feasibility of using heat pipe cooling in drilling applications. The effect of parameters such as depth of the heat pipe within the drill, heat pipe diameter, heat flux input magnitude and length of the heat input zone is analyzed. From the results it can be conclude that from both numerical studies and initial experiments the use of a heat pipe inside the drill reduces the temperature field significantly.

2.5 Introduction to nanofluids

It is well known fact that conventional fluids such as water, ethylene glycol (EG) and engine oils have low thermal conductivity and the efficiency of heat transfer with a very small temperature difference is limited. There is a need for energy efficient working fluids to improve the energy conversion system. However the coefficient of convective heat transfer depends on thermal conductivity of the fluid. The thermal conductivity of fluid is improved by adding micrometer or millimeter sized solid materials to the base fluids. The solid additives improves the thermal conductivity of the base fluid the practical applications are limited due to the clogging of flow channels, sedimentation of large particles and causing pressure drops. The above drawbacks are overwhelmed by using a new class of fluids called nanofluids.Choi in Argonne National Laboratory introduced the concept of nanofluids. Nanofluids are a new class of solid-liquid composite materials consisting of solid nanoparticles (in the range of 1-100 nm) or carbon nanotubes, dispersed in a heat transfer fluid such as ethylene glycol, water or oil Choi (1995).

2.5.1 Techniques used in synthesis of nanofluids

Several researchers carried out the synthesis of nanofluids using two step and single step method. In case of two step method, the nanoparticles are produced initially and then it is added into the working fluid in case of single step method the dispersion of nanoparticle is done directly in to the working fluid

2.5.1.1 Synthesis of nanofluids using two step method

The preparation of nanofluids is done by mixing the nanoparticles directly into the base fluid. The nanoparticles are produced at first step and then it is added in to the base fluid as a second step. Xuan and Li (2000) presented a procedure for preparing a nanofluid which is a suspension consisting of nano phase powders and a base liquid. Two different kinds of nanofluids are prepared by varying the base fluid. The first one is the transformer oil based nanofluid which is prepared by adding Cu nanoparticles by 2 and 5 Vol%, respectively and the suspension are stabilized with the oleic acid. The second is the preparation of water based copper nanofluid in which Cu nanoparticles are added by 5 Vol% and laurate salt is added to stabilize the suspension.

Patel et. al. (2003) measured the thermal conductivity of Au nanopaticles in water and tolune and the size of the nanoparticles used in this study is of 10-20 nm in diameter by adding citrate as the stabilization agent. Putnam et. al. (2006) prepared nanofluid which consisted the mixtures of C60–C70 fullerence in toluene and alkanethiolate stabilized Au nanoparticles in ethanol and toluene by using two step processes for measuring thermal conductivity. Murshed et. al. (2005) prepared two kinds of nanofluids of which one is in spherical shaped TiO_2 nanoparticles of diameter 15 nm and the other one is rod shaped TiO_2 nanoparticles of 10 nm in diameter and 40 nm in length for comparing the thermal conductivity.

Wang et. al. (1999) and Lee et. al. (1999) measured the thermal conductivity of Al_2O_3 and CuO nanofluid which is prepared by two step method using different base fluids such as water, vacuum pump fluid, engine oil, and ethylene glycol. Experimental results show that the thermal conductivities of nanoparticle–fluid

mixtures are higher than that of the base fluids. Wang et. al. (2006) prepared water-based multiwall carbon nanotube dispersed nanofluids using sodium dodecyl sulfate (SDS) dispersions, since the fibers are entangled in the aqueous suspension. However, the heat transfer performance of the nanofluids is affected by the addition of dispersions in fluids, especially at high temperature. Hong et.al. (2005) prepared Fe nanofluids with ethylene glycol using Fe nanocrystalline powder which is synthesized by a chemical vapour condensation process. To improve the suspension of the nanoparticles, sonication is carried out with high-powered pulses to improve the dispersion of nanoparticles in the preparation of nanofluids. After, sonication nanofluids exhibit an enhancement of thermal conductivity. Thermal conductivity of a Fe nanofluid is increased nonlinearly up to 18% as the volume fraction of particles is increased up to 0.55 Vol.%.

Liu et. al. (2005) using a two-step method prepared CNT nanofluids using ethylene glycol and synthetic engine oil for measuring thermal conductivity of the nanofluids and the volume concentration of CNT–ethylene glycol suspensions is below 1.0 Vol. % and that of CNT–synthetic engine oil suspensions is below 2.0 Vol. %. Results indicate that the CNT–synthetic engine oil suspension has a much higher enhanced thermal conductivity ratio than that of the CNT–ethylene glycol suspension. The two-step method for preparing nanofluids is a process by dispersing nanoparticles into base liquids. This step-by step method isolates the preparation of the nanofluids from the preparation of nanoparticles. As a result, agglomeration of nanoparticles may take place in both steps, especially in the process of drying, storage, and transportation of nanoparticles. The agglomeration will not only result in the settlement and clogging of microchannels, but also decrease the thermal conductivity. Simple techniques such as ultrasonic agitation or the addition of surfactants to the fluids are often used to minimize particle aggregation and improve dispersion behavior. Since nanopowder synthesis techniques have already been scaled up to industrial production levels by several companies, there are potential economic advantages in using two-step synthesis methods that rely on the use of such powders. But an important problem that needs to be solved is the stabilization of the suspension prepared.

2.5.1.2 Synthesis of nanofluids using single step method

Eastman and Choi (2001) has used a one-step physical synthesis method to prepare nanofluids, in which Cu vapor was directly condensed into nanoparticles by contact with a flowing low vapor pressure liquid (ethylene glycol) and the effective thermal conductivity of ethylene glycol was shown to be increased up to 40% for a nanofluid consisting of ethylene glycol containing approximately 0.3 Vol% Cu nanoparticles of mean diameter, 10 nm. Liu et. al. (2006) used the technique of chemical reduction method for synthesis of nanofluids containing Cu nanoparticles in water without using surfactant as the dispersant. Thus the synthesized copper nanofluid shows improved thermal conductivity when compared to pure fluids.

Hong et.al. (2005) employed chemical vapour condensation process to synthesis Fe nanofluids with ethylene glycol. The thermal conductivity of a Fe nanofluid is increased nonlinearly up to 18% as the volume fraction of particles is increased up to 0.55 Vol. %. Lo et. al. (2005) developed submerged arc nanosynthesis system for preparing Cu-based nanofluids with different morphologies and using various dielectric liquids by selecting pure copper as an electrode as well as the work piece material. Also the advantage of this method is that allows the production of uniform and well-dispersed copper nanoparticles without any aggregation.Zhu et. al. (2004) presented a novel one-step chemical method for preparing copper nanofluids by reducing $CuSO_4 \cdot 5H_2O$ with $NaH_2PO_2 \cdot H_2O$ in ethylene glycol under microwave irradiation. By this method nonagglomerated and stably suspended Cu nanofluids were obtained. This method also found to be a fast and efficient for preparing Cu nanofluids.

The single-step method is a process of combining the preparation of nanoparticles with the synthesis of nanofluids, for which the nanoparticles are directly prepared by physical vapour deposition (PVD) technique or liquid chemical method. In this method the processes of drying, storage, transportation, and dispersion of nanoparticles are avoided, so the agglomeration of nanoparticles is minimized and the stability of fluids is increased. But a disadvantage of this method is that only low vapour pressure fluids are compatible with the process. This limits the application of the method.

2.6 Conventional heat pipe using nanofluids

Do et. al. (2010) experimentally investigated the effect of nanofluids on the thermal performance of circular screen mesh wick heat pipes using water-based Al_2O_3 nanofluids with the volume fraction of 1.0 and 3.0 Vol.%. The wall temperature distributions and the thermal resistances between the evaporator and the adiabatic sections are measured and compared with those for the heat pipe using DI water. The average evaporator wall temperatures of the heat pipes using the water-based Al_2O_3 nanofluids are much lower than that of the heat pipe using DI water. The thermal resistance of the heat pipe using the water-based Al_2O_3 nanofluids with the volume fraction of 3.0 Vol. % is significantly reduced by about 40% at the evaporator-adiabatic section. The experimental results also show that the water-based Al_2O_3 nanofluids as the working fluid instead of DI water can enhance the maximum heat transport rate of the heat pipe.

Naphon et. al. (2008) fabricated a heat pipe from the straight copper tube with the outer diameter and length of 15, 600 mm, respectively to study the enhancement of heat pipe thermal efficiency with de-ionic water, alcohol, and nanofluids (alcohol and titanium nanoparticles of diameter 21 nm) as working fluids. The parameters considered in this study are effects of % charge amount of working fluid, heat pipe tilt angle and % nanoparticles volume concentrations. Experimental results indicate that the presence of nanoparticle enhances the thermal performance of heat pipe thermal efficiency. Tsaia et. al. (2004) investigated the thermal resistance of conventional circular heat pipe of length 170 mm and an outer diameter of 6 mm which employed aqueous solution of gold nanofluid and DI water as a working fluid. Furthermore, the thermal resistance of the heat pipes with nanoparticle solution is lower than that of DI water. The experimental results proved that a higher thermal performance of the new coolant can provide a substitute for conventional DI water in vertical circular meshed heat pipe.

Shukla et. al. (2010) carried out experimental investigation on cylindrical copper heat pipe of outer diameter 19.5 mm and length 400 mm by using three different working fluids such as DI water, silver colloidal and copper water for different heat input in the range of 100-250W.The experimental result showed a reduction in wall

temperature for the heat pipes operated with nanofluids and also the efficiency is enhanced by 14% when compared to the heat pipe using base fluid as working fluid. Shafahi et. al. (2010) studied the thermal performance of a cylindrical heat pipe containing different nanofluids (Al_2O_3, CuO, and TiO_2).The thermal resistance of the heat pipe is found to be reduced due to the presence of nanoparticles in the liquid and hence the thermal performance of the heat pipe is enhanced. It also showed that smaller particles have greater impact on the effect on the temperature gradient along with the heat pipe.

Kang et. al. (2009) studied the heat transfer performance of sintered circular heat pipe with silver nanofluids with the heating power range of 30–70W.The size of the silver nanoparticles used were 10 nm and 35 nm respectively with the concentrations of 1 mg/L, 10 mg/L, and 100 mg/L respectively. The heating power input was 20W higher than DI Water and indicated the nanoparticle size has independent effect on the thermal performance. Mousa (2011) studied the performance of circular heat pipe experimentally using nanofluids under different operating conditions including heat input rate, filling ratio, and volume fraction of the nano-particle in water, the working fluids are pure water and Al_2O_3-water based nanofluid. Under optimum condition the thermal resistance decreases with increasing Al_2O_3-water based nanofluid compared to that of pure water. Kempers et. al. (2006) performed experimental investigation to determine the effect of the number of mesh layers and amount of working fluid on the heat transfer performance of copper-water heat pipes with screen mesh wicks. It was found that the effective thermal resistance decreases with an increase in heat flux, and approaches an approximately constant value at higher heat fluxes. For all orientations, the maximum heat transfer through the heat pipe is increased as the number of mesh layers of the wick was increased, as expected.

Saleh et. al. (2013) performed an experimental investigation on a conventional screen-mesh wick heat pipe to investigate the effect of nanoparticles in a nanofluid.The experiments were performed to measure the temperature distribution and thermal resistance of the heat pipe. The experimental results showed temperature distribution and thermal resistance tend to decrease as the concentration and the crystallite size of the nanoparticle is increased. Hajian et.al. (2012) studied experimentally about the transient and steady state thermal performances of a

medium-sized cylindrical stainless steel meshed heat pipe, utilizing both DI-water and silver nanofluid, as the working fluids. Thermal resistance and response time were used for describing the steady state and transient behavior of the heat pipe. The results showed that a decrease in thermal resistance was obtained for the heat pipe using DI-water nanofluid when compared to heat pipe using DI-water as working fluid.

2.7 Modeling and parameter optimization

Chiang and Chang (2007) applied systematic experimental design based on the response surface methodology (RSM) to identify the effects of machining parameters on the performance of shrinkage and warpage.The centered central composite design (CCD) has been adopted for the experiment structure. The quadratic model of RSM associated sequential approximation optimization (SAO) method is used to find the optimum value of machining parameters. The results of analysis of variance (ANOVA) and conducting confirmation experiments demonstrate that the quadratic models of the shrinkage and warpage are fairly well fitted with the experimental values. Silva et. al. (2011) optimized the biodiesel production process by the application of factorial design 2^4 and response surface methodology. He also investigated the combined effects of temperature, catalyst concentration, reaction time and molar ratio of alcohol in relation to oil. The authors showed that response surface methodology was a suitable method to optimize the operating conditions in order to maximize the ethyl esters production and minimize the glycerol production.

Abhang and Hameedullah (2010) planned experimental runs according to 24+8 added centre point factorial design of experiments to investigate power consumption in turning EN-31 steel with tungsten carbide tool under different cutting conditions and statistically analyzed the data using Analysis of Variance technique. The first order and second order power consumption prediction models were developed by using response surface methodology. Response surface method is found to be a successful technique to perform trend analysis of power consumption in metal cutting with respect to various combinations of design variables (metal cutting speed, feed rate, depth of cut and tool nose radius).Natarajan et. al. (2011) focused on response surface methodology (RSM) for the multiple response optimization in micro-end

milling operation to achieve maximum metal removal rate (MRR) and minimum surface roughness. In this work, second-order quadratic models were developed for MRR and surface roughness, considering the spindle speed, feed rate and depth of cut as the cutting parameters, using central composite design and used for multiple-response optimization by desirability function approach to determine the optimum machining parameters. The optimized machining parameters are validated experimentally, and it is observed that the response values are in good agreement with the predicted values.

Based on response surface method (RSM) Aruna and Dhanalaksmi (2012) carried out optimization of the surface roughness when turning Inconel 718 with cermet inserts. By using central composite design, second-order quadratic models are developed for surface roughness, considering the cutting speed, feed rate and depth of cut as the cutting parameters to determine the optimum machining parameters. Recently Saedon et. al. (1683) developed first and second order tool life models for micro milling hardened tool steel AISI D2 62 HRC in terms of cutting speed, feed per tooth and depth of cut, using response surface methodology. Central composite design (CCD) was employed in developing the tool life model in relation to independent variables as primary cutting parameters. The adequacy of the predictive model was verified using analysis of variance (ANOVA) at 5% significant level and found to be adequate.

Magesh et. al. (2011) studied the effects of substrate concentration, PH and temperature on ethanol concentration were optimized using a full factorial central composite design experiment and optimized the process conditions using response surface methodology. The quadratic model indicated that substrate concentration of 33g/l, PH 5.52 and a temperature of 30.13^{o}C were found to be optimum for maximum ethanol concentration of 8.64g/l. Statistical analysis of full factorial central composite design of the experiments revealed that the substrate concentration was the most significant variable compared to the PH and temperature.

Dhara et.al. (2006) used response optimization technique to optimize the process parameters such as lamp current, pulse frequency, pulse width and air pressure. The objectives were depth of groove and recast layer. In the first and second step

optimization of individual response and optimization of both the response has been carried out subjected to different conditions. In this technique the composite desirability is close to 1 and hence it can be concluded that all the working parameters are within the working range.

Karthikeyan et.al. (2001) developed a polynomial model for the various EDM characteristic such as metal removal rate, tool wear rate and surface roughness in terms of the process parameters such as volume fraction of SiC, current and pulse time. The models were used to optimize the EDM characteristics using non-linear goal programming.

The Box-Behnken design is one option of response surface experimental design. As an independent quadratic design, it doesn't contain any embedded fractorial design, in which the treatment combinations are at the midpoints of edges of the design space and at the center. The designs are rotatable (or nearly rotatable) and require 3 levels for each factor (-1, 0, 1).The advantages of the Box-Behnken design are it requires only 3 levels for each factor, it is a rotatable design and when number of the factors is 3 or 4, the total number for experimental runs is less that of a central composite design (Box 1987).

Response surface methodology was undertaken by Fang and Shen (2010) to optimize the polyethylenimine-mediated transient transfection of suspension cultured HEK 293-F cells. A total of 15 combinations were designed according to Box-Behnken design to identify the effects of DNA concentration, polyethylenimine concentration and incubation time on transient transfection efficiency. Analysis of variance demonstrated that the experimental values fit well with a quadratic model. The RSM-optimized transient transfection resulted in greater production of human tissue prokallikrein (TproK) than non-RSM optimized conditions.

Fu et.al.(2006) employed statistics-based experimental design with response surface methodology to investigate the effect of operation conditions on photoelectrocatalytic oxidation of fulvic acid (FA) using a Ti/TiO_2 electrode in a photoreactor.The Box-Behnken design was employed including the three key variables (initial pH, potassium peroxodisulphate ($K_2S_2O_8$) and bias potential).

Results from the above study show that response surface methodology is one of the suitable methods to optimize the best operating conditions in multi-factor operating environment for the purpose of obtaining maximum FA degradation. The quadratic equation developed in this study shows the presence of a high correlation between observed and predicated values.Balasubramanian et.al. (2012) aims to optimize the foaming conditions for tomato juice using three level Box-Behnken experimental design of response surface methodology by considering three process parameters namely concentration of egg albumin (EA) as foaming agent, carboxy methyl cellulose (CMC) as foam stabilizer and whipping time (WT) was optimized. The Box behnken design of RSM was found effective in determining the optimum zone within the experimental region.

Response surface methodology using Box-Behnken design by Wani et.al. (2012) employed the multivariate approach which enables substantial improvement in the method developed method using fewer experiments, without wastage of large volumes of organic solvents, which leads to high analysis cost. By the use of quadratic regression analysis, equations were developed to describe the behavior of the response as simultaneous functions of the selected independent variables and the results obtained using response surface predictions were in good agreement with the experimental results. Therefore, Box-Behnken statistical design used in determining the optimum experimental conditions such as concentration of DDQ, temperature and time was reliable and effective.

2.8 Problem identification

The performance of heat pipe is influenced by many parameters such as the heat input, type of heat pipe, porosity and permeability of wick structure, the type and amount of working fluid, heat pipe material and geometry of heat pipe. From the literature survey it is clear that the heat pipe using DI Water and aqueous solutions is limited to maximum heat transfer rate and thermal performance which leads to the applications of heat pipe using nanofluids.To overcome the above drawbacks many researchers carried out experiments on different types of heat pipes of different geometries by using various types of nanofluids.

The literature survey also indicates that different combinations of heat pipes and working fluids are used of which conventional heat pipe with screen mesh wick structure is found to be superior due to its ease of fabrication, enhanced thermal performance and application. Parameters such as angle of inclination, filling ratio, heat input, heat pipe material and working fluids found to influence the heat transfer characteristics of heat pipe. Also literatures on the inclined heat pipes and filling ratio are limited and till now no work has been carried out on the conventionl heat pipe with screen mesh wick using TiO_2 nanofluids and CuO nanofluids.

In this work the heat transfer characteristics of conventional screen mesh wick pipe is analyzed using three different working fluids such as DI Water, TiO_2 nanofluid and CuO nanofluid by considering the above mentioned parameters. The outer envelope of the heat pipe is chosen as copper. The reasons behind selecting copper tube are: Compatibility with both the working fluid and the external environment is very high. Thermal conductivity is also higher than the other container materials such as stainless steel, mild steel etc, Copper facilitates the ease of fabrication, including weldability, machineability and ductility and also there are some other important properties required for heat pipe container like porosity, wettability, strength to weight ratio which is more important in spacecraft applications etc.

CHAPTER- 3

EXPERIMENTAL SET-UP AND PROCEDURE

The heat pipe is designed with the help of literature survey and also according to the text book Heat Pipe Theory and Practice by Chi (1976). Also this chapter includes the properties of base working fluid (DI Water), preparation and characterization of titanium di-oxide and copper oxide nanofluid and the description of experimental set-up and procedure followed in experimental work.

3.1 Design and specifications of heat pipe

Heat pipe material		: Copper
Working fluid		: DI Water
Wick material		: Stainless steel
Total length of pipe	L_t	: 0.6 m
Evaporator length	L_e	: 0.15 m
Adiabatic length	La	: 0.3 m
Condenser length	L_c	: 0.15 m
Outer diameter of the pipe	d_o	: 22 x 10^{-3} m
Inner diameter of the pipe	d_i	: 20.8 x 10^{-3} m
Thickness of the pipe	t	: 1.2 x10^{-3} m
Wick permeability	k	: 3.672 x 10^{-10} m^2
Mesh size	n	: 60 in^{-1}
Mesh wire diameter	d	: 0.2286 x 10^{-3} m
No of wires/unit	N	: 2365 m^{-1}
No of layers		: 2

Wick porosity

$$\varepsilon = 1 - (1.05\pi dN)/4 = 1 - \frac{1.05 \text{ x } \pi \text{ x } 0.2286 \text{ x } 10^{-3} \text{x } 2365}{4}$$

$$\varepsilon : 0.5543$$

Wick permeability

$$k = \frac{d^2\varepsilon^3}{122\,(1-\varepsilon)^2} = \frac{(0.2286\,x\,10^{-3})^2(0.5543)^3}{122\,(1-0.5543)^2}$$

$$k : 3.672 \text{ X } 10^{-10} \text{ m}^2$$

3.1.1 Properties of working fluid

Working fluid		: DI Water
Boiling point		: $100^{o}C$
Latent heat,	L	: 2257 kJ / kg
Liquid density,	ρ_l	: 957.85 kg / m^3
Vapour density,	ρ_v	: 0.59773 kg / m^3
Liquid thermal conductivity,	K_e	: 0.613 W / m K
Liquid viscosity ,	μ_l	: 0.278 $x10^{-3}$ N-sec / m^2
Vapor viscosity,	μ_v	: 0.0121 $x10^{-3}$ N-sec / m^2
Liquid surface tension,	σ	: 58.91 $x10^{-3}$ N / m
Molecular weight,	M	: 18 kg / kg-mol
Gas constant,	R	: 8314 J / kg-mol-K
Nucleation radius,	r_n	: 2.54 $x10^{-7}$ m

3.2 Preparation and characterization of nanofluids

3.2.1 Equipments used for characterization of nanofluids

The equipments which were used for characterization of nanofluids are SEM, EDXS, XRD and KD2 Pro thermal analyzer.

3.2.1.1 Scanning electron microscope (SEM)

A scanning electron microscope (SEM) as shown in Figure 3.1 is a type of electron microscope that produces the images of a sample by scanning it with a focused beam of electrons. The electrons interact with electrons in the sample, producing various signals that can be detected and that contain information about the sample's surface topography and composition. The electron beam is generally scanned in a raster scan pattern, and the beam's position is combined with the detected signal to produce an image. SEM can achieve resolution better than 1 nanometer. Specimens can be observed in high vacuum, low vacuum and environmental SEM specimens can be observed in wet conditions.

The types of signals produced by a SEM include secondary electrons (SE), back-scattered electrons (BSE), characteristic X-rays, light (cathode luminescence) (CL),

specimen current and transmitted electrons. The SEM can produce very high-resolution images of a sample surface, revealing details less than 1 nm in size. A wide range of magnifications is possible, from about 10 times (about equivalent to that of a powerful hand-lens) to more than 500,000 times, about 250 times the magnification limit of the best light microscopes.

In a typical SEM, an electron beam is thermionically emitted from an electron gun fitted with a tungsten filament cathode. Tungsten is normally used in thermionic electron guns because it has the highest melting point and lowest vapour pressure of all metals, thereby allowing it to be heated for electron emission, and because of its low cost. Other types of electron emitters include lanthanum hexaboride (LaB_6) cathodes, which can be used in a standard tungsten filament SEM if the vacuum system is upgraded and FEG, which may be of the cold-cathode type using tungsten single crystal emitters or the thermally assisted Schottky type, using emitters of zirconium oxide.

Figure 3.1 Scanning electron microscope

The electron beam, which typically has an energy ranging from 0.2 keV to 40 keV, is focused by one or two condenser lenses to a spot about 0.4 nm to 5 nm in diameter. The beam passes through pairs of scanning coils or pairs of deflector plates in the electron column, typically in the final lens, which deflect the beam in the x and y axes so that it scans in a faster fashion over a rectangular area of the sample surface.

When the primary electron beam interacts with the sample, the electrons lose energy by repeated random scattering and absorption within a tear drop-shaped volume of the specimen known as the interaction volume, which extends from less than 100 nm to around 5 µm into the surface. The SEM used in this study is of Make: Hitachi, Model: S-3400N**,** resolution: 3nm@30kV and magnification: 5X to 300,000X.

3.2.1.2 Energy-dispersive X-ray spectroscopy (EDXS)

Energy-dispersive X-ray spectroscopy (EDXS) is an analytical technique which is used for the elemental analysis or chemical characterization of a sample. It relies on the investigation of an interaction of some source of X-ray excitation and a sample. The intensity or area of a peak in an EDX spectrum is proportional to the concentration of the corresponding element in the specimen. For determining elemental content, the electron-beam current is assumed to be uniform throughout the specimen and electron channeling is avoided by avoiding strong diffraction conditions. Energy Dispersive X-ray Analysis (EDXA) technique is used for performing chemical analysis in conjunction with Scanning Electron Microscopy (SEM) and Transmission Electron Microscopy (TEM).It is not a surface science technique. The analytical data is acquired in the form of digitized spectra, viewed during accumulation on a computer monitor, which displays the number of X-rays, I, detected as a function of E, the X-ray energy.

An electron beam strikes the surface of conducting sample (SEM) .The energy of the beam is typically in the range of 10-20 keV. This causes X-rays to be emitted from the irradiated material. The energy of the X-rays emitted depends on the material under examination. The X-rays are generated in a region about 2 microns in depth (SEM), and thus EDX is not a surface science technique. By moving the electron beam across the material and 2-D (two dimensional) image of each element in the sample can be acquired. Due to the low X-ray intensity, images usually take a number of hours to be acquired. Elements of low atomic number are difficult to detect by EDX. A Beryllium window is often used to protect the SiLi detector in the EDX system. The absorption of the soft X-rays precludes the detection of elements below an atomic number of 11 (Na). In windowless EDX systems, elements with as low

atomic number as 4 (Be) have been detected, but the problems involved get progressively worse as the atomic number is reduced.

3.2.1.3 X-Ray diffractometer

An X-ray diffractometer which is shown if Figure 3.2 illuminates a sample of material with X-rays of known wavelength, moving the sample and detector in order to measure the intensity of the diffracted radiation as a function of beam and sample orientation. From the resulting intensity versus angle plot much can be inferred about the structure of the material. A diffractometer can be used to make a diffraction pattern of any crystalline solid. With a diffraction pattern an investigator can identify an unknown mineral, or characterize the atomic-scale structure of an already identified mineral.

Diffraction occurs as waves interact with a regular structure whose repeat distance is about the same as the wavelength. The phenomenon is common in the natural world, and occurs across a broad range of scales. For example, light can be diffracted by a grating having scribed lines spaced on the order of a few thousand angstroms, about the wavelength of light. It happens that X-rays have wavelengths on the order of a few angstroms, the same as typical interatomic distances in crystalline solids. That means X-rays can be diffracted from minerals which, by definition, are crystalline and have regularly repeating atomic structures.

.

Figure 3.2 PAnalytical X'Pert PRO diffractometer

The crystal size of the particle is calculated using the Debye-Scherrer formula as shown in equation 3.1.

$$D = \frac{0.89\,\lambda}{\beta \cos\theta} \qquad \text{Eq. 3.1}$$

Where D is the size of the particle, λ is the X-ray wavelength (1.5406), β is the peak width and theta is the Braggs angle.

3.2.1.4 KD2 Pro thermal analyser

The KD2 Pro is a battery-operated, menu-driven device. It consists of a handheld microcontroller and sensor needles (Figure.3.3). The KD2's sensor needle contains both a heating element and a thermistor. The controller module contains a battery, a 16-bit microcontroller/AD converter, and power control circuit. The thermal conductivity measurement assumes: (i) the long heat source can be treated as an infinitely long heat source (ii) the medium is both homogeneous and isotropic, and at uniform initial temperature, T_0. The sensor needle used is KS-1 which is made of stainless steel having a length of 60 mm and a diameter of 1.3 mm, and closely approximates the infinite line heat source which gives least disturbance to the sample during measurements. The sensor needle can be used for measuring thermal conductivity of fluids in the range of 0.2–2 W/mK with an accuracy of ±5%.

Figure 3.3 KD2 Pro thermal analyzer

Each measurement cycle consists of 90s. During the first 30 s, the instrument will equilibrate which is then followed by heating and cooling of sensor needle for 30 s each. At the end of the cycle, the controller computes the thermal conductivity using the change in temperature (ΔT) – time data from equation 3.2.

$$K = \frac{q(\ln t_2 - \ln t_1)}{4\pi(\Delta T_2 - \Delta T_2)} \qquad \text{Eq. 3.2}$$

Where q is constant heat rate applied to an infinitely long and small line source, ΔT_1 and ΔT_2 are the changes in the temperature at times t_1 and t_2 respectively.

The KD2 analyzer used in our experiments collects data at 1 s intervals during a 30 s heating time and a 30 s cooling time. The final 20 points during heating and cooling are used in a simultaneous least squares computation which determines the thermal conductivity. Temperature is measured by a 16 bit analog to digital converter. All of the computations are done by an internal 16 bit microcontroller, and the result is displayed. The calibration of the sensor needle is carried out first by measuring thermal conductivity of distilled water and glycerine. The measured values for distilled water and glycerin are 0.611 and 0.292 W/mK respectively which are in agreement with the literature values of 0.613 and 0.285 W/mK respectively within ±5% accuracy (Hagen 1999, Vargaftik 1975, Kothandaraman 2007). The calibration of the KD2 Pro sensor needle is carried out at room temperature (32^0C) and the uncertainty in measurements is calculated as ±2% on the basis of 95% confidence level.

3.3 Synthesis of titanium di-oxide nanofluid

Titanium di-oxide nanofluid is prepared by wet chemical method. The used chemicals are titanium tetrachloride, sodium hydroxide and hydrochloric acid. They are purchased from aldrich chemicals and are in analytical grade. The synthesis involves single step process i.e. the preparation of titanium di-oxide nanoparticle is carried out along with the nanofluids.In this preparation process, 100 ml of deionised water is taken in a 500 ml of beaker. To this 0.51 gm of titanium tetrachloride is added along with one gram of sodium hydroxide pellets. The reaction mixture is heated along with magnetic stirring and the process is carried out for one hour (Figure 3.4). As a result white colour precipitate solution is formed after the reaction and then the mixture is cooled to room temperature.

Figure 3.4 Preparation of titanium di-oxide nanofluid using magnetic stirrer cum hot plate

The PH value of the so formed titanium di-oxide wet precipitate is neutralized by adding droplets of hydrochloric acid. Then the titanium di-oxide wet precipitate is washed with deionised water to remove the impurity ions present in the solution. Titanium di-oxide nanofluids are obtained by dispersing the wet precipitate into the required amount of deionised water under ultrasonic vibration (Figure 3.5) for about four hours to have uniform dispersion of titanium di-oxide nanoparticles in the base fluid i.e. (DI Water).

Figure 3.5 Ultrasonication of titanium di-oxide nanofluid

3.3.1 Characterization of titanium di-oxide nanofluid

The characterization of titanium di-oxide nanoparticles were done by XRD, SEM, EDXA and KD2 Pro thermal analyzer. Using the instrument PAnalytical X'Pert PRO diffractometer the structural determination and estimation of crystalline size were carried out. The average size of the nanoparticle was calculated using Debye-Scherrer equation 3.1 and it was 20 nm.The image for XRD is shown in Figure 3.6.

Scanning electron microscope and energy dispersive X-ray analysis (EDXA) is done using the instrument Hitachi, model: S-3400 N for surface morphology and chemical analysis. The result showed that the titanium di-oxide nanoparticle is spherical in shape is shown in Figure 3.7 and the presence of Ti and O elements are confirmed (Figure 3.8). Figure 3.9 shows the image of dispersed titanium di-oxide nanoparticle in base fluid (DI Water) and the thermal conductivity is measured using KD2 Pro thermal analyzer, Decagon Devices, Inc., USA. The value is found to be 0.6507W/mK which showed an increase of 5.8 % when compared to DI Water (0.613 W/mK).

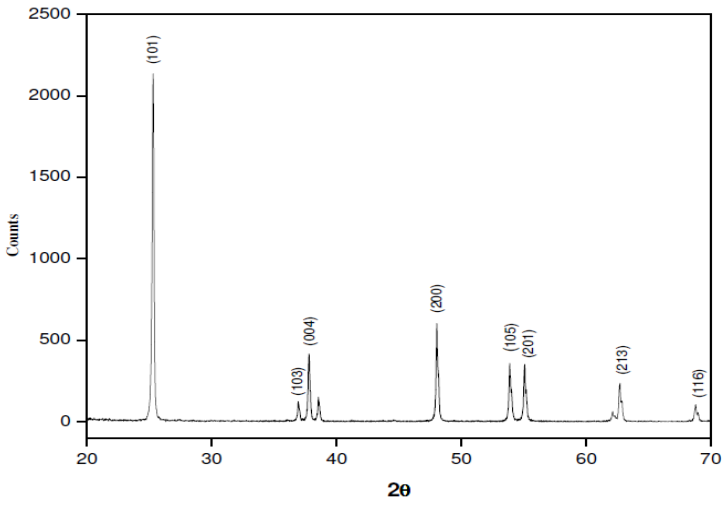

Figure 3.6 X-ray diffractogram for titanium di-oxide nanoparticle

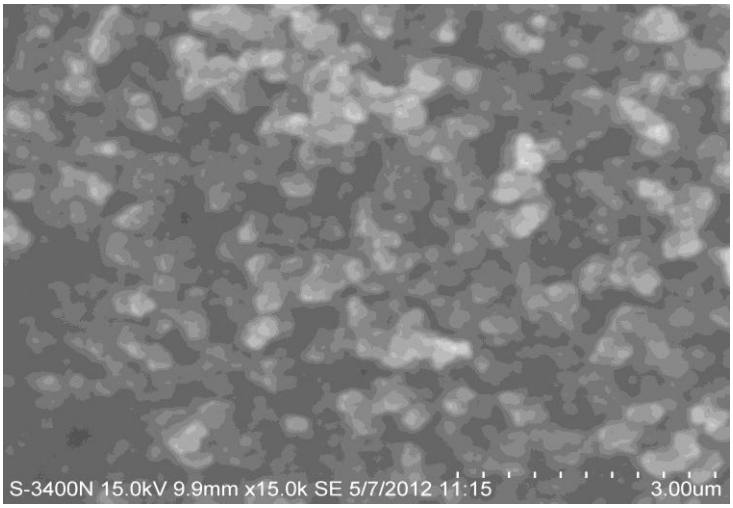

Figure 3.7 SEM image for the titanium di-oxide nanoparticle

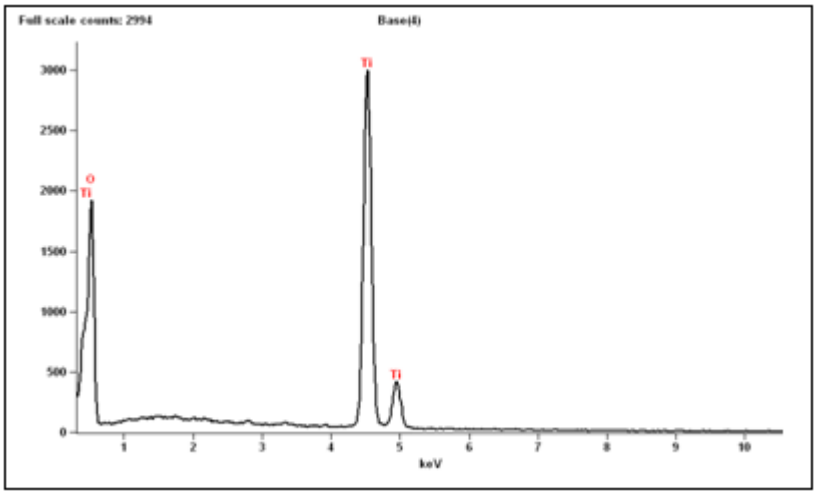

Figure 3.8 EDXA image for titanium di-oxide nanoparticle

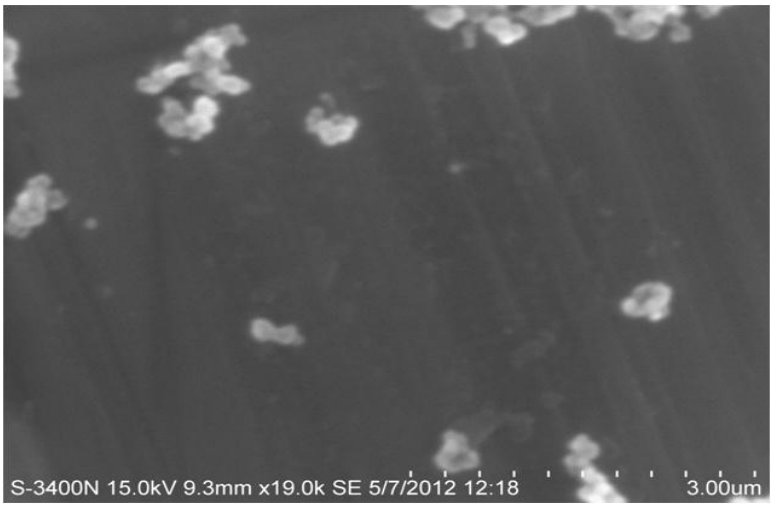

Figure 3.9 SEM image for titanium di-oxide nanofluid

3.4 Synthesis of copper oxide nanofluid

Copper oxide nanofluid has been prepared by wet chemical method. The chemicals such as copper chloride, sodium hydroxide and hydrochloric acid are purchased from Aldrich chemicals and they are in analytical grade. Since the method involves single step process, the preparation of copper oxide nanoparticle is carried out along with nanofluids.In this preparation process 100 ml of deionised water is taken in a 500 ml of beaker. To this 0.51 gm of copper chloride is added along with one gram of sodium hydroxide pellets. The reaction mixture is heated along with magnetic stirring and the process is carried out for one hour (Figure 3.10). As a result the colour of the solution changes from blue to black after the reaction and then the mixture is cooled to room temperature.

Figure 3.10 Preparation of copper oxide nanofluid using magnetic stirrer cum hot plate

The PH value of the so formed copper oxide wet precipitate is neutralized by adding droplets of hydrochloric acid. Then the copper oxide wet precipitate is washed with deionised water to remove the impurity ions present in the solution. Copper oxide nanofluids are obtained by dispersing the wet precipitate into the required amount of deionised water under ultrasonic vibration (Figure 3.11) for about four hours to have uniform dispersion of copper oxide nanoparticles.

Figure 3.11 Ultrasonication of copper oxide nanofluid

3.4.1 Characterization of copper oxide nanofluid

The characterization of copper oxide nanoparticles were done by XRD for structural determination and estimation of crystalline size using the instrument PAnalytical X'Pert PRO diffractometer and the average size of the nanoparticle were calculated using Debye-Scherrer equation 3.1 and it was 20 nm and image for XRD is shown in Figure 3.12.

Scanning Electron Microscope and Energy Dispersive X-ray Analysis (EDXA) is done using the instrument Hitachi, model: S-3400 N for surface morphology and chemical analysis. The result showed that the copper oxide nanoparticle is spherical in shape (Figure 3.13) and the presence Cu and O elements are confirmed from Figure 3.14. Figure 3.15 shows the image of dispersed copper oxide nanoparticle in base fluid and the thermal conductivity is measured using KD2 Pro thermal analyzer, Decagon Devices, Inc., USA. The value is found to be 0.698 W/mK and showed an increase of 12.4 % when compared to DI Water (0.613 W/mK).

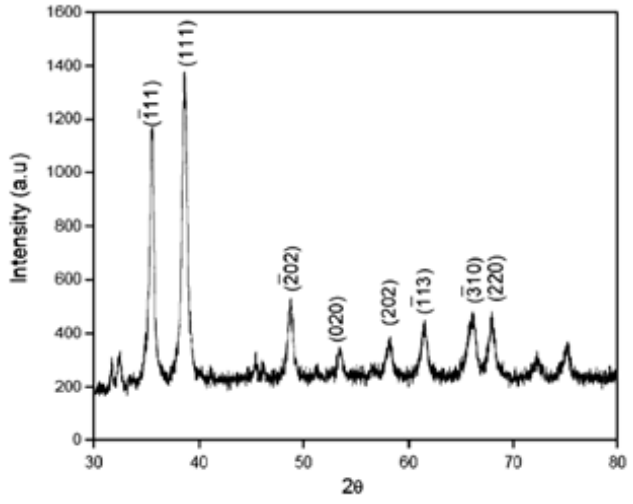

Figure 3.12 X-ray diffractogram for the copper oxide nanoparticle

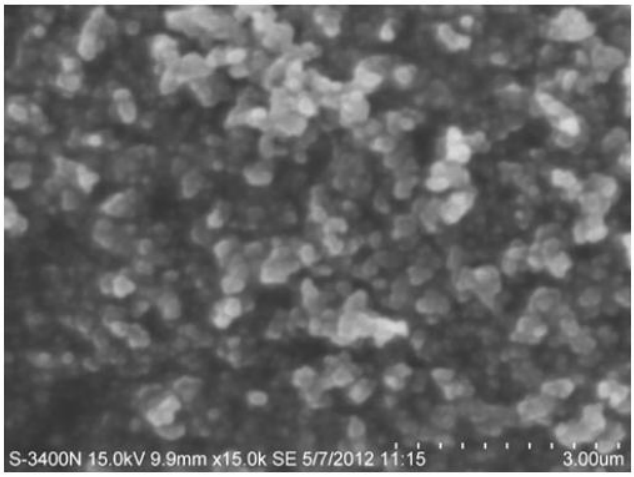

Figure 3.13 SEM image for the copper oxide nanoparticle

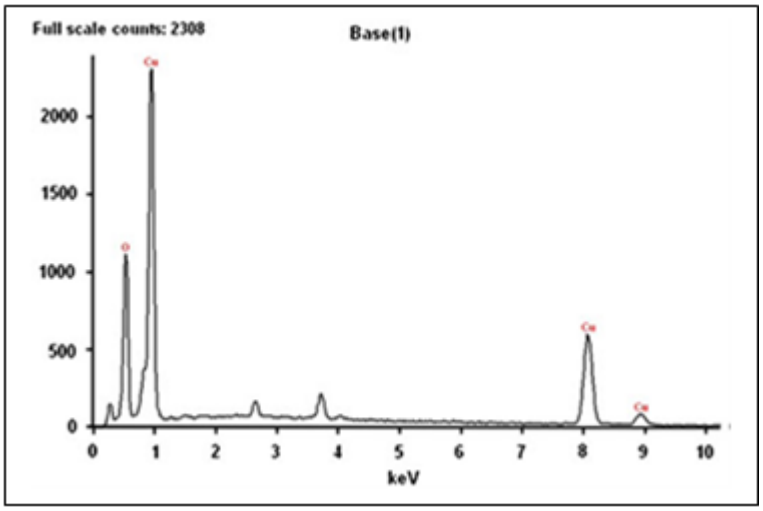

Figure 3.14 EDXA image for copper oxide nanoparticle

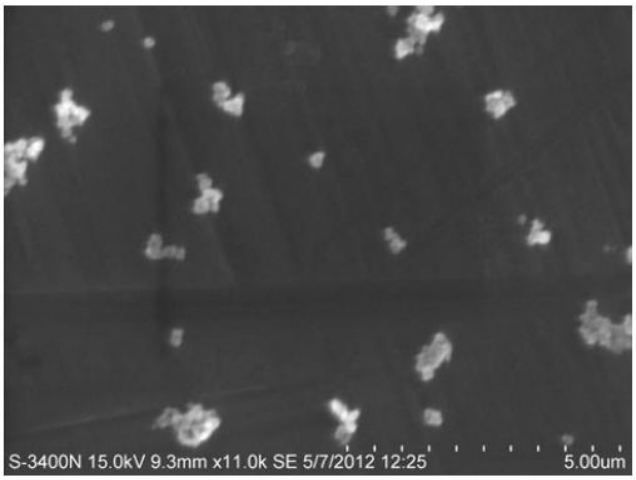

Figure 3.15 SEM image for copper oxide nanofluid

3.5 Experimental set-up and procedure

In this experimental study the experiments are carried out on full factorial design and Table 3.1 shows the working fluids, experimental parameters and their levels used .Figure 3.16 shows the schematic experimental diagram which is used for testing the performance of heat pipe and the Photographic view of experimental set-up is shown in Figure 3.17.

Table 3.1 Experimental parameters and their levels

Working fluids	**Parameters**	**Units**	**Levels**			
DI Water	Angle of inclination	Degree (deg.)	0	30	60	90
TiO_2 Nanofluid	Heat input	Watt (W)	40	50	60	70
CuO Nanofluid	Filling ratio	Percentage (%)	25	50	75	100

Copper tube is used as a material for fabrication of heat pipe due to its higher thermal conductance and compatibility with the working fluid. The outer diameter, inner diameter, thickness and length are 22 mm, 20.8 mm, 1.2 mm and 600 mm respectively. Stainless steel screen mesh (number 160) wick of two layers is used as wick of the heat pipe and the wire diameter of the screen mesh is 0.2286 mm.

The heat pipe has three sections namely evaporator section, adiabatic section and condenser section. The evaporator section is 150 mm in length and an electric heater is applied on the circumference of the evaporator section to provide the required heat supply and a wattmeter with the required power range and a variac has been integrated into the electric heater circuit to evaluate the exact power supplied to the evaporator region.

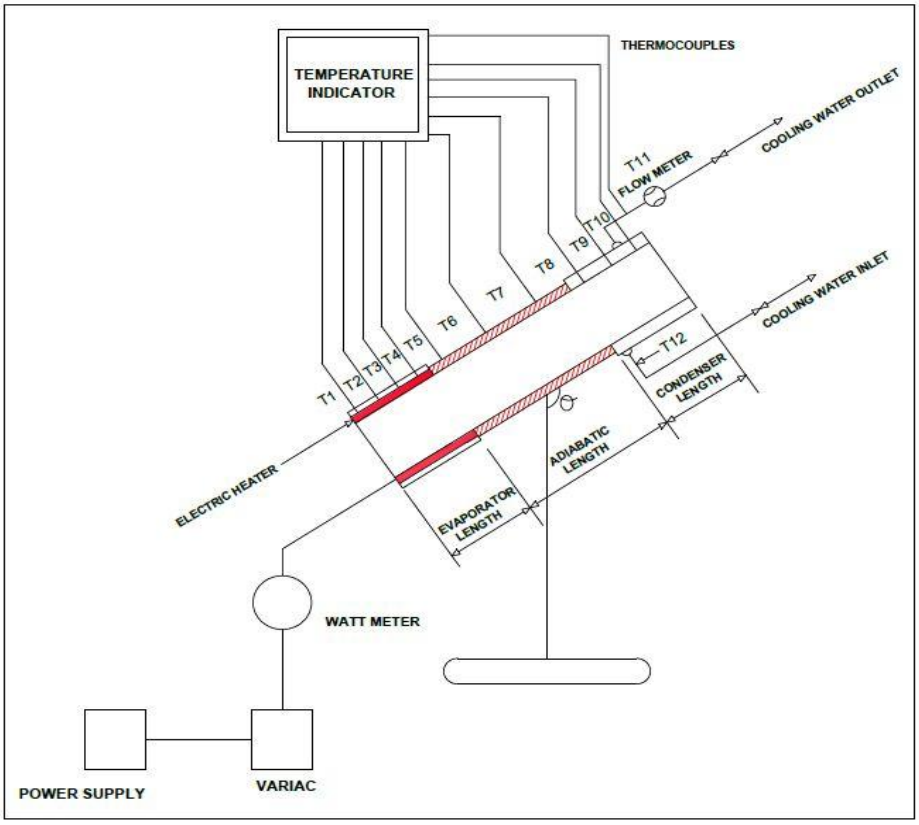

Figure 3.16 Schematic experimental diagram

The evaporator section is followed by adiabatic section which is of 300 mm in length and both the sections are insulated by glass wool (0.33W/mK) to prevent the heat loss from these regions. The condenser section is 150 mm in length and is cooled by circulating water to maintain a constant temperature of 30^0C ± 1^0C at the inlet section and flow rate of 0.08 kg/min is kept constant by using flow meter with uncertainty ±0.01L/min.

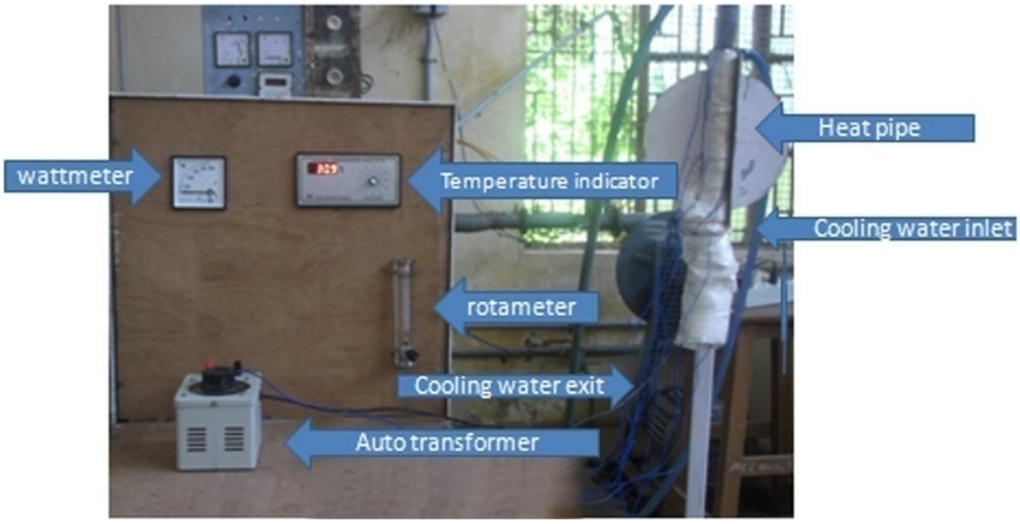

Figure 3.17 Photographic view of experimental set-up

The cooling water circuit is incorporated in the condenser section of the heat pipe using a 150 mm long water jacket with an inner diameter of 30 mm and outer diameter of 34 mm and water is used inside the cooling jacket. The water flow rate is measured by a rotameter on the inlet line of the jacket. The inlet and outlet temperatures of the cooling water are measured using two copper constantan thermocouples Twelve K-type thermocouples are brazed on the outer surface of the heat pipe at various locations which include four at the evaporator region, three at the adiabatic region, three at condenser region and the remaining two at the inlet and outlet of the cooling water circuit. The K-type thermocouples are calibrated against quartz thermometer and the uncertainty of the measurement is $\pm 0.1^{0}$C. Three identical heat pipes of same dimensions have been fabricated to carry out the experiment for different working fluids i.e. DI Water, TiO_2 and CuO nanofluids.

For each new charging the same heat pipe is used. Before filling up the working fluid, the heat pipe is evacuated by the vacuum pump to remove the dissolved gases and after evacuation the heat pipe is initially filled with 25% filling ratio of the working fluid. Filling ratio means the percentage of the evaporator section volume that is filled by the working fluids. The type of vacuum pump used in this experiment is of model DOA-P707-AA and 1/8 HP.The evaporator region is heated using the power supply to the required value with the help of auto transformer. The vacuum pressure is measured using the vacuum gauge which is attached in the condenser section. The temperatures are measured along the length of the heat pipe at various

locations when the steady state condition has been reached. Then the experiments are repeated for different filling ratio (25%, 50%, 75% and 100%), angle of inclination (0^0,30^0,60^0 and 90^0) and various working fluids (DI Water, TiO_2 and CuO nanofluids).

The thermal resistance of the heat pipe (R) is calculated by using the formula

$$R = \frac{(T_e - T_c)}{Q} \left[\frac{K}{W}\right] \quad \text{Eq. 3.3}$$

Where

T_e - Average wall temperature of the evaporator section (K)

T_c - Average wall temperature of the condenser section (K) and

Q - Heat supplied at the evaporator region of the heat pipe (W) and

The overall heat transfer coefficient is calculated using the formula

$$U = \frac{Q}{AX\Delta T} \left[\frac{W}{m^2K}\right] \quad \text{Eq. 3.4}$$

Where

U - Overall heat transfer coefficient (W/m^2K)

Q - Heat input (W)

A- Cross sectional area of the heat pipe (m^2) and

ΔT – Change in average wall temperature of evaporator and condenser section (K)

The experimental results for DI Water, TiO_2 nanofluid and CuO nanofluid operated heat pipe are calculated using the equation 3.3 and 3.4 and shown in Tables 3.2, 3.3 and 3.4.

Table 3.2 Experimental results for heat transfer characteristics of DI Water heat pipe

Ex. No	Heat input (W)	Angle of inclination (Deg.)	Filling ratio (%)	Thermal resistance (K/W)	Overall heat transfer coefficient (W/m^2K)
1	40	0	25	1.99	1482.3
2	40	0	50	1.81	1659.1
3	40	0	75	1.58	1900.6
4	40	0	100	1.70	1735.2
5	40	30	25	1.84	1603.2
6	40	30	50	1.69	1776.9
7	40	30	75	1.48	2029.0
8	40	30	100	1.59	1855.2
9	40	60	25	1.72	1745.9
10	40	60	50	1.60	1876.8
11	40	60	75	1.39	2122.1
12	40	60	100	1.49	1979.7
13	40	90	25	1.64	1831.0
14	40	90	50	1.56	1937.4
15	40	90	75	1.30	2269.1
16	40	90	100	1.44	2048.5
17	50	0	25	1.73	1705.0
18	50	0	50	1.65	1787.7
19	50	0	75	1.39	2160.4
20	50	0	100	1.51	1953.5
21	50	30	25	1.61	1843.6
22	50	30	50	1.54	1950.0
23	50	30	75	1.32	2234.7
24	50	30	100	1.42	2077.3
25	50	60	25	1.56	1925.0
26	50	60	50	1.46	2056.8
27	50	60	75	1.23	2398.2
28	50	60	100	1.38	2137.5
29	50	90	25	1.50	2002.0
30	50	90	50	1.40	2107.0
31	50	90	75	1.14	2587.5
32	50	90	100	1.28	2304.5
33	60	0	25	1.62	1820.8
34	60	0	50	1.49	2015.4
35	60	0	75	1.30	2310.0

Contd…

Ex. No	Heat input (W)	Angle of inclination (Deg.)	Filling ratio (%)	Thermal resistance (K/W)	Overall heat transfer coefficient (W/m^2K)
36	60	0	100	1.40	2107.0
37	60	30	25	1.54	1950.0
38	60	30	50	1.37	2191.9
39	60	30	75	1.19	2478.8
40	60	30	100	1.28	2304.5
41	60	60	25	1.45	2071.0
42	60	60	50	1.31	2292.3
43	60	60	75	1.15	2565.0
44	60	60	100	1.24	2378.9
45	60	90	25	1.35	2224.4
46	60	90	50	1.22	2461.4
47	60	90	75	1.03	2863.9
48	60	90	100	1.10	2681.6
49	70	0	25	1.33	2217.9
50	70	0	50	1.27	2364.5
51	70	0	75	1.15	2587.5
52	70	0	100	1.23	2398.2
53	70	30	25	1.20	2502.5
54	70	30	50	1.13	2657.5
55	70	30	75	1.01	2920.6
56	70	30	100	1.09	2706.2
57	70	60	25	1.11	2633.7
58	70	60	50	1.04	2887.5
59	70	60	75	0.93	3171.8
60	70	60	100	1.00	2948.8
61	70	90	25	1.07	2756.8
62	70	90	50	0.97	3041.0
63	**70**	**90**	**75**	**0.86**	**3430.0**
64	70	90	100	0.91	3241.0

Table 3.3 Experimental results for heat transfer characteristics of TiO_2 nanofluid heat pipe

Ex. No	Heat input (W)	Angle of inclination (Deg.)	Filling ratio (%)	Thermal resistance (K/W)	Overall heat transfer coefficient (W/m^2K)
1	40	0	25	1.74	1695.3
2	40	0	50	1.55	1937.4
3	40	0	75	1.36	2208.0
4	40	0	100	1.44	2048.5
5	40	30	25	1.61	1832.2
6	40	30	50	1.41	2129.7
7	40	30	75	1.27	2364.5
8	40	30	100	1.33	2217.9
9	40	60	25	1.47	2042.8
10	40	60	50	1.32	2275.0
11	40	60	75	1.17	2521.2
12	40	60	100	1.23	2398.2
13	40	90	25	1.37	2191.9
14	40	90	50	1.28	2346.0
15	40	90	75	1.08	2731.3
16	40	90	100	1.18	2499.8
17	50	0	25	1.54	1915.0
18	50	0	50	1.38	2176.0
19	50	0	75	1.19	2523.5
20	50	0	100	1.26	2341.0
21	50	30	25	1.37	2153.2
22	50	30	50	1.28	2346.0
23	50	30	75	1.13	2610.4
24	50	30	100	1.17	2521.2
25	50	60	25	1.33	2257.8
26	50	60	50	1.18	2499.8
27	50	60	75	1.05	2809.3
28	50	60	100	1.12	2633.7
29	50	90	25	1.24	2421.7
30	50	90	50	1.12	2681.2
31	50	90	75	0.95	3105.1
32	50	90	100	1.04	2836.3
33	60	0	25	1.34	2201.3
34	60	0	50	1.30	2310.0
35	60	0	75	1.04	2887.5
36	60	0	100	1.20	2458.2
37	60	30	25	1.25	2402.0
38	60	30	50	1.17	2566.6
39	60	30	75	0.97	3041.0

Contd…

Ex. No	Heat input (W)	Angle of inclination (Deg.)	Filling ratio (%)	Thermal resistance (K/W)	Overall heat transfer coefficient (W/m^2K)
40	60	30	100	1.08	2731.3
41	60	60	25	1.18	2566.6
42	60	60	50	1.11	2705.4
43	60	60	75	0.90	3277.6
44	60	60	100	1.04	2836.3
45	60	90	25	1.08	2780.5
46	60	90	50	1.02	2944.7
47	60	90	75	0.78	3781.8
48	60	90	100	0.92	3206.3
49	70	0	25	1.01	2920.6
50	70	0	50	0.94	3194.6
51	70	0	75	0.82	3597.3
52	70	0	100	0.88	3352.1
53	70	30	25	0.88	3412.5
54	70	30	50	0.80	3753.7
55	70	30	75	0.68	4338.0
56	70	30	100	0.74	3986.2
57	70	60	25	0.79	3801.3
58	70	60	50	0.72	4170.8
59	70	60	75	0.61	4835.8
60	70	60	100	0.65	4538.2
61	70	90	25	0.73	4113.7
62	70	90	50	0.65	4620.0
63	**70**	**90**	**75**	**0.54**	**5462.6**
64	70	90	100	0.57	5175.0

Table 3.4 Experimental results for heat transfer characteristics of CuO nanofluid heat pipe

Ex. No	Heat input (W)	Angle of inclination (Deg.)	Filling ratio (%)	Thermal resistance (K/W)	Overall heat transfer coefficient (W/m^2K)
1	40	0	25	1.35	2185.0
2	40	0	50	1.23	2441.4
3	40	0	75	1.05	2860.0
4	40	0	100	1.11	2657.5
5	40	30	25	1.23	2398.3
6	40	30	50	1.09	2755.0
7	40	30	75	0.96	3128.1
8	40	30	100	1.01	2920.6
9	40	60	25	1.09	2755.0
10	40	60	50	1.00	3003.0
11	40	60	75	0.86	3430.0
12	40	60	100	0.91	3241.5
13	40	90	25	0.99	3033.3
14	40	90	50	0.93	3229.0
15	40	90	75	0.77	3830.9
16	40	90	100	0.86	3430.0
17	50	0	25	1.19	2478.8
18	50	0	50	1.06	2833.0
19	50	0	75	0.86	3491.8
20	50	0	100	0.97	3041.0
21	50	30	25	1.05	2860.0
22	50	30	50	0.96	3128.1
23	50	30	75	0.81	3641.7
24	50	30	100	0.87	3390.6
25	50	60	25	0.98	3064.2
26	50	60	50	0.87	3451.7
27	50	60	75	0.73	4040.8
28	50	60	100	0.81	3641.7
29	50	90	25	0.89	3374.2
30	50	90	50	0.80	3753.7
31	50	90	75	0.64	4609.1
32	50	90	100	0.74	3986.2
33	60	0	25	0.95	3161.0
34	60	0	50	0.89	3374.2
35	60	0	75	0.72	4170.8
36	60	0	100	0.80	3687.3
37	60	30	25	0.86	3491.0
38	60	30	50	0.77	3900.0
39	60	30	75	0.64	4609.1

Contd…

Ex. No	Heat input (W)	Angle of inclination (Deg.)	Filling ratio (%)	Thermal resistance (K/W)	Overall heat transfer coefficient (W/m^2K)
40	60	30	100	0.69	4275.2
41	60	60	25	0.78	3850.0
42	60	60	50	0.71	4229.5
43	60	60	75	0.58	5085.9
44	60	60	100	0.63	4682.3
45	60	90	25	0.69	4352.0
46	60	90	50	0.63	4766.6
47	60	90	75	0.46	6412.7
48	60	90	100	0.53	5565.7
49	70	0	25	0.73	4040.8
50	70	0	50	0.68	4416.2
51	70	0	75	0.59	4999.7
52	70	0	100	0.64	4609.2
53	70	30	25	0.58	5177.5
54	70	30	50	0.54	5561.1
55	70	30	75	0.48	6145.5
56	70	30	100	0.51	5784.0
57	70	60	25	0.49	6128.5
58	70	60	50	0.45	6673.3
59	70	60	75	0.39	7563.7
60	70	60	100	0.42	7023.4
61	70	90	25	0.42	7150.0
62	70	90	50	0.38	7902.6
63	**70**	**90**	**75**	**0.33**	**8938.9**
64	70	90	100	0.35	8428.2

CHAPTER 4

RESULTS AND DISCUSSION

4.1 Heat transfer characteristics of heat pipe using DI water as a working fluid.

4.1.1 Effect of angle of inclination, filling ratio, and heat input on thermal resistance of heat pipe for DI Water as working fluid

From the experimental results the thermal resistance of DI Water operated heat pipe is calculated using the equation 3.3 and the results are tabulated and shown in Tables from 4.1 to 4.4.

Table 4.1 Thermal resistance of heat pipe using DI water for 25% filling ratio

Heat input (W)	Thermal resistance (K/W)			
	Angle of inclination (deg.)			
	0	**30**	**60**	**90**
40	1.99	1.84	1.72	1.64
50	1.73	1.61	1.56	1.50
60	1.62	1.54	1.45	1.35
70	1.33	1.20	1.11	1.07

Table 4.2 Thermal resistance of heat pipe using DI water for 50% filling ratio

Heat input (W)	Thermal resistance (K/W)			
	Angle of inclination (deg.)			
	0	**30**	**60**	**90**
40	1.81	1.69	1.60	1.56
50	1.65	1.54	1.46	1.40
60	1.49	1.37	1.31	1.22
70	1.27	1.13	1.04	0.97

Table 4.3 Thermal resistance of heat pipe using DI water for 75% filling ratio

Heat input (W)	Thermal resistance (K/W)			
	Angle of inclination (deg.)			
	0	**30**	**60**	**90**
40	1.58	1.48	1.39	1.30
50	1.39	1.32	1.23	1.14
60	1.30	1.19	1.15	1.03
70	1.15	1.01	0.93	0.86

Table 4.4 Thermal resistance of heat pipe using DI water for 100% filling ratio

Heat input (W)	Thermal resistance (K/W)			
	Angle of inclination (deg.)			
	0	**30**	**60**	**90**
40	1.70	1.59	1.49	1.44
50	1.51	1.42	1.38	1.28
60	1.40	1.28	1.24	1.10
70	1.23	1.09	1.00	0.91

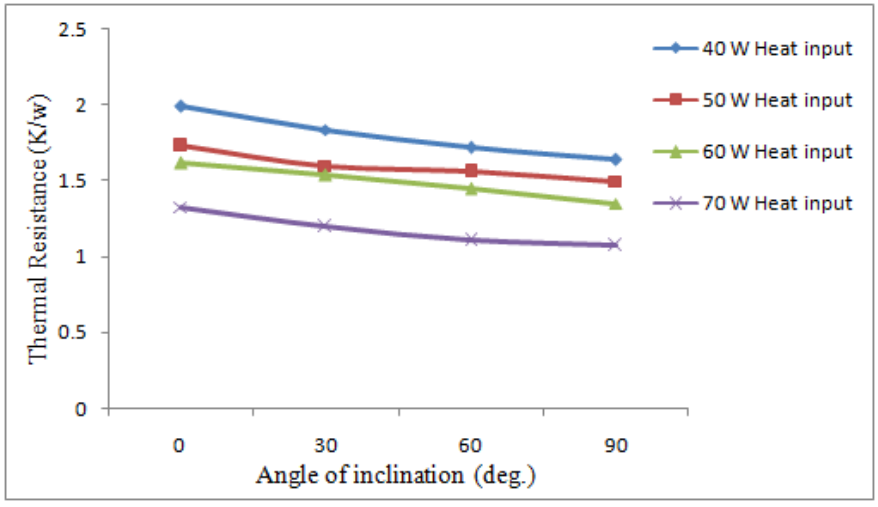

Figure 4.1 Thermal resistance of heat pipe using DI water for 25% filling ratio at various angle of inclination and heat input

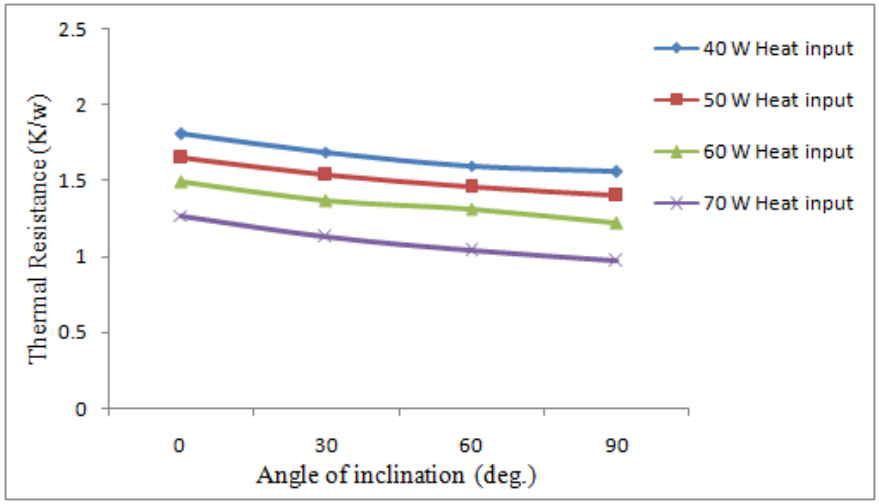

Figure 4.2 Thermal resistance of heat pipe using DI water for 50% filling ratio at various angle of inclination and heat input

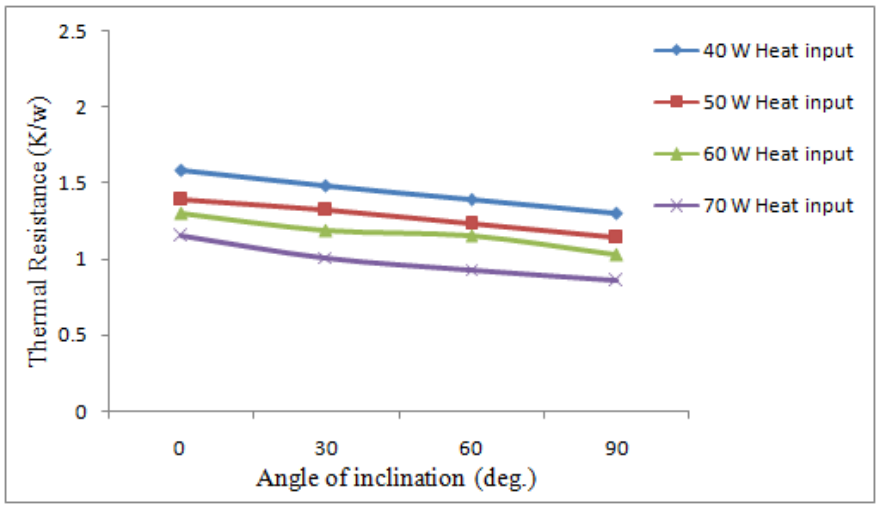

Figure 4.3 Thermal resistance of heat pipe using DI water for 75% filling ratio at various angle of inclination and heat input

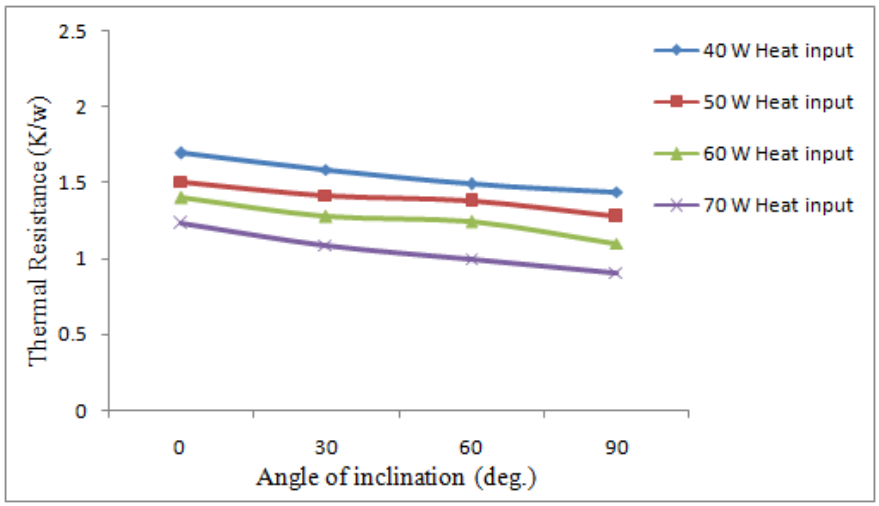

Figure 4.4 Thermal resistance of heat pipe using DI water for 100% filling ratio at various angle of inclination and heat input

Figures 4.1 to 4.4 shows the effect of angle of inclination, filling ratio, and heat input on thermal resistance of the heat pipe operated with DI Water as working fluid. When the angle of inclination increases from 0^0 to 90^0 degree the thermal resistance decreases. The lowest thermal resistance value is obtained when the heat pipe is operated at 90^0 angle of inclination. For the heat input is concerned the thermal resistance is higher at low heat input i.e. 40W this is due to the fact at low heat input a relatively solid liquid film resides in the evaporator section. However the thermal resistance decreases rapidly as the heat input is increased and this tendency is a common characteristic of the heat pipe as indicated by Hopkins et. al. (1999). Hence the heat pipe operated at 40 W heat input shows higher thermal resistance compared to the heat pipe operated at higher heat input i.e.70 W.

The thermal resistance value decreases when the filling ratio is increased from 25% to 75% and any increase in filling ratio beyond that i.e. 100% the thermal resistance increases. This is due to the reason when the heat pipe is operated with lower filling ratio with fixed heat input the working fluid evaporates easily and thus less time period available for the condensed working fluid present in the condenser section to flow back to the evaporator section, as a result dry out occurs at the evaporator section thus affecting the phase change phenomenon of the working fluid which leads to higher thermal resistance as indicated by Teng et. al. (2010).

Similarly when the filling ratio is high (i.e. 100%) the temperature available at the evaporator section is found to be lesser than the actual temperature needed for the evaporation of the working fluid, hence the movement of the vapour from the evaporator section to the condenser section is very less due to the larger volume of the working fluid, in addition a lesser space is available in the heat pipe for the movement of the vapour which leads to increase in higher pressure inside the heat pipe thus affecting the evaporation of the working fluid, as a result the thermal resistance increases. The lowest thermal resistance is obtained when the heat pipe is operated at an inclination angle of 90^0, 75% filling ratio and 70 W heat input.

4.1.2 Effect of angle of inclination, filling ratio, and heat input on overall heat transfer coefficient of heat pipe for DI Water as working fluid

From the experimental results the overall heat transfer coefficient of DI Water operated heat pipe is calculated using the equation 3.4 and the results are tabulated and shown in Tables from 4.5 to 4.8.

Table 4.5 Overall heat transfer coefficient of DI water heat pipe for 25% filling ratio

Heat input (W)	Overall heat transfer coefficient (W/m^2K)			
	Angle of inclination (deg.)			
	0	**30**	**60**	**90**
40	1482.3	1603.2	1745.9	1831.0
50	1705.0	1843.6	1925.0	2002.0
60	1820.8	1950.0	2071.0	2224.4
70	2217.9	2502.5	2633.7	2756.8

Table 4.6 Overall heat transfer coefficient of DI water heat pipe for 50% filling ratio

Heat input (W)	Overall heat transfer coefficient (W/m^2K)			
	Angle of inclination (deg.)			
	0	**30**	**60**	**90**
40	1659.1	1776.9	1876.8	1937.4
50	1787.7	1950.0	2056.8	2107.0
60	2015.4	2191.9	2292.3	2461.4
70	2364.5	2657.5	2887.5	3041.0

Table 4.7 Overall heat transfer coefficient of DI water heat pipe for 75% filling ratio

Heat input (W)	Overall heat transfer coefficient (W/m^2K)			
	Angle of inclination (deg.)			
	0	**30**	**60**	**90**
40	1900.6	2029.0	2122.1	2269.1
50	2160.4	2234.7	2398.2	2587.5
60	2310.0	2478.8	2565.0	2863.9
70	2587.5	2920.6	3171.8	3430.0

Table 4.8 Overall heat transfer coefficient of DI water heat pipe for 100% filling ratio

Heat input (W)	Overall heat transfer coefficient (W/m^2K))			
	Angle of inclination (deg.)			
	0	**30**	**60**	**90**
40	1735.2	1855.2	1979.7	2048.5
50	1953.5	2077.3	2137.5	2304.5
60	2107.0	2304.5	2378.9	2681.6
70	2398.2	2706.2	2949.8	3241.0

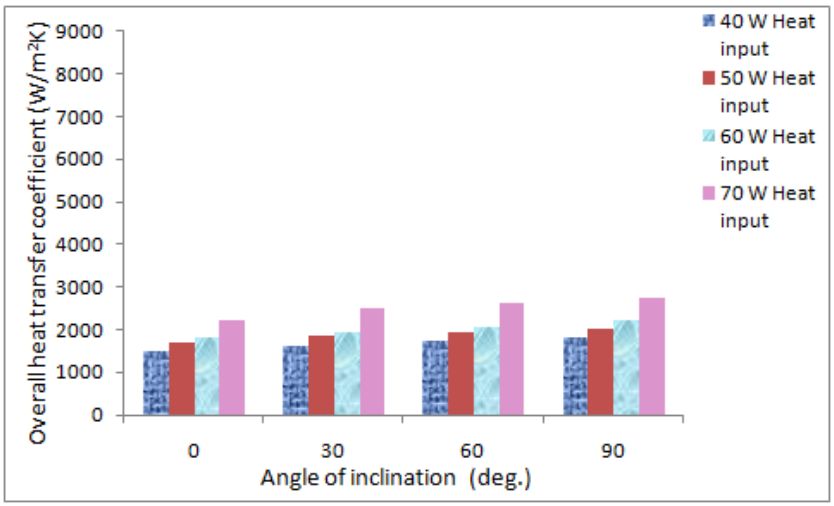

Figure 4.5 Overall heat transfer coefficient of DI water heat pipe for 25% filling ratio at various angle of inclination and heat input

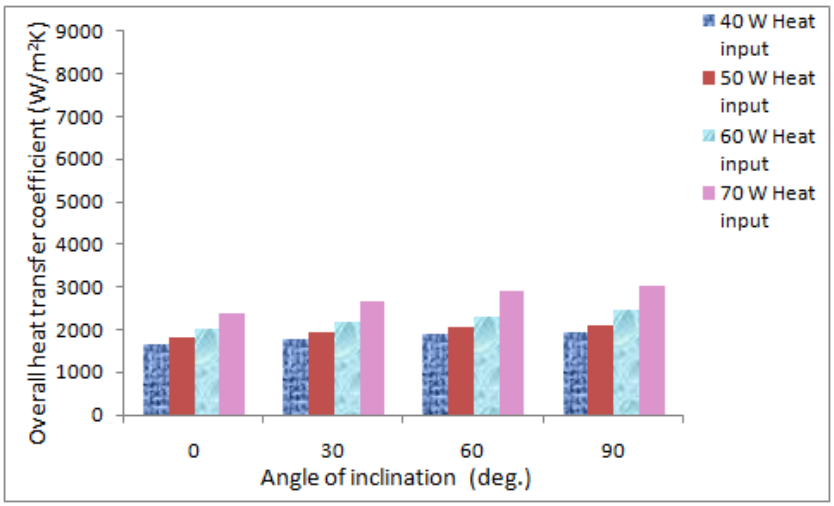

Figure 4.6 Overall heat transfer coefficient of DI water heat pipe for 50% filling ratio at various angle of inclination and heat input

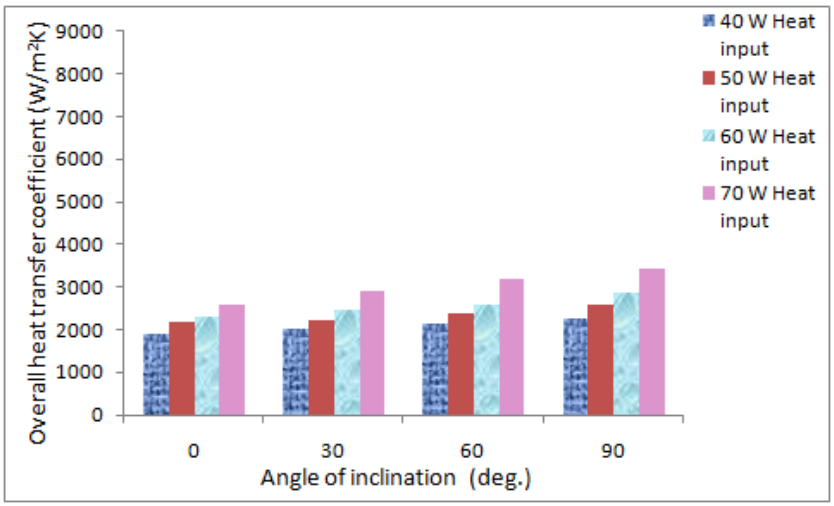

Figure 4.7 Overall heat transfer coefficient of DI water heat pipe for 75% filling ratio at various angle of inclination and heat input

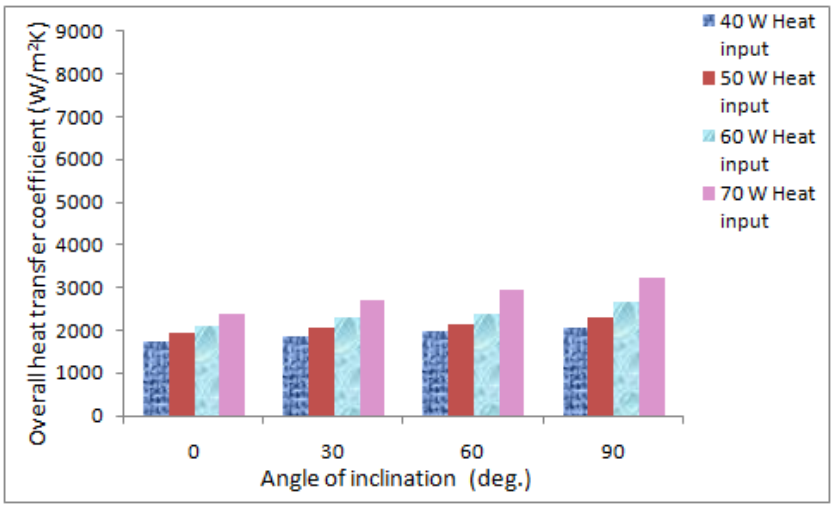

Figure 4.8 Overall heat transfer coefficient of DI water heat pipe for 100% filling ratio at various angle of inclination and heat input

The variation of overall heat transfer coefficient of DI Water working fluid for different angle of inclination (0^0,30^0,60^0 and 90^0), filling ratio (25%, 50%, 75% and 100%) and different heat input (40W, 50W, 60W and 70W) is shown in figures from 4.5 to 4.8.The graphs indicate that the overall heat transfer coefficient increases as the angle of inclination increases from 0^0 to 90^0.The minimum value of overall heat transfer coefficient is obtained when the heat pipe is operated in horizontal position (i.e.0^0) and the maximum value is obtained when the heat pipe is operated in vertical

position (i.e.90^0) from the horizontal and this is due to increase in the temperature difference between the evaporator and condenser sections.

When the filling ratio is increased from 25% to 100% the overall heat transfer coefficient increases up to 75%. Any increase beyond the overall heat transfer coefficient starts decreasing and the highest value is obtained when the heat pipe is operated at 75% filling ratio. The overall heat transfer coefficient is increased with increase in heat input i.e. from 40 w to 70 W. At 70 W heat input the heat pipe shows maximum overall heat transfer coefficient. The highest overall heat transfer coefficient is obtained when the heat pipe is operated at an inclination angle of 90^0, 75% filling ratio and 70 W heat input.

4.2 Heat transfer characteristics of heat pipe using TiO_2 nanofluid as working fluid

4.2.1 Effect of angle of inclination, filling ratio, and heat input on thermal resistance of heat pipe for TiO_2 nanofluid as working fluid

From the experimental results the thermal resistance of heat pipe operated with TiO_2 nanofluid is calculated using the equation 3.3. The results are tabulated and shown in Tables from 4.9 to 4.12.

Table 4.9 Thermal resistance of heat pipe using TiO_2 nanofluid for 25% filling ratio

Heat input (W)	Thermal resistance (K/W)			
	Angle of inclination (deg.)			
	0	**30**	**60**	**90**
40	1.74	1.61	1.47	1.37
50	1.54	1.37	1.33	1.24
60	1.34	1.25	1.18	1.08
70	1.01	0.88	0.79	0.73

Table 4.10 Thermal resistance of heat pipe using TiO_2 nanofluid for 50% filling ratio

Heat input (W)	Thermal resistance (K/W)			
	Angle of inclination (deg.)			
	0	**30**	**60**	**90**
40	1.55	1.41	1.32	1.28
50	1.38	1.28	1.18	1.12
60	1.30	1.17	1.11	1.02
70	0.94	0.80	0.72	0.65

Table 4.11 Thermal resistance of heat pipe using TiO_2 nanofluid for 75% filling ratio

Heat input (W)	Thermal resistance (K/W)			
	Angle of inclination (deg.)			
	0	**30**	**60**	**90**
40	1.36	1.27	1.17	1.08
50	1.19	1.13	1.05	0.95
60	1.04	0.97	0.90	0.78
70	0.82	0.68	0.61	0.54

Table 4.12 Thermal resistance of heat pipe using TiO_2 nanofluid for 100% filling ratio

Heat input (W)	Thermal resistance (K/W)			
	Angle of inclination (deg.)			
	0	**30**	**60**	**90**
40	1.44	1.33	1.23	1.18
50	1.26	1.17	1.12	1.04
60	1.20	1.08	1.04	0.92
70	0.88	0.74	0.65	0.57

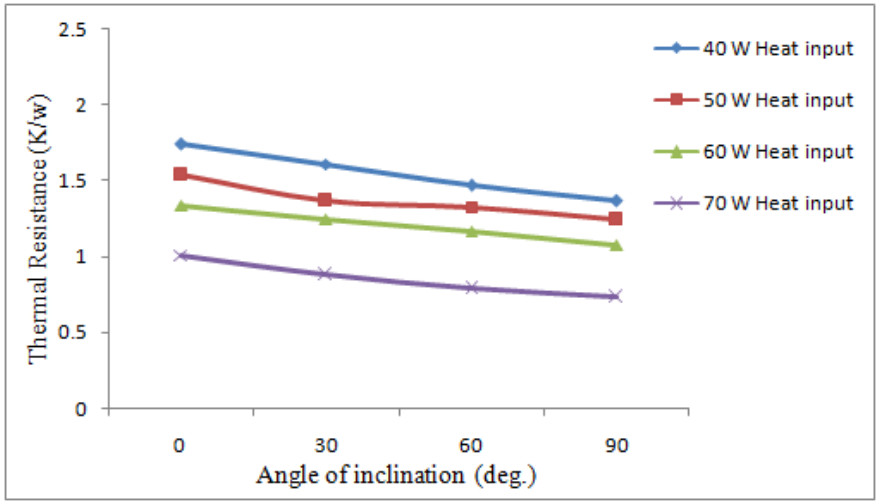

Figure 4.9 Thermal resistance of heat pipe using TiO_2 nanofluid for 25% filling ratio at various angle of inclination and heat input

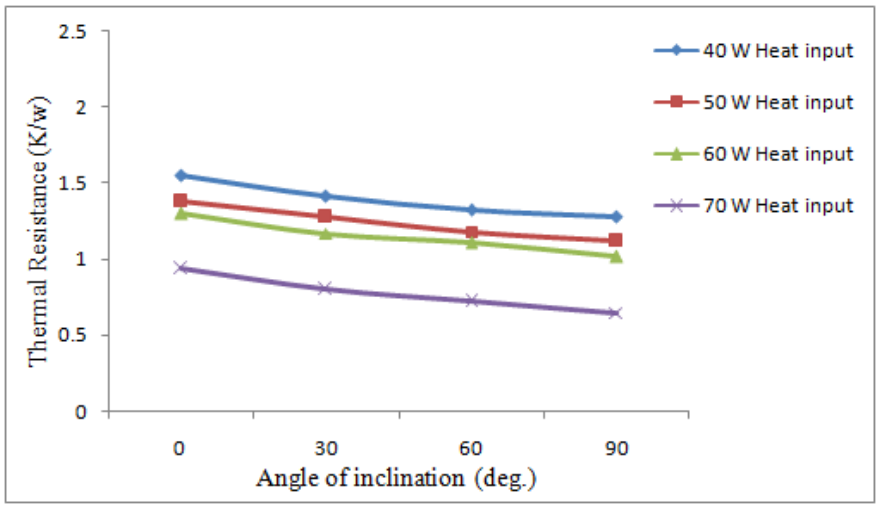

Figure 4.10 Thermal resistance of heat pipe using TiO_2 nanofluid for 50% filling ratio at various angle of inclination and heat input

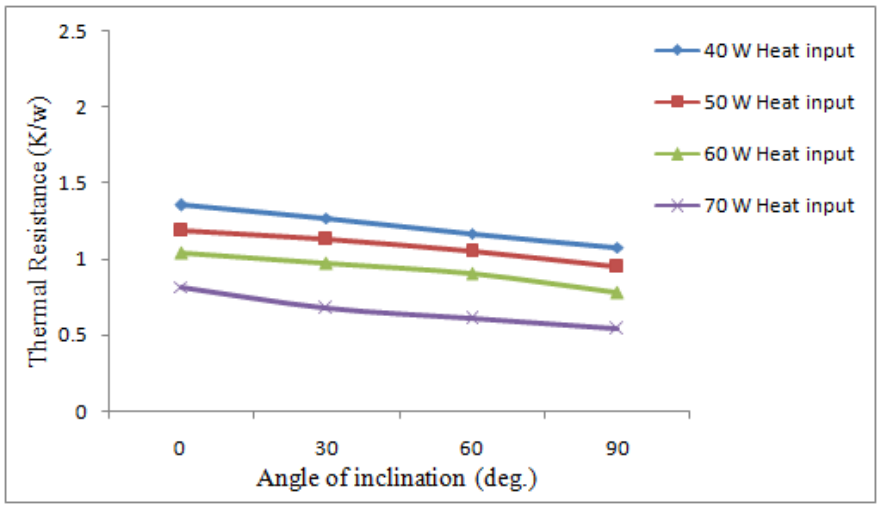

Figure 4.11 Thermal resistance of heat pipe using TiO_2 nanofluid for 75% filling ratio at various angle of inclination and heat input

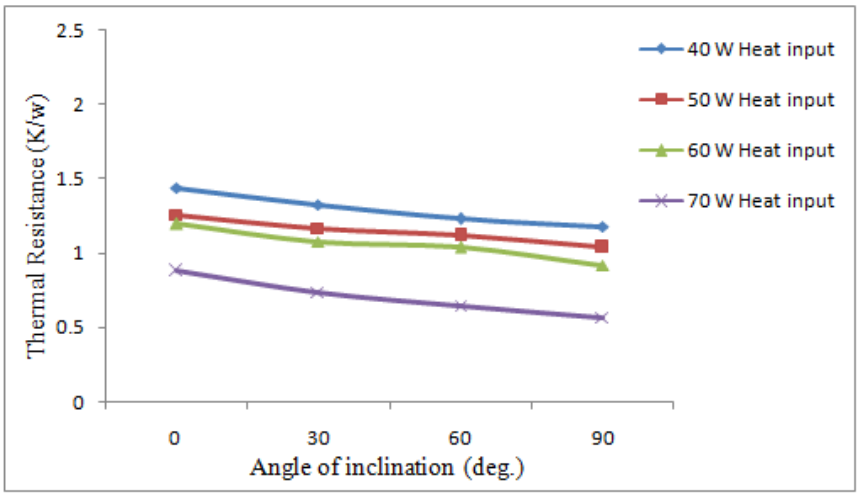

Figure 4.12 Thermal resistance of heat pipe using TiO_2 nanofluid for 100% filling ratio at various angle of inclination and heat input

Figure 4.9 to 4.12 shows the variation of thermal resistance of heat pipe operated with TiO_2 nanofluid for different angle of inclination (0^0,30^0,60^0 and 90^0), filling ratio (25%, 50%, 75% and 100%), different heat input (40W, 50W, 60W and 70W).The results show that the thermal resistance value is found to decrease when the angle of inclination is increased from 0^0 to 90^0. At 25% filling ratio the heat pipe shows higher thermal resistance due to the occurrence of dry out phenomenon at the evaporator section which affects the phase phenomenon of the working fluid as mentioned by

Teng et al 2010. For further increase in filling ratio from 25% to 75% the value of thermal resistance decreases and the highest value is found to occur when the heat pipe is operated at 75% filling ratio. At 100% filling ratio the thermal resistance is found to increase due to the reason lesser space is available in the heat pipe for the movement of the vapour thus affecting the evaporation of the working fluid. As far as heat input is concerned the thermal resistance is higher at 40W heat input and when the heat input is increased further the thermal resistance decreases and found to be minimum at 70 W heat input. Hence the lowest thermal resistance is obtained when the heat pipe is operated at an inclination angle of 90^0, filling ratio 75% and heat input 70 W.

4.2.2 Effect of angle of inclination, filling ratio, and heat input on overall heat transfer coefficient for TiO_2 nanofluid as working fluid

From the experimental results the overall heat transfer coefficient of heat pipe operated with TiO_2 nanofluid is calculated using the equation 3.4 and the results are tabulated and shown in Tables from 4.13 to 4.16.

Table 4.13 Overall heat transfer coefficient of heat pipe using TiO_2 nanofluid for 25% filling ratio

Heat input (W)	Overall heat transfer coefficient (W/m^2K)			
	Angle of inclination (deg.)			
	0	**30**	**60**	**90**
40	1695.3	1832.2	2042.8	2191.9
50	1915.0	2153.2	2257.8	2421.7
60	2201.3	2402.0	2566.6	2780.5
70	2920.6	3412.5	3801.3	4113.7

Table 4.14 Overall heat transfer coefficient of heat pipe using TiO_2 nanofluid for 50% filling ratio

Heat input (W)	Overall heat transfer coefficient (W/m^2K)			
	Angle of inclination (deg.)			
	0	**30**	**60**	**90**
40	1937.4	2129.7	2275.0	2346.0
50	2176.0	2346.0	2499.8	2681.2
60	2310.0	2566.6	2705.4	2944.7
70	3194.6	3753.7	4170.8	4620.0

Table 4.15 Overall heat transfer coefficient of heat pipe using TiO_2 nanofluid for 75% filling ratio

Heat input (W)	Overall heat transfer coefficient (W/m^2K)			
	Angle of inclination (deg.)			
	0	**30**	**60**	**90**
40	2208.0	2364.5	2521.2	2731.3
50	2523.5	2610.4	2809.3	3105.1
60	2887.5	3041.0	3277.6	3781.8
70	3597.3	4338.0	4835.8	5462.6

Table 4.16 Overall heat transfer coefficient of heat pipe using TiO_2 nanofluid for 100% filling ratio

Heat input (W)	Overall heat transfer coefficient (W/m^2K))			
	Angle of inclination (deg.)			
	0	**30**	**60**	**90**
40	2048.5	2217.9	2398.2	2499.8
50	2341.1	2521.2	2633.7	2836.3
60	2458.2	2731.3	2836.3	3206.3
70	3352.1	3986.2	4538.2	5175.0

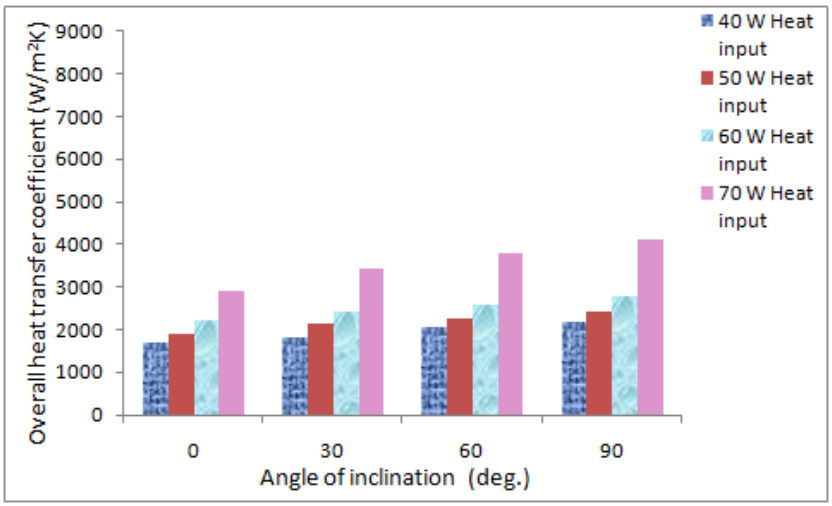

Figure 4.13 Overall heat transfer coefficient of heat pipe using TiO_2 nanofluid for 25% filling ratio at various angle of inclination and heat input

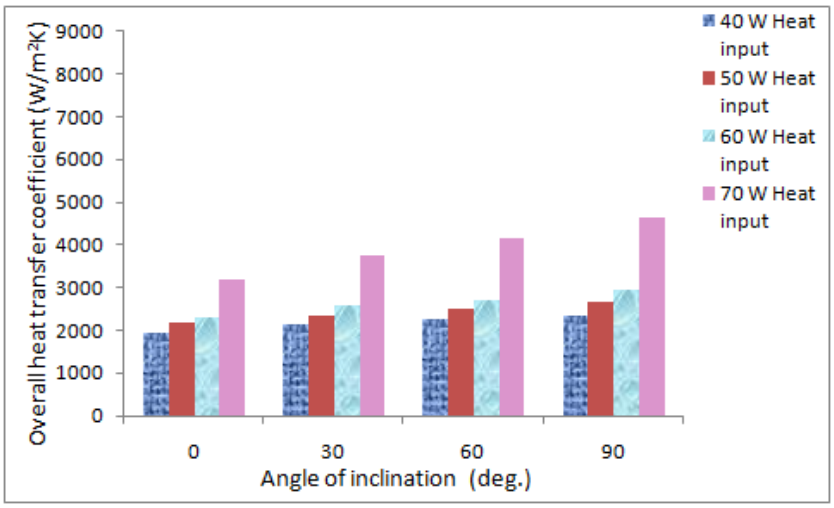

Figure 4.14 Overall heat transfer coefficient of heat pipe using TiO_2 nanofluid for 50% filling ratio at various angle of inclination and heat input

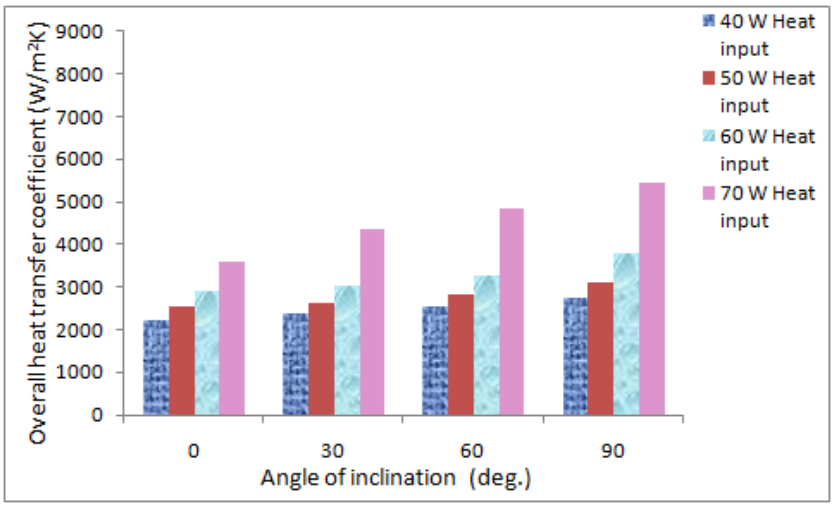

Figure 4.15 Overall heat transfer coefficient of heat pipe using TiO_2 nanofluid for 75% filling ratio at various angle of inclination and heat input

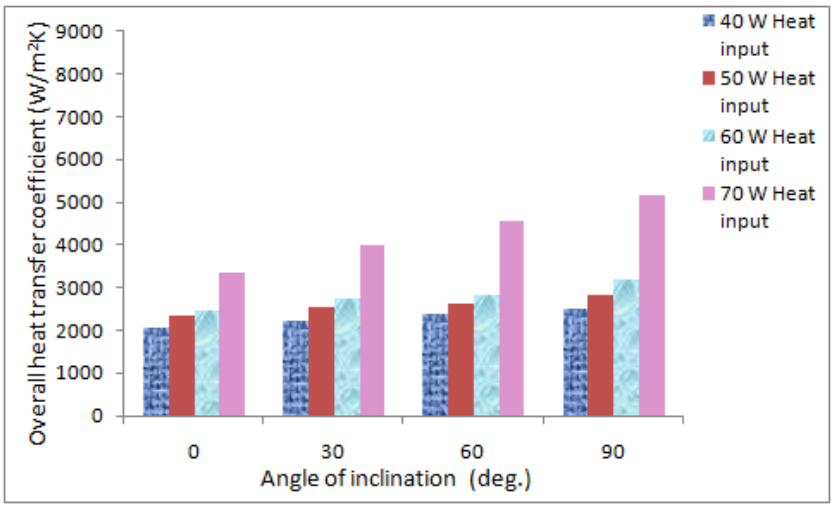

Figure 4.16 Overall heat transfer coefficient of heat pipe using TiO_2 nanofluid for 100% filling ratio at various angle of inclination and heat input

The variation of overall heat transfer coefficient of heat pipe using TiO_2 nanofluid for different angle of inclination (0^0,30^0,60^0 and 90^0), filling ratio (25%, 50%, 75% and 100%), and different heat input (40W, 50W, 60W and 70W) are shown in Figures from 4.13 to 4.16. The lowest value of overall heat transfer coefficient is obtained when the heat pipe is operated at 0^0 angle of inclination and the its value increases when the angle of inclination is increased from 0^0 to 90^0.The highest value of overall heat transfer coefficient is obtained when the heat pipe is operated at 90^0 angle of inclination. When the heat pipe is operated at 25% filling ratio the value of overall

heat transfer coefficient is found to be lesser and when the filling ratio is increased from 25% to 75% its value starts increasing and the highest value is obtained at 75% filling ratio. Whereas when the filling ratio is increased from 75% to 100% the value of overall heat transfer coefficient decreases. For heat input is concerned at 40 W heat input the heat pipe shows lowest value of overall heat transfer coefficient and its value increases when the heat input is increased from 40 W to 70 W and the highest value is obtained when the heat pipe is operated at 70 W heat input. Of all combinations of operating parameters used the heat pipe shows highest overall heat transfer coefficient when it is operated at an inclination angle of 90^0, 75% filling ratio and 70 W heat input.

4.3 Heat transfer characteristics of heat pipe using CuO nanofluid as working fluid

4.3.1 Effect of angle of inclination, filling ratio, and heat input on thermal resistance for CuO nanofluid as working fluid

From the experimental results the thermal resistance of heat pipe operated with CuO nanofluid is calculated using the equation 3.3. The results are tabulated and shown in Tables from 4.17 to 4.20.

Table 4.17 Thermal resistance of heat pipe using CuO nanofluid for 25% filling ratio

Heat input (W)	Thermal resistance (K/W)			
	Angle of inclination (deg.)			
	0	**30**	**60**	**90**
40	1.35	1.23	1.09	0.99
50	1.19	1.05	0.98	0.89
60	0.95	0.86	0.78	0.69
70	0.73	0.58	0.49	0.42

Table 4.18 Thermal resistance of heat pipe using CuO nanofluid for 50% filling ratio

Heat input (W)	Thermal resistance (K/W)			
	Angle of inclination (deg.)			
	0	**30**	**60**	**90**
40	1.23	1.09	1.00	0.93
50	1.06	0.96	0.87	0.80
60	0.89	0.77	0.71	0.63
70	0.68	0.54	0.45	0.38

Table 4.19 Thermal resistance of heat pipe using CuO nanofluid for 75% filling ratio

Heat input (W)	Thermal resistance (K/W)			
	Angle of inclination (deg.)			
	0	**30**	**60**	**90**
40	1.05	0.96	0.86	0.77
50	0.86	0.81	0.73	0.64
60	0.72	0.64	0.58	0.46
70	0.59	0.48	0.39	0.33

Table 4.20 Thermal resistance of heat pipe using CuO nanofluid for 100% filling ratio

Heat input (W)	Thermal resistance (K/W)			
	Angle of inclination (deg.)			
	0	**30**	**60**	**90**
40	1.11	1.01	0.91	0.86
50	0.97	0.87	0.81	0.74
60	0.80	0.69	0.63	0.53
70	0.64	0.51	0.42	0.35

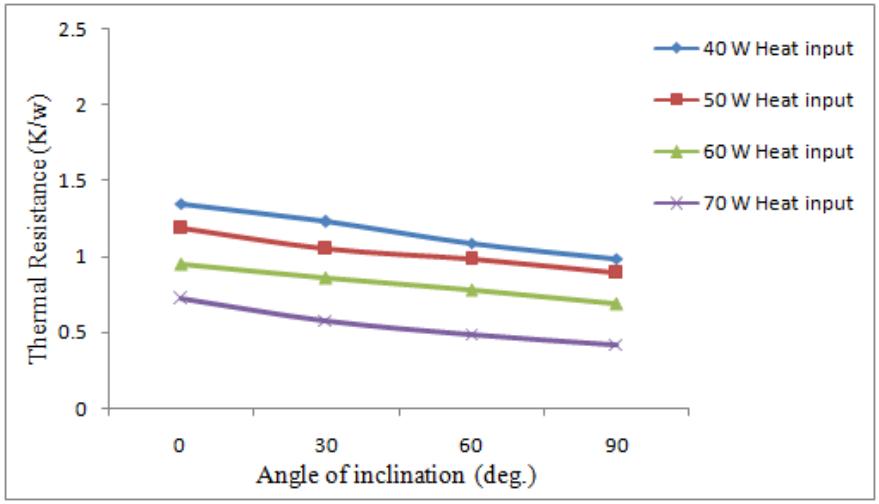

Figure 4.17 Thermal resistance of heat pipe using CuO nanofluid for 25% filling ratio at various angle of inclination and heat input

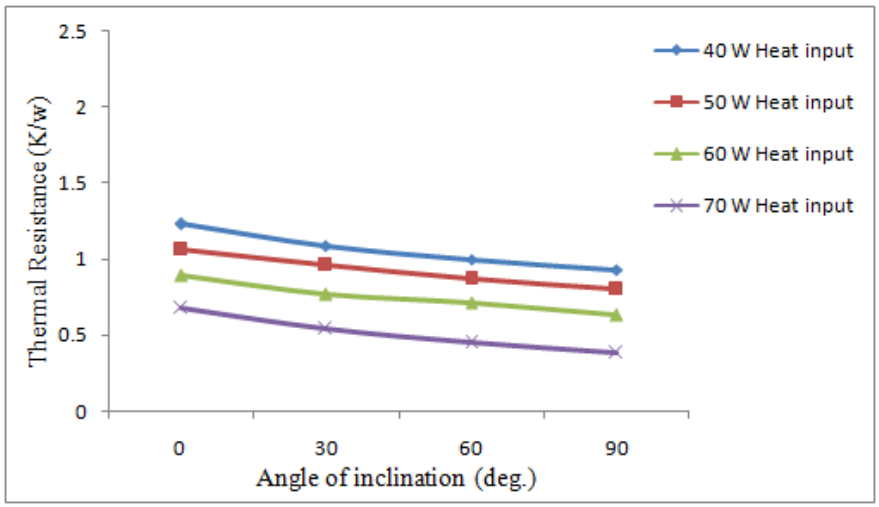

Figure 4.18 Thermal resistance of heat pipe using CuO nanofluid for 50% filling ratio at various angle of inclination and heat input

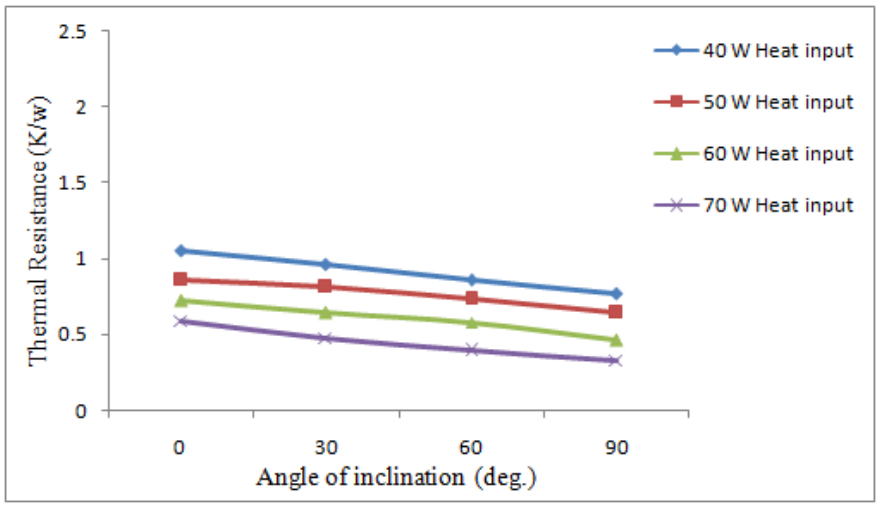

Figure 4.19 Thermal resistance of heat pipe using CuO nanofluid for 75% filling ratio at various angle of inclination and heat input

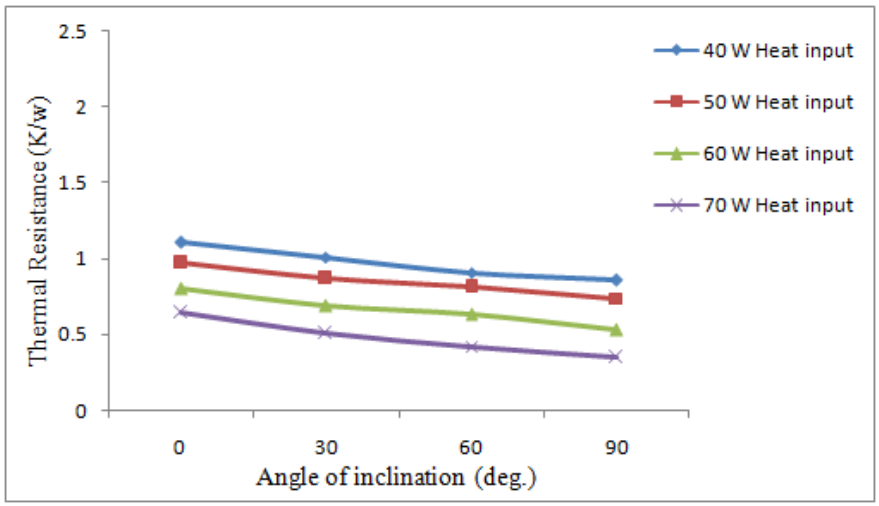

Figure 4.20 Thermal resistance of heat pipe using CuO nanofluid for 100% filling ratio at various angle of inclination and heat input

The variation of thermal resistance of heat pipe operated with CuO nanofluid for different angle of inclination (0^0,30^0,60^0 and 90^0), filling ratio (25%, 50%, 75% and 100%) and different heat input (40W, 50W, 60W and 70W) is shown in Figures from 4.17 to 4.20.The results from the graph indicate that when the heat pipe is operated at 0^0 angle of inclination the value of thermal resistance is found to be higher and when the angle of inclination is increased from 0^0 to 90^0 the value of thermal resistance decreases. When the heat pipe is operated at 25% filling ratio the value of thermal resistance is found to be higher and when the filling ratio is increased from 25% to 75% the value of thermal resistance decreases and when the filling ratio is increased

from 75% to 100% its value increases. For heat input parameter the heat pipe shows higher thermal resistance at 40 W heat input and the thermal resistance exhibits a decreasing trend when the heat input is increased from 40 W to 70 W. The heat transfer rate is increased due to increase of vapor density which is consistent with the result found by Jon (1999) and Kim (1999).

4.3.2 Effect of angle of inclination, filling ratio, and heat input on overall heat transfer coefficient of heat pipe using CuO nanofluid

From the experimental results the overall heat transfer coefficient of heat pipe operated with CuO nanofluid is calculated using the equation 3.4 and the results are tabulated and shown in tables from 4.21 to 4.24.

Table 4.21 Overall heat transfer coefficient of heat pipe using CuO nanofluid for 25% filling ratio

Heat input (W)	Overall heat transfer coefficient (W/m^2K)			
	Angle of inclination (deg.)			
	0	**30**	**60**	**90**
40	2185.0	2398.3	2755.0	3033.3
50	2478.8	2860.0	3064.4	3374.2
60	3161.0	3491.8	3850.0	4352.0
70	4040.8	5177.5	6128.5	7150.0

Table 4.22 Overall heat transfer coefficient of heat pipe using CuO nanofluid for 50% filling ratio

Heat input (W)	Overall heat transfer coefficient (W/m^2K)			
	Angle of inclination (deg.)			
	0	**30**	**60**	**90**
40	2441.4	2755.0	3003.0	3229.0
50	2833.0	3128.1	3451.7	3753.7
60	3374.2	3900.0	4229.5	4766.6
70	4416.2	5561.1	6673.3	7902.6

Table 4.23 Overall heat transfer coefficient of heat pipe using CuO nanofluid for 75% filling ratio

Heat input (W)	Overall heat transfer coefficient (W/m^2K)			
	Angle of inclination (deg.)			
	0	**30**	**60**	**90**
40	2860.0	3128.1	3430.0	3830.9
50	3491.8	3641.7	4040.8	4609.1
60	4170.8	4609.1	5085.9	6412.7
70	4999.7	6145.5	7563.7	8938.9

Table 4.24 Overall heat transfer coefficient of heat pipe using CuO nanofluid for 100% filling ratio

Heat input (W)	Overall heat transfer coefficient (W/m^2K))			
	Angle of inclination (deg.)			
	0	**30**	**60**	**90**
40	2657.5	2920.6	3241.5	3430.0
50	3041.0	3390.6	3641.7	3986.2
60	3687.3	4275.2	4682.3	5565.7
70	4609.2	5784.0	7023.4	8428.2

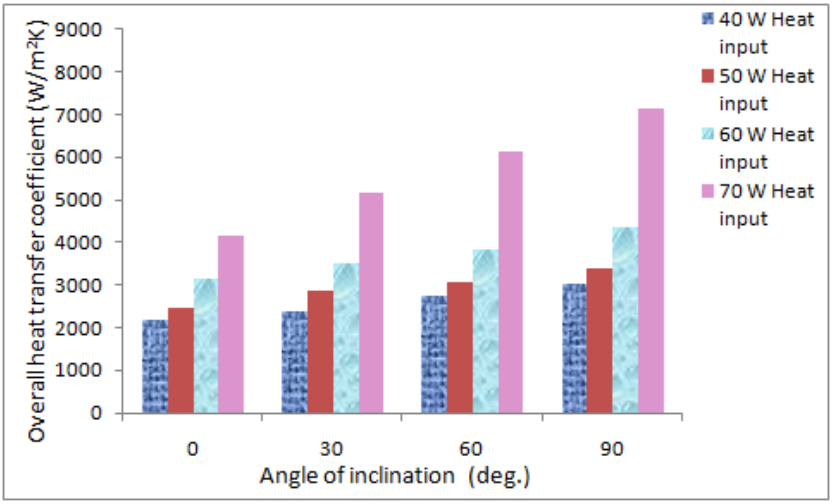

Figure 4.21 Overall heat transfer coefficient of heat pipe using CuO nanofluid for 25% filling ratio at various angle of inclination and heat input

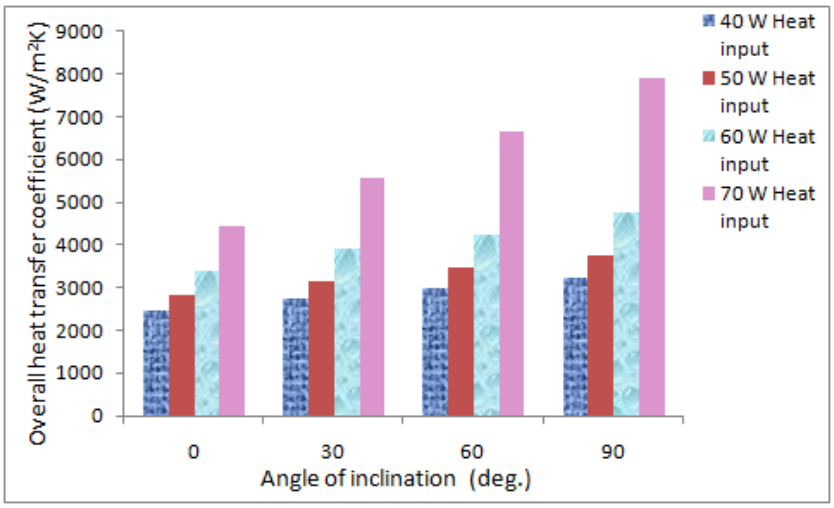

Figure 4.22 Overall heat transfer coefficient of heat pipe using CuO nanofluid for 50% filling ratio at various angle of inclination and heat input

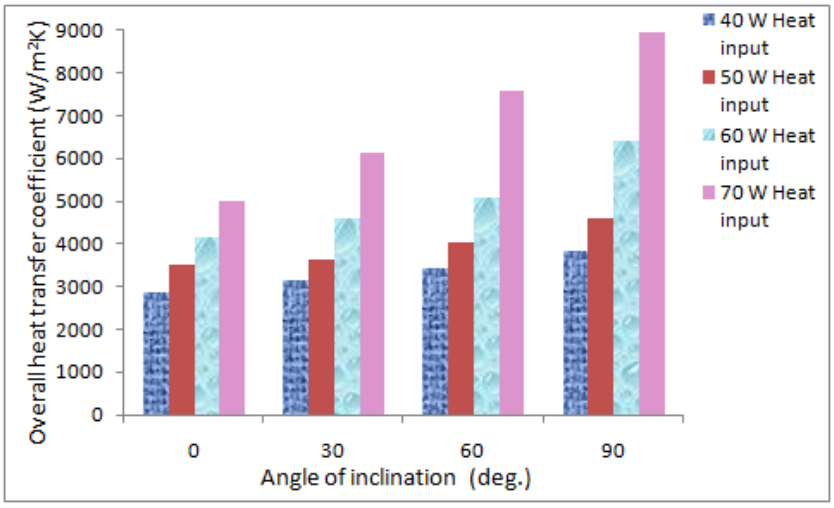

Figure 4.23 Overall heat transfer coefficient of heat pipe using CuO nanofluid for 75% filling ratio at various angle of inclination and heat input

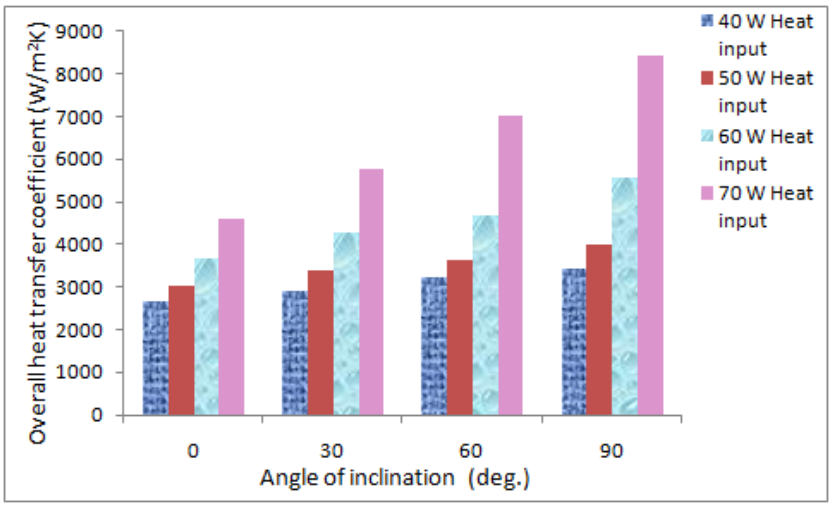

Figure 4.24 Overall heat transfer coefficient of heat pipe using CuO nanofluid for 100% filling ratio at various angle of inclination and heat input

The variation of overall heat transfer coefficient of heat pipe using CuO nanofluid for different angle of inclination (0^0,30^0,60^0 and 90^0), filling ratio (25%, 50%, 75% and 100%), and different heat input (40W, 50W, 60W and 70W) are shown in Figures 4.21 to 4.24. The heat pipe shows minimum value of overall heat transfer coefficient when it is operated at 0^0 angle of inclination and when the angle of inclination is increased from 0^0 to 90^0 the overall heat transfer coefficient increases and reaches its maximum value at angle 90^0 of inclination. The graphs also indicates that at 25% filling ratio the heat pipe shows minimum value of overall heat transfer coefficient and its value increases when the filling ratio is increased from 25% to 75% and reaches a maximum value when it is operated at 75% filling ratio. Further when the filling ratio is increased from 75% to 100% the value of overall heat transfer coefficient decreases. For heat input is concerned at 40 W heat input the heat pipe shows lowest value of overall heat transfer coefficient and its value increases when the heat input is increased from 40 W to 70 W and the highest value is obtained when the heat pipe is operated at 70 W heat input. Of all combinations of operating parameters used the heat pipe shows highest overall heat transfer coefficient when it is operated at an inclination angle of 90^0, 75% filling ratio and 70 W heat input.

4.4 Comparison of heat transfer characteristics of heat pipe using DI water, TiO_2 nanofluid and CuO nanofluid

4.4.1 Effect of angle of inclination, filling ratio, and heat input on thermal resistance

A thermal resistance comparison of heat pipe using DI Water, TiO_2 nanofluid and CuO nanofluid is carried out. From the experimental results the thermal resistance value of heat pipe for the above three working fluids is calculated by the equation 3.3 and the results are tabulated and shown in Tables from 4.25 to 4.28.

Table 4.25 Thermal resistance for DI Water, TiO_2 nanofluid and CuO nanofluid for 25% filling ratio

Heat input (W)	Working Fluids	Thermal resistance (K/W)			
		Angle of inclination (deg.)			
		0	**30**	**60**	**90**
40	DI Water	1.99	1.84	1.72	1.64
	TiO_2 nanofluid	1.74	1.61	1.47	1.37
	CuO nanofluid	1.35	1.23	1.09	0.99
50	DI Water	1.73	1.61	1.56	1.50
	TiO_2 nanofluid	1.54	1.37	1.33	1.24
	CuO nanofluid	1.19	1.05	0.98	0.89
60	DI Water	1.62	1.54	1.45	1.35
	TiO_2 nanofluid	1.34	1.25	1.18	1.08
	CuO nanofluid	0.95	0.86	0.78	0.69
70	DI Water	1.33	1.20	1.11	1.07
	TiO_2 nanofluid	1.01	0.88	0.79	0.73
	CuO nanofluid	0.72	0.58	0.49	0.42

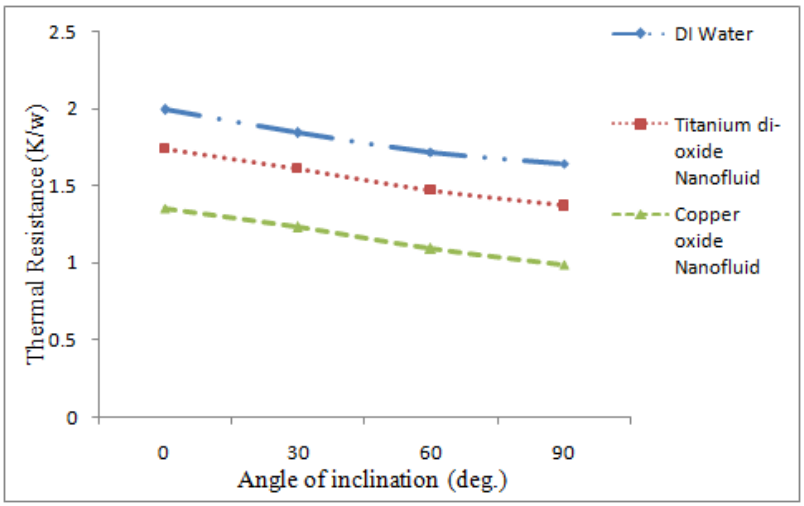

Figure 4.25 Comparison of thermal resistance for DI Water, TiO_2 nanofluid and CuO nanofluid for 25% filling ratio and 40W heat input

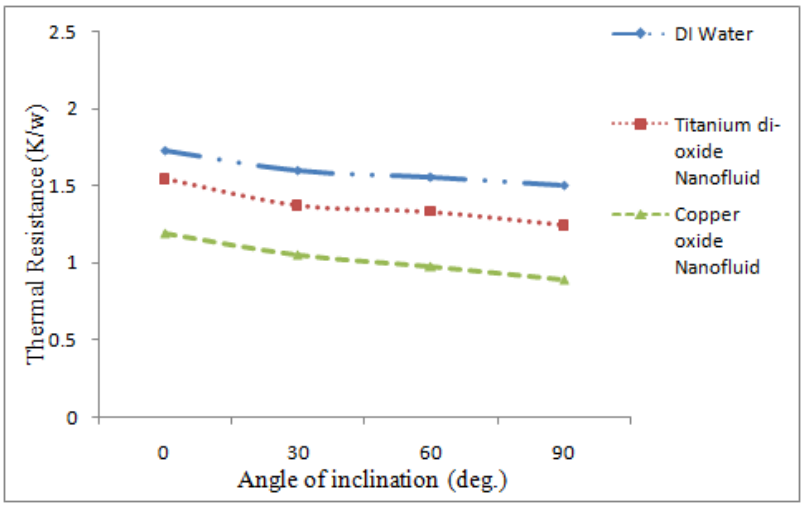

Figure 4.26 Comparison of thermal resistance for DI Water, TiO_2 nanofluid and CuO nanofluid for 25% filling ratio and 50W heat input

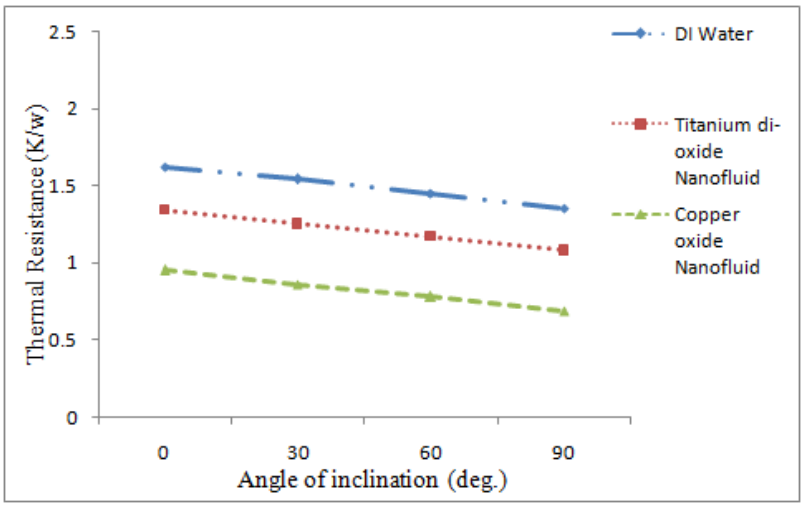

Figure 4.27 Comparison of thermal resistance for DI Water, TiO_2 nanofluid and CuO nanofluid for 25% filling ratio and 60W heat input

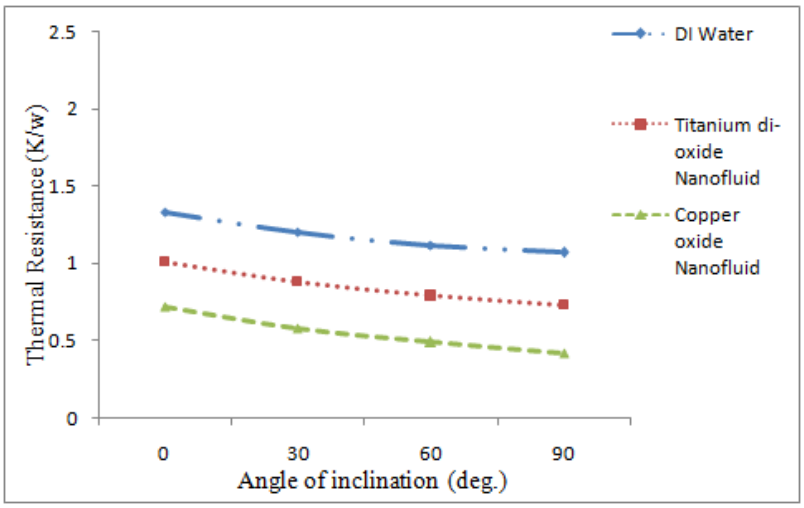

Figure 4.28 Comparison of thermal resistance for DI Water, TiO_2 nanofluid and CuO nanofluid for 25% filling ratio and 70W heat input

Table 4.26 Thermal resistance for DI Water, TiO_2 nanofluid and CuO nanofluid for 50% filling ratio

Heat input (W)	Working Fluids	Thermal resistance (K/W)			
		Angle of inclination (deg.)			
		0	**30**	**60**	**90**
40	DI Water	1.81	1.69	1.60	1.56
	TiO_2 nanofluid	1.55	1.41	1.32	1.28
	CuO nanofluid	1.23	1.09	1.00	0.93
50	DI Water	1.65	1.54	1.46	1.40
	TiO_2 nanofluid	1.38	1.28	1.18	1.12
	CuO nanofluid	1.06	0.96	0.87	0.80
60	DI Water	1.49	1.37	1.31	1.22
	TiO_2 nanofluid	1.30	1.17	1.11	1.02
	CuO nanofluid	0.89	0.77	0.71	0.63
70	DI Water	1.27	1.13	1.04	0.97
	TiO_2 nanofluid	0.94	0.80	0.72	0.65
	CuO nanofluid	0.68	0.54	0.45	0.38

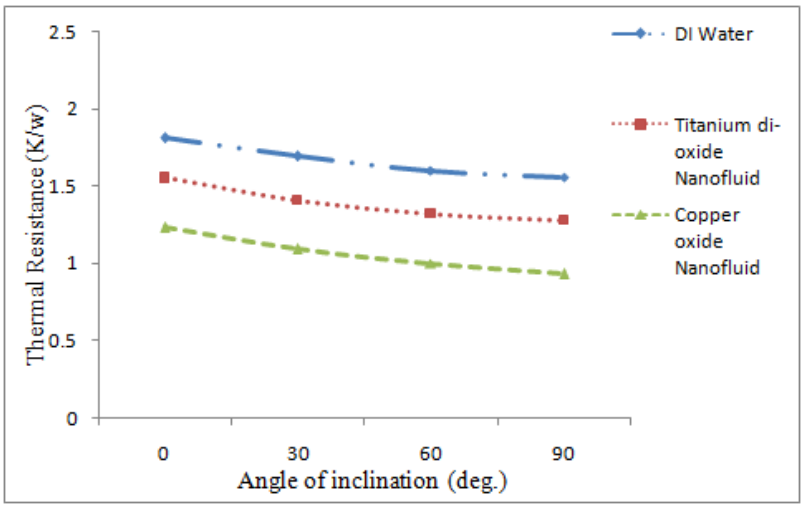

Figure 4.29 Comparison of thermal resistance for DI Water, TiO_2 nanofluid and CuO nanofluid for 50% filling ratio and 40W heat input

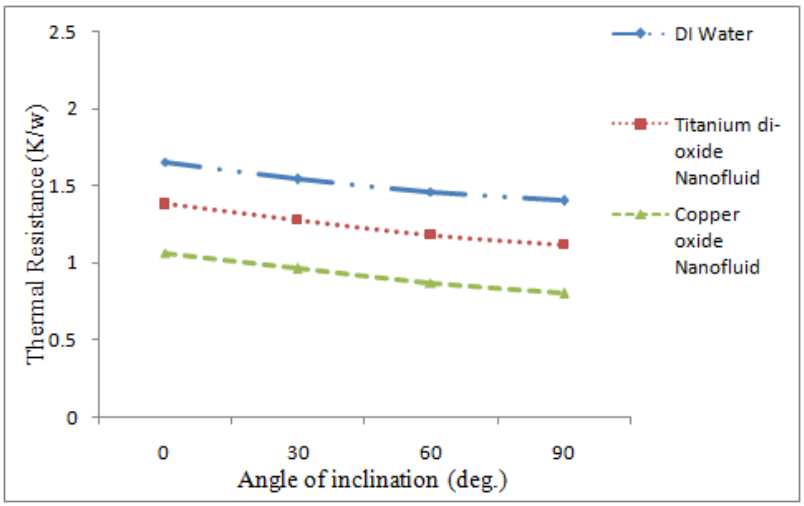

Figure 4.30 Comparison of thermal resistance for DI Water, TiO_2 nanofluid and CuO nanofluid for 50% filling ratio and 50W heat input

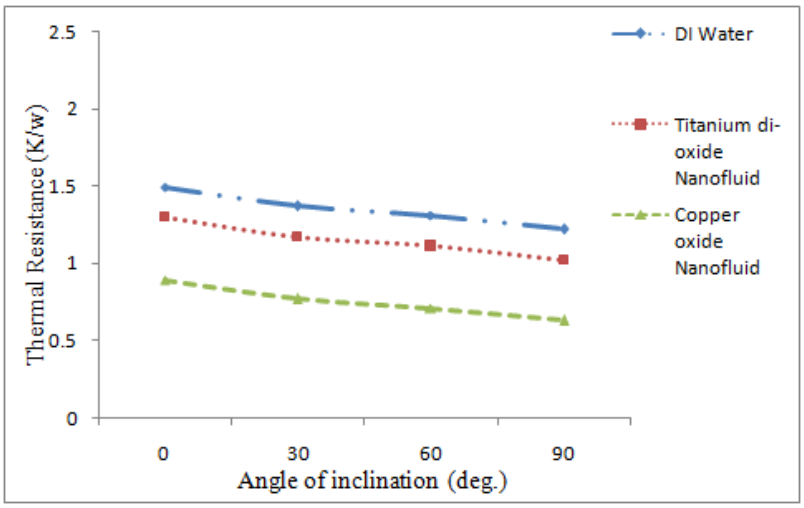

Figure 4.31 Comparison of thermal resistance for DI Water, TiO_2 nanofluid and CuO nanofluid for 50% filling ratio and 60W heat input

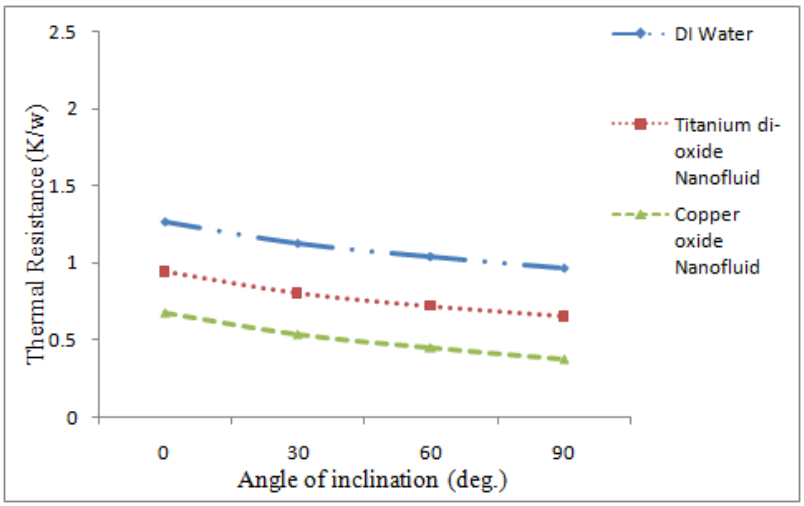

Figure 4.32 Comparison of thermal resistance for DI Water, TiO_2 nanofluid and CuO nanofluid for 50% filling ratio and 70W heat input

Table 4.27 Thermal resistance for DI Water, TiO_2 nanofluid and CuO nanofluid for 75% filling ratio

Heat input (W)	Working Fluids	Thermal resistance (K/W)			
		Angle of inclination (deg.)			
		0	**30**	**60**	**90**
40	DI Water	1.58	1.48	1.39	1.30
	TiO_2 nanofluid	1.36	1.27	1.17	1.08
	CuO nanofluid	1.05	0.96	0.86	0.77
50	DI Water	1.39	1.32	1.23	1.14
	TiO_2 nanofluid	1.19	1.13	1.05	0.95
	CuO nanofluid	0.86	0.81	0.73	0.64
60	DI Water	1.30	1.19	1.15	1.03
	TiO_2 nanofluid	1.04	0.97	0.90	0.78
	CuO nanofluid	0.72	0.64	0.58	0.46
70	DI Water	1.15	1.01	0.93	0.86
	TiO_2 nanofluid	0.82	0.68	0.61	0.54
	CuO nanofluid	0.59	0.48	0.39	0.33

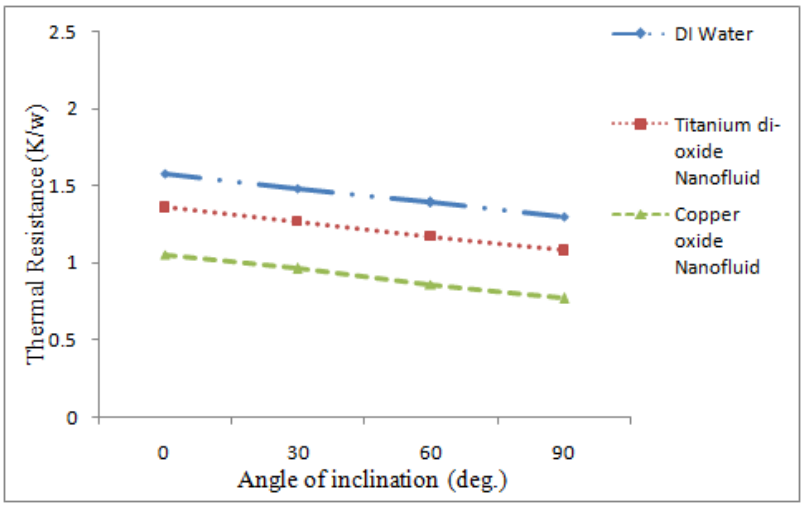

Figure 4.33 Comparison of thermal resistance for DI Water, TiO_2 nanofluid and CuO nanofluid for 75% filling ratio and 40W heat input

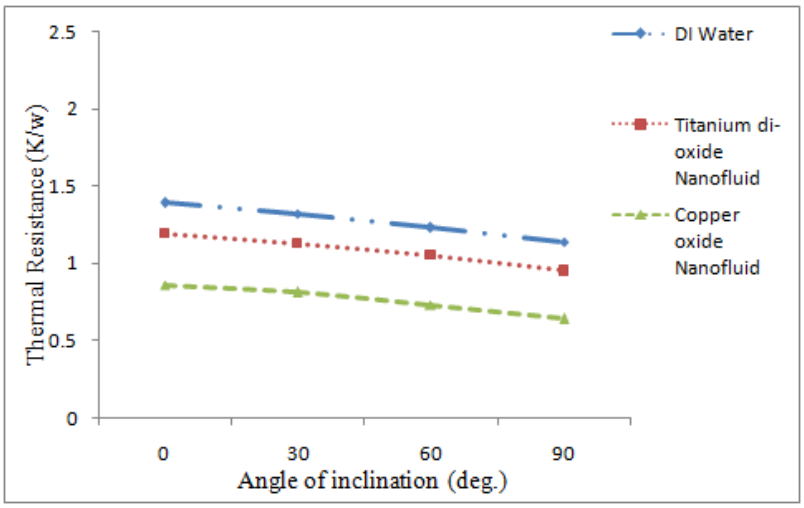

Figure 4.34 Comparison of thermal resistance for DI Water, TiO_2 nanofluid and CuO nanofluid for 75% filling ratio and 50W heat input

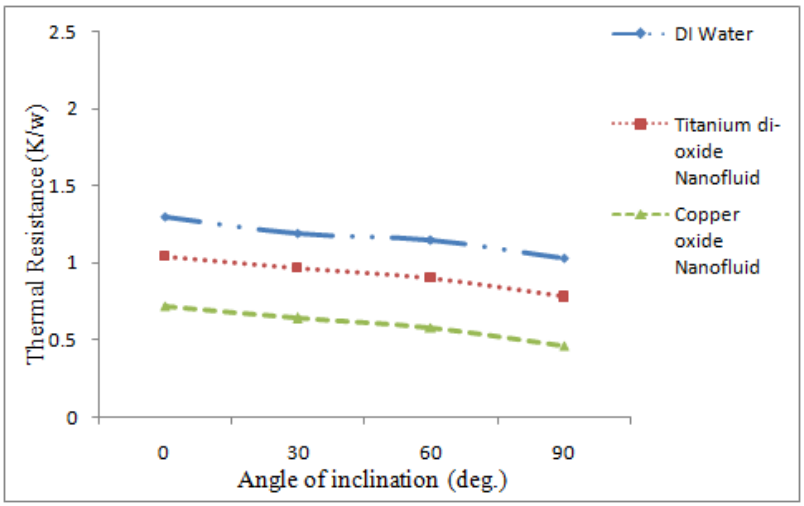

Figure 4.35 Comparison of thermal resistance for DI Water, TiO_2 nanofluid and CuO nanofluid for 75% filling ratio and 60W heat input

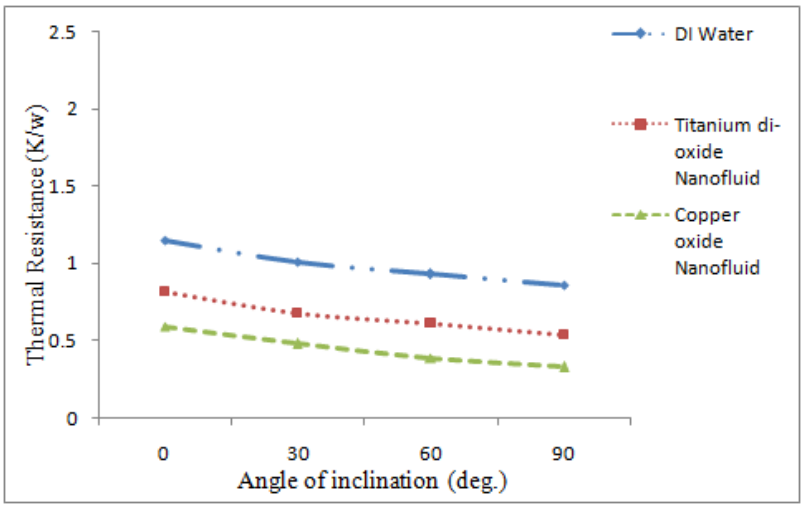

Figure 4.36 Comparison of thermal resistance for DI Water, TiO_2 nanofluid and CuO nanofluid for 75% filling ratio and 70W heat input

Table 4.28 Thermal resistance for DI Water, TiO_2 nanofluid and CuO nanofluid for 100% filling ratio

Heat input (W)	Working Fluids	Thermal resistance (K/W)			
		Angle of inclination (deg.)			
		0	**30**	**60**	**90**
40	DI Water	1.70	1.59	1.49	1.44
	TiO_2 nanofluid	1.44	1.33	1.23	1.18
	CuO nanofluid	1.11	1.01	0.91	0.86
50	DI Water	1.51	1.42	1.38	1.28
	TiO_2 nanofluid	1.26	1.17	1.12	1.04
	CuO nanofluid	0.97	0.87	0.81	0.74
60	DI Water	1.40	1.28	1.24	1.10
	TiO_2 nanofluid	1.20	1.08	1.04	0.92
	CuO nanofluid	0.80	0.69	0.63	0.53
70	DI Water	1.23	1.09	1.00	0.91
	TiO_2 nanofluid	0.88	0.74	0.65	0.57
	CuO nanofluid	0.64	0.51	0.42	0.35

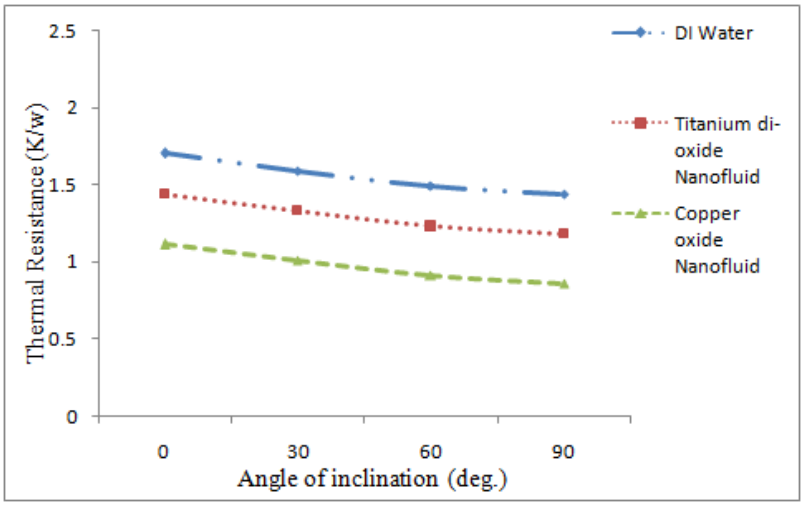

Figure 4.37 Comparison of thermal resistance for DI Water, TiO_2 nanofluid and CuO nanofluid for 100% filling ratio and 40W heat input

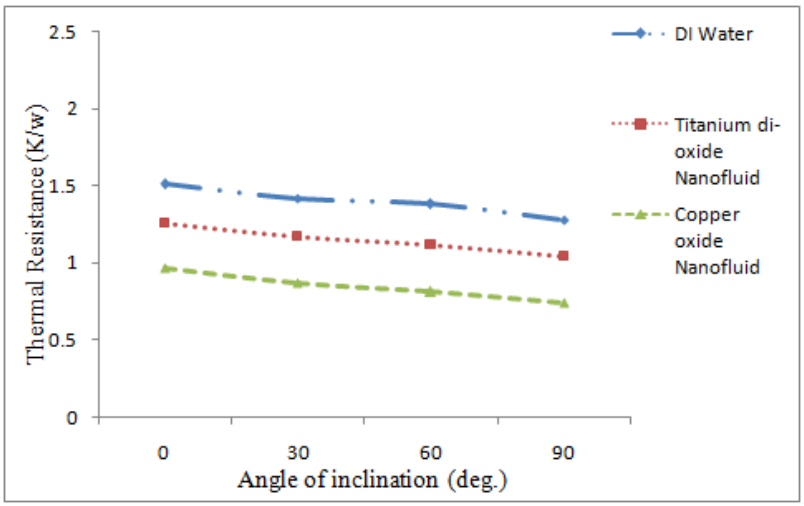

Figure 4.38 Comparison of thermal resistance for DI Water, TiO_2 nanofluid and CuO nanofluid for 100% filling ratio and 50W heat input

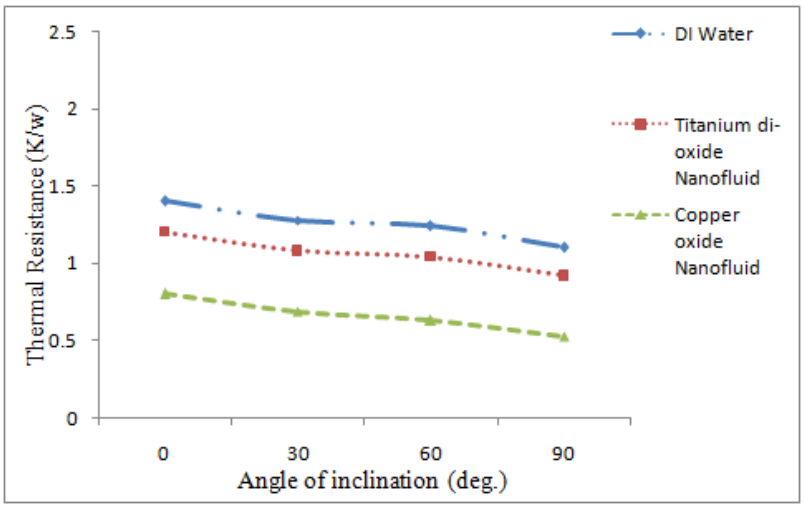

Figure 4.39 Comparison of thermal resistance for DI Water, TiO_2 nanofluid and CuO nanofluid for 100% filling ratio and 60W heat input

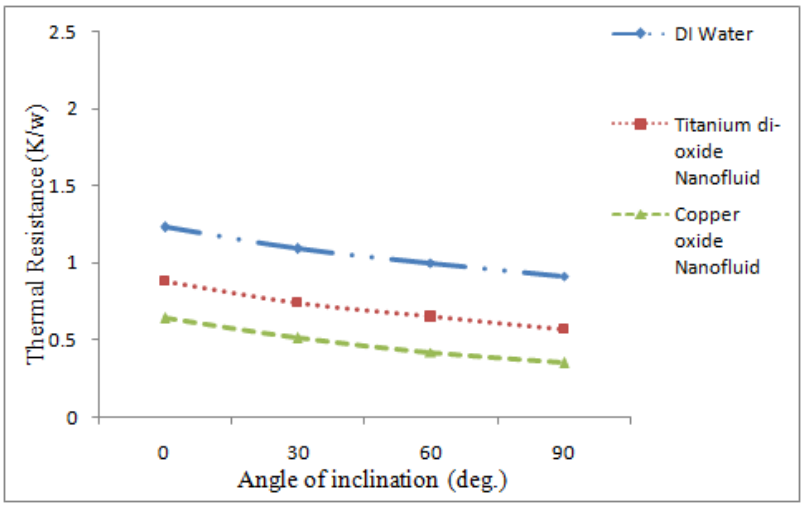

Figure 4.40 Comparison of thermal resistance for DI Water, TiO_2 nanofluid and CuO nanofluid for 100% filling ratio and 70W heat input

Figures 4.25 to 4.40 shows that when the angle of inclination increases from 0^0 to 90^0 the thermal resistance decreases for all the three working fluids. At 0^0 degree angle of inclination the heat pipe using DI Water shows higher thermal resistance when compared to heat pipe using TiO_2 nanofluid and CuO nanofluid also the heat pipe using TiO_2 nanofluid shows higher thermal resistance when compared to heat pipe using CuO nanofluid. Similar results are obtained at an inclination angle of 30^0,60^0 and 90^0 for all the working fluids.

At 25% filling ratio the heat pipe using DI Water shows higher thermal resistance when compared to heat pipe using TiO_2 nanofluid and CuO nanofluid and the heat pipe using CuO nanofluid shows lesser thermal resistance when compared to the heat pipe using TiO_2 nanofluid.Also at filling ratio of 50%,75% and 100% similar results are obtained. At 40W heat input the heat pipe using DI Water shows higher thermal resistance when compared to heat pipe using TiO_2 nanofluid and CuO nanofluid and similar results are obtained for when the heat pipes operated at 50 W, 60 W and 70 W heat input.

An optimum thermal resistance value is obtained when the heat pipe is operated at 90^0 angle of inclination, 75% filling ratio and 70 W heat input for all the working fluids. Hence a comparison is made at the above mentioned operating parameters. Since the thermal conductivity of CuO nanofluid is found to higher than TiO_2

nanofluid and DI Water, the heat pipe using CuO nanofluid shows lower thermal resistance when compared to heat pipe using TiO_2 nanofluid and DI Water, the decrease in percentage was about 37.2% and 62% respectively.

4.4.2 Effect of angle of inclination, filling ratio, and heat input on overall heat transfer coefficient

An overall heat transfer coefficient comparison of heat pipe using DI Water, TiO_2 nanofluid and CuO nanofluid is carried out. From the experimental results the overall heat transfer coefficient value of heat pipe using the above three working fluids is calculated by the equation 3.4 and the results are tabulated and shown in tables from 4.29 to 4.32.

Table 4.29 Overall heat transfer coefficient for DI Water, TiO_2 nanofluid and CuO nanofluid for 25% filling ratio

Heat input (W)	Working Fluids	Overall heat transfer coefficient (W/m^2K)			
		Angle of inclination (deg.)			
		0	**30**	**60**	**90**
40	DI Water	1482.3	1603.2	1745.9	1831.0
	TiO_2 nanofluid	1695.3	1832.2	2042.8	2191.9
	CuO nanofluid	2185.0	2398.3	2755.0	3033.3
50	DI Water	1705.0	1843.6	1925.0	2002.0
	TiO_2 nanofluid	1915.0	2153.2	2257.8	2421.7
	CuO nanofluid	2478.8	2860.0	3064.4	3374.2
60	DI Water	1820.8	1950.0	2071.0	2224.4
	TiO_2 nanofluid	2201.3	2402.0	2566.6	2780.5
	CuO nanofluid	3161.0	3491.8	3850.0	4352.0
70	DI Water	2217.9	2502.5	2633.7	2756.8
	TiO_2 nanofluid	2920.6	3412.5	3801.3	4113.7
	CuO nanofluid	4040.8	5177.5	6128.5	7150.0

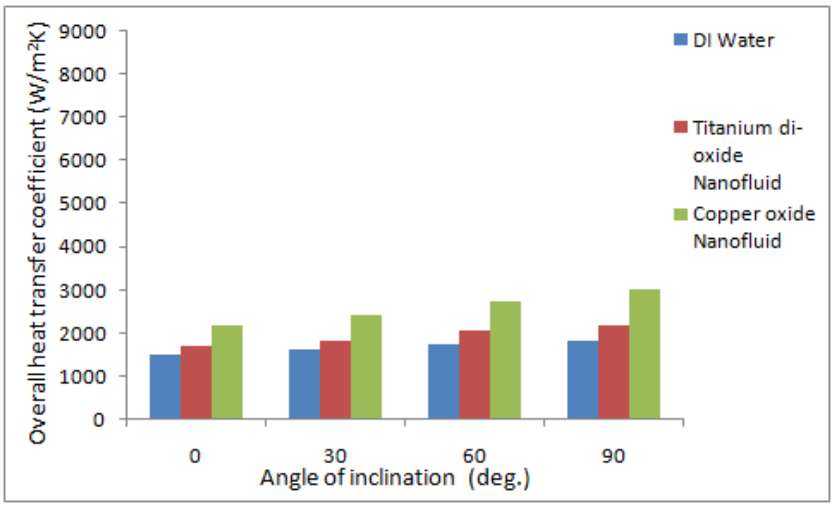

Figure 4.41 Comparison of overall heat transfer coefficient for DI Water, TiO_2 nanofluid and CuO nanofluid for 25% filling ratio and 40W heat input

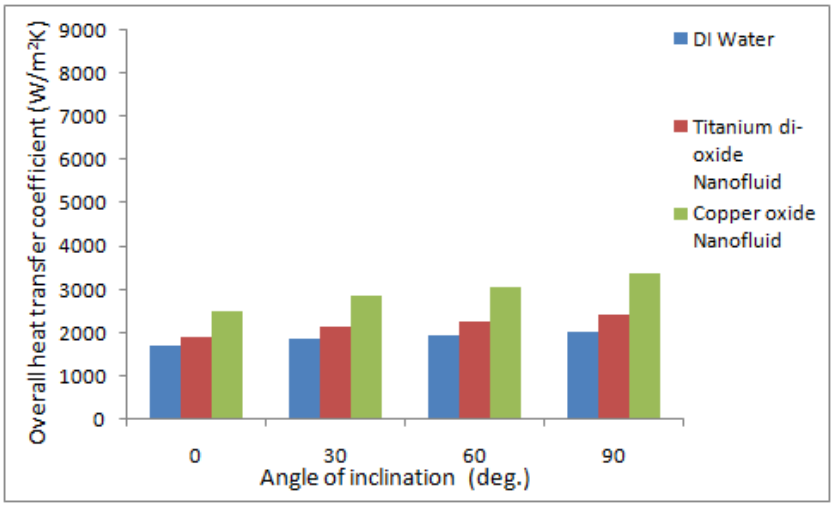

Figure 4.42 Comparison of overall heat transfer coefficient for DI Water, TiO_2 nanofluid and CuO nanofluid for 25% filling ratio and 50W heat input

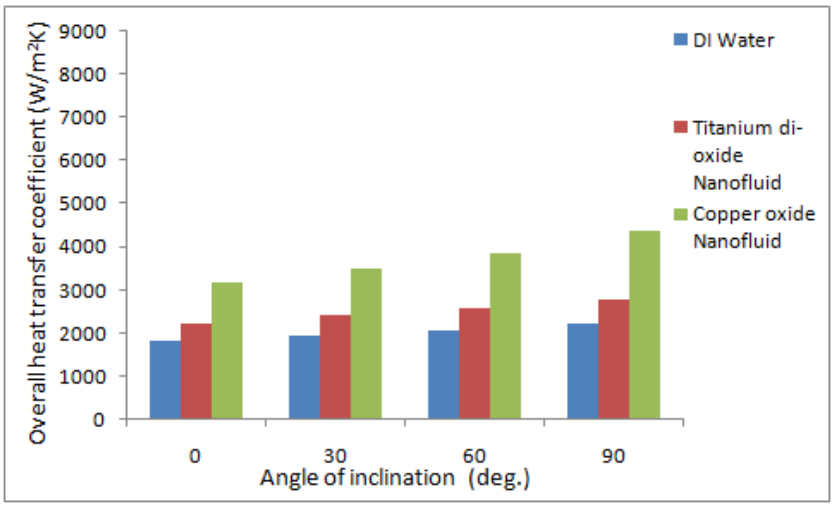

Figure 4.43 Comparison of overall heat transfer coefficient for DI Water, TiO_2 nanofluid and CuO nanofluid for 25% filling ratio and 60W heat input

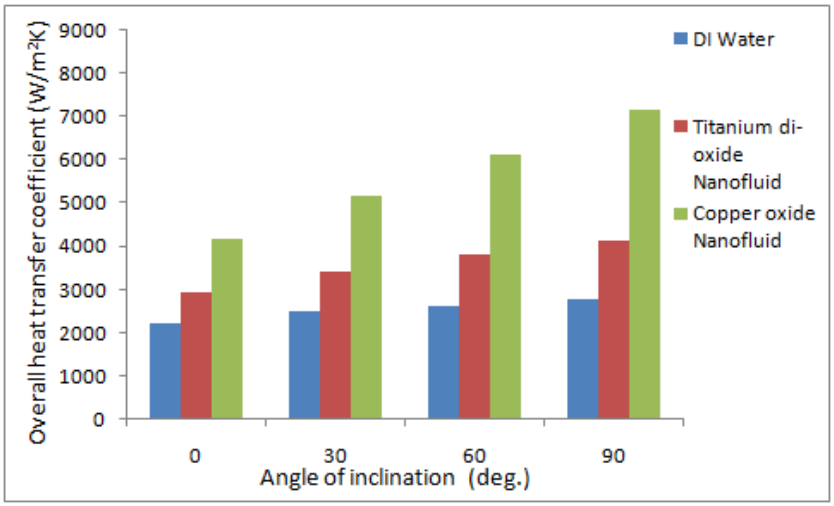

Figure 4.44 Comparison of overall heat transfer coefficient for DI Water, TiO_2 nanofluid and CuO nanofluid for 25% filling ratio and 70W heat input

Table 4.30 Overall heat transfer coefficient for DI Water, TiO_2 nanofluid and CuO nanofluid for 50% filling ratio

Heat input (W)	Working Fluids	Overall heat transfer coefficient (W/m^2K)			
		Angle of inclination (deg.)			
		0	**30**	**60**	**90**
40	DI Water	1659.1	1776.9	1876.8	1937.4
	TiO_2 nanofluid	1937.4	2129.7	2275.0	2346.0
	CuO nanofluid	2441.4	2755.0	3003.0	3229.0
50	DI Water	1787.7	1950.0	2056.8	2107.0
	TiO_2 nanofluid	2176.0	2346.0	2499.8	2681.2
	CuO nanofluid	2833.0	3128.1	3451.7	3753.7
60	DI Water	2015.4	2191.9	2292.3	2461.4
	TiO_2 nanofluid	2310.0	2566.6	2705.4	2944.7
	CuO nanofluid	3374.2	3900.0	4229.5	4766.6
70	DI Water	2364.5	2657.5	2887.5	3041.0
	TiO_2 nanofluid	3194.6	3753.7	4170.8	4620.0
	CuO nanofluid	4416.2	5561.1	6673.3	7902.6

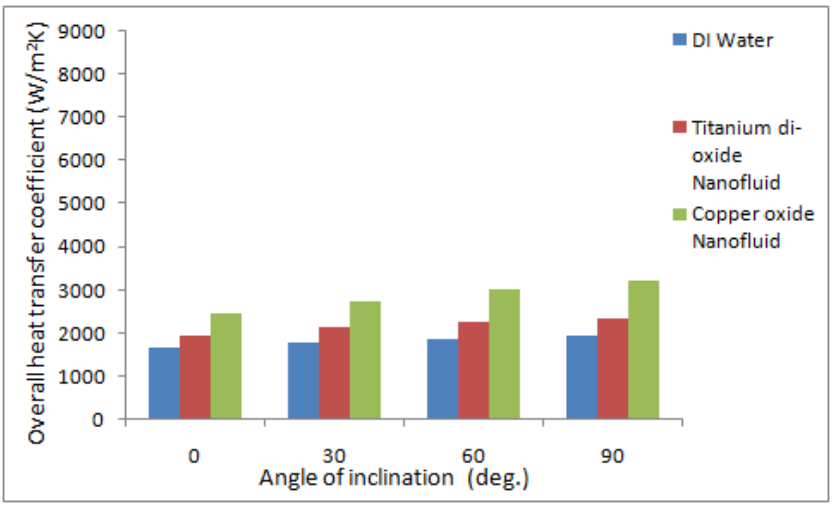

Figure 4.45 Comparison of overall heat transfer coefficient for DI Water, TiO_2 nanofluid and CuO nanofluid for 50% filling ratio and 40W heat input

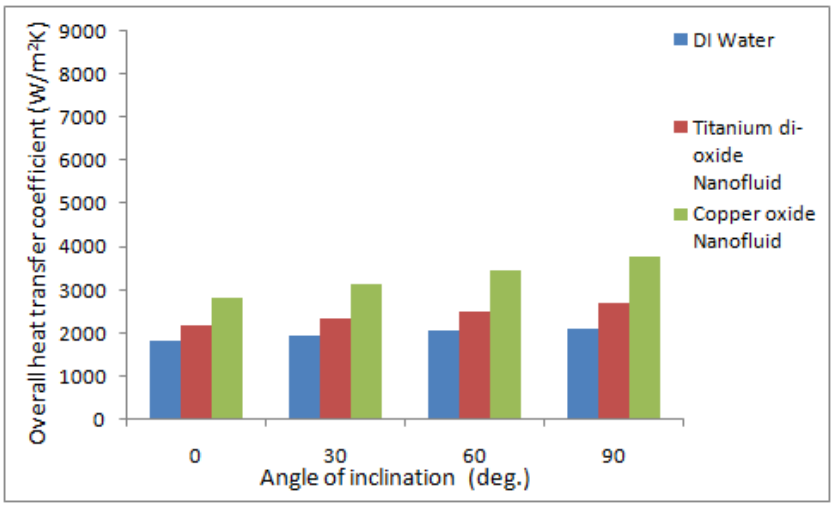

Figure 4.46 Comparison of overall heat transfer coefficient for DI Water, TiO_2 nanofluid and CuO nanofluid for 50% filling ratio and 50W heat input

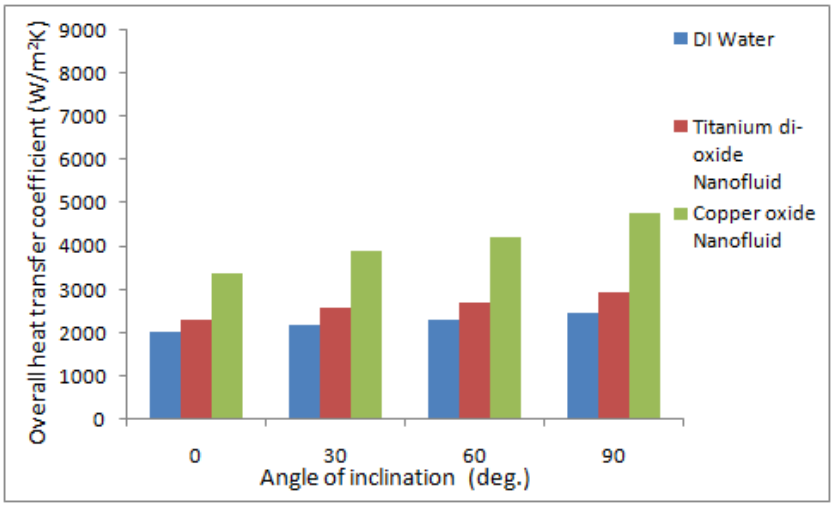

Figure 4.47 Comparison of overall heat transfer coefficient for DI Water, TiO_2 nanofluid and CuO nanofluid for 50% filling ratio and 60W heat input

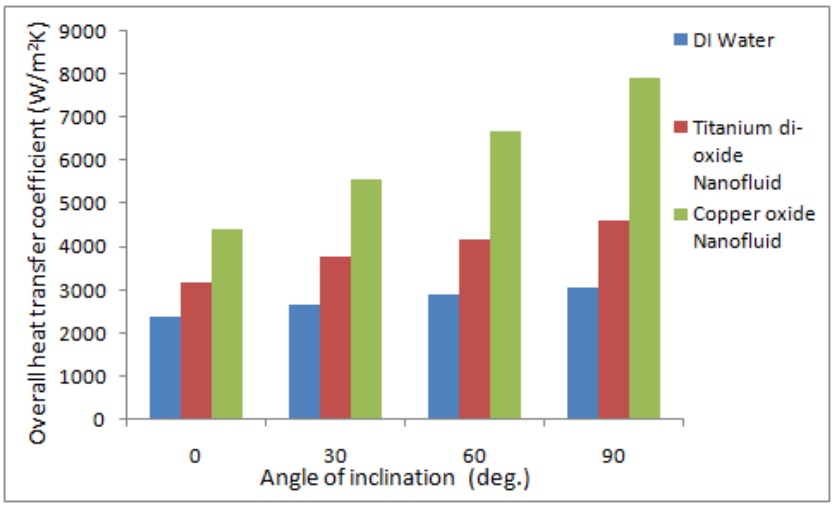

Figure 4.48 Comparison of overall heat transfer coefficient for DI Water, TiO_2 nanofluid and CuO nanofluid for 50% filling ratio and 70W heat input

Table 4.31 Overall heat transfer coefficient for DI Water, TiO_2 nanofluid and CuO nanofluid for 75% filling ratio

Heat input (W)	Working Fluids	Overall heat transfer coefficient (W/m^2K)			
		Angle of inclination (deg.)			
		0	**30**	**60**	**90**
40	DI Water	1900.6	2029.0	2122.1	2269.1
	TiO_2 nanofluid	2208.0	2364.5	2521.2	2731.3
	CuO nanofluid	2860.0	3128.1	3430.0	3830.9
50	DI Water	2160.4	2234.7	2398.2	2587.5
	TiO_2 nanofluid	2523.5	2610.4	2809.3	3105.1
	CuO nanofluid	3491.8	3641.7	4040.8	4609.1
60	DI Water	2310.0	2478.8	2565.0	2863.9
	TiO_2 nanofluid	2887.5	3041.0	3277.6	3781.8
	CuO nanofluid	4170.8	4609.1	5085.9	6412.7
70	DI Water	2587.5	2920.6	3171.8	3430.0
	TiO_2 nanofluid	3597.3	4338.0	4835.8	5462.6
	CuO nanofluid	4999.7	6145.5	7563.7	8938.9

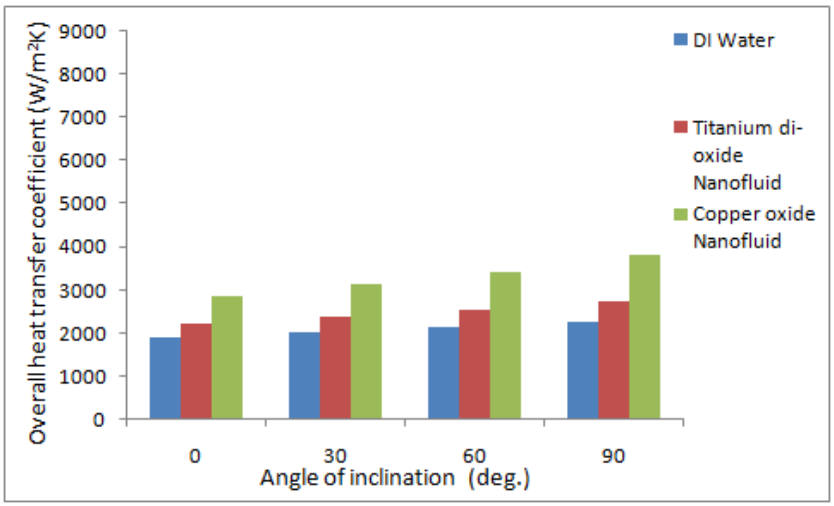

Figure 4.49 Comparison of overall heat transfer coefficient for DI Water, TiO_2 nanofluid and CuO nanofluid for 75% filling ratio and 40W heat input

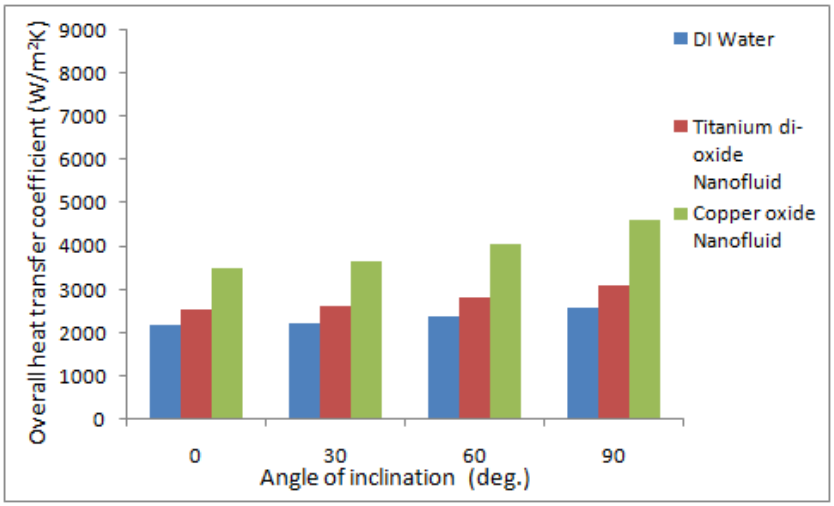

Figure 4.50 Comparison of overall heat transfer coefficient for DI Water, TiO_2 nanofluid and CuO nanofluid for 75% filling ratio and 50W heat input

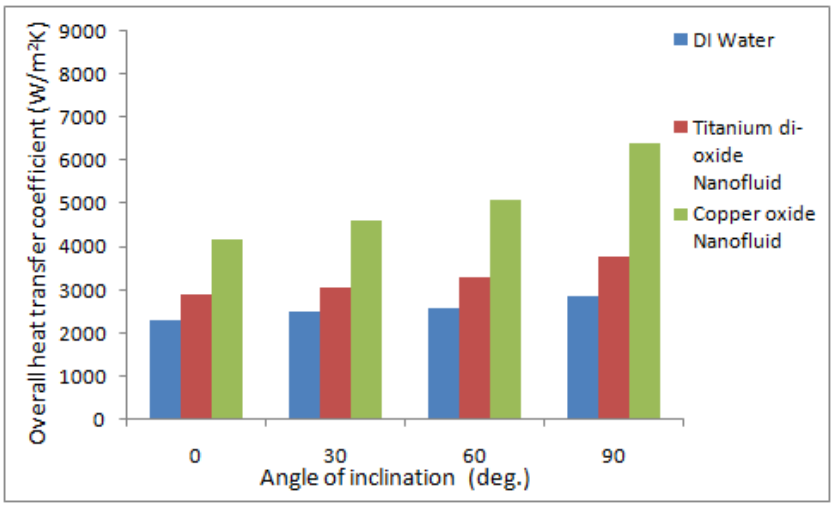

Figure 4.51 Comparison of overall heat transfer coefficient for DI Water, TiO_2 nanofluid and CuO nanofluid for 75% filling ratio and 60W heat input

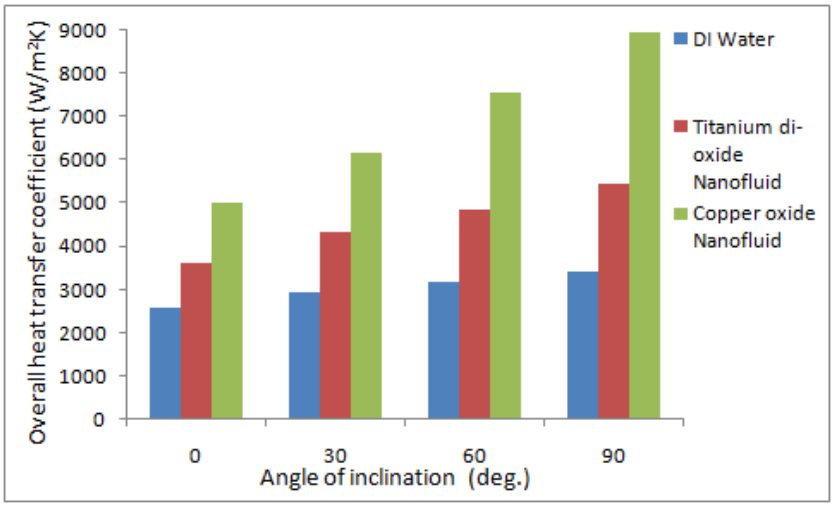

Figure 4.52 Comparison of overall heat transfer coefficient for DI Water, TiO_2 nanofluid and CuO nanofluid for 75% filling ratio and 70W heat input

Table 4.32 Overall heat transfer coefficient for DI Water, TiO_2 nanofluid and CuO nanofluid for 100% filling ratio

Heat input (W)	Working Fluids	Overall heat transfer coefficient (W/m^2K)			
		Angle of inclination (deg.)			
		0	**30**	**60**	**90**
40	DI Water	1735.2	1855.2	1979.7	2048.5
	TiO_2 nanofluid	2048.5	2217.9	2398.2	2499.8
	CuO nanofluid	2657.5	2920.6	3241.5	3430.0
50	DI Water	1953.5	2077.3	2137.5	2304.5
	TiO_2 nanofluid	2341.0	2521.2	2633.7	2836.3
	CuO nanofluid	3041.0	3390.6	3641.7	3986.2
60	DI Water	2107.0	2304.5	2378.9	2681.6
	TiO_2 nanofluid	2458.2	2731.3	2836.3	3206.3
	CuO nanofluid	3687.3	4275.2	4682.3	5565.7
70	DI Water	2398.2	2706.2	2949.8	3241.0
	TiO_2 nanofluid	3352.1	3986.2	4538.2	5175.0
	CuO nanofluid	4609.2	5784.0	7023.4	8428.2

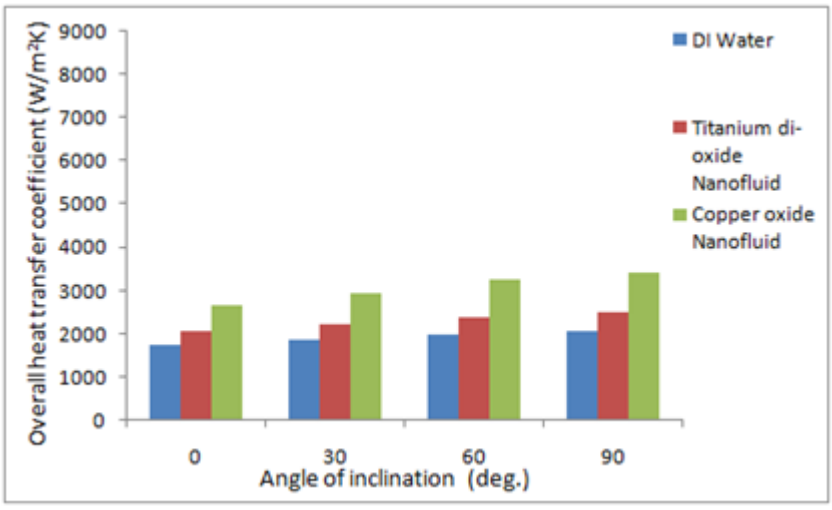

Figure 4.53 Comparison of overall heat transfer coefficient for DI Water, TiO_2 nanofluid and CuO nanofluid for 100% filling ratio and 40W heat input

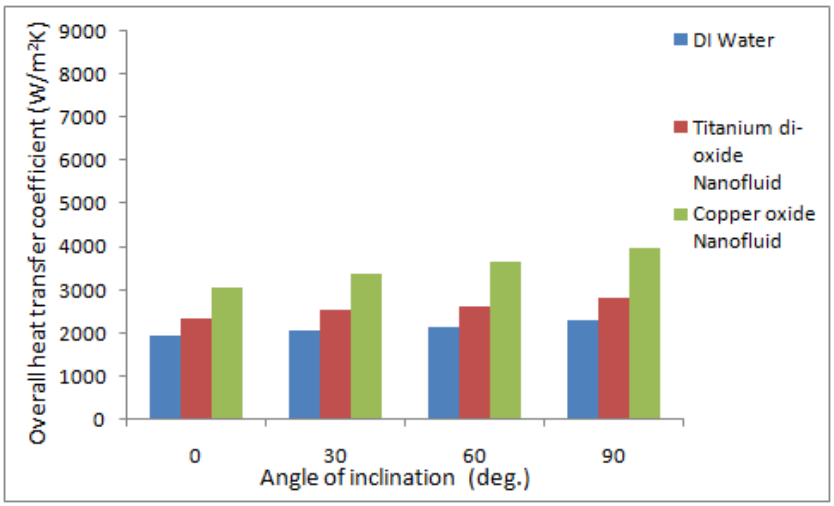

Figure 4.54 Comparison of overall heat transfer coefficient for DI Water, TiO_2 nanofluid and CuO nanofluid for 100% filling ratio and 50W heat input

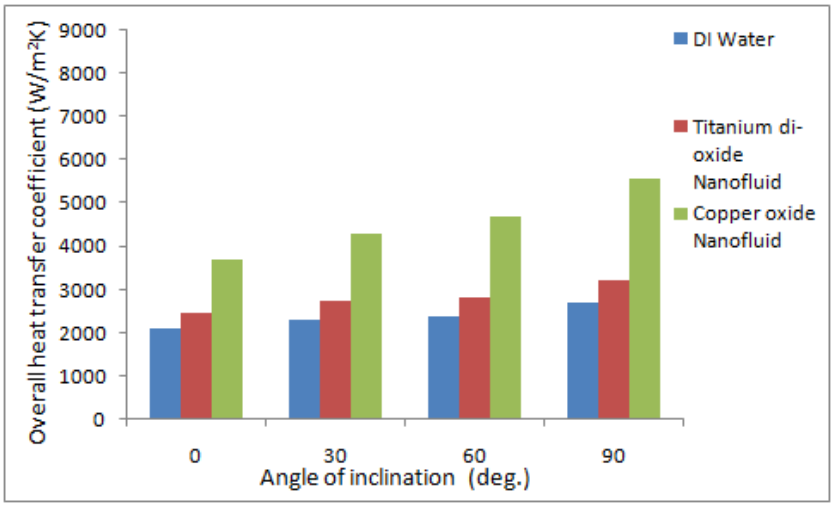

Figure 4.55 Comparison of overall heat transfer coefficient for DI Water, TiO_2 nanofluid and CuO nanofluid for 100% filling ratio and 60W heat input

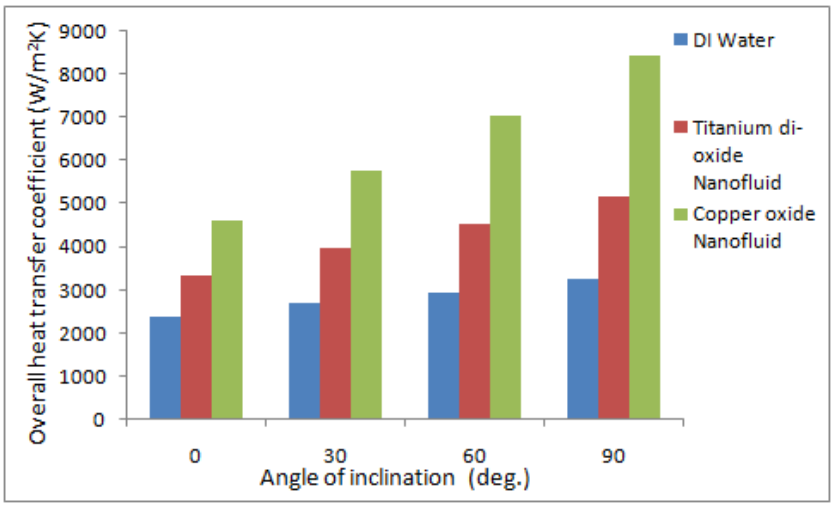

Figure 4.56 Comparison of overall heat transfer coefficient for DI Water, TiO_2 nanofluid and CuO nanofluid for 100% filling ratio and 70W heat input

Figures 4.41 to 4.56 show that when the angle of inclination increases from 0^0 to 90^0 the overall heat transfer coefficient increases for all the three working fluids. At 0^0 degree angle of inclination the heat pipe using DI Water shows lower overall heat transfer coefficient when compared to heat pipe using TiO_2 nanofluid and CuO nanofluid. The heat pipe using TiO_2 nanofluid shows lower overall heat transfer coefficient when compared to heat pipe using CuO nanofluid. Similar results are obtained at an inclination angle of 30^0,60^0 and 90^0 for all the working fluids.

At 25% filling ratio the heat pipe using DI Water shows lower overall heat transfer coefficient when compared to heat pipe using TiO_2 nanofluid and CuO nanofluid and the heat pipe using CuO nanofluid shows higher overall heat transfer coefficient when compared to the heat pipe using TiO_2 nanofluid. Also at filling ratio of 50%, 75% and 100% similar results are obtained. At 40 W heat input the heat pipe using DI Water shows lower overall heat transfer coefficient when compared to heat pipe using TiO_2 nanofluid and CuO nanofluid and similar results are obtained for the heat pipes operated at 50 W, 60 W and 70 W heat input.

An optimum overall heat transfer coefficient value is obtained when the heat pipe is operated at 90^0 angle of inclination, 75% filling ratio and 70 W heat input for all the working fluids. Hence a comparison is made from the above mentioned operating

parameters. Since the thermal conductivity and heat capacity of CuO nanofluid is found to higher than TiO_2 nanofluid and DI Water, the heat pipe using CuO nanofluid shows higher overall heat transfer coefficient when compared to heat pipe using TiO_2 nanofluid and DI Water and the increase in percentage is about 63.6% and 160.6% respectively.

4.5 Reasons for heat transfer enhancement

In general the thermal performance of heat pipes increases with increase in operating temperature. The reason is due to the changes in thermo physical properties of the working fluid with the operating temperature.The decrease in thermal resistance for CuO nanofluid and TiO_2 nanofluid heat pipe is due to the following reasons. The first is the presence of nanoparticles in the DI Water increases the thermal conductivity of the base fluid (DI Water).The nanoparticle can absorb liquid molecules and cause the formation of molecular nanolayer on the surface of the nanoparticles (Yu et. al. 2007 and Keblinski 2002).The second reason is that presence of nanoparticle in the DI Water decreases the solid liquid contact angle and thus makes the liquid extend in the mesh and hence the capillary force is increased in the heat pipe.

Third a change in the heating surface characteristics occurs due to the formation of thin porous layer on the surface of the heat pipe which increases the solid-liquid wettability and the capillary force. The fourth reason is due to the large number of smaller nucleation sites created at the evaporator section of the heat pipe which produces smaller bubbles and increase the heat transfer between the evaporator walls to working fluid (Collier and Thome 1996).The overall heat transfer coefficient of heat pipe operated with CuO nanofluid and TiO_2 nanofluid is found to be higher than the heat pipe operated with DI Water. The reason for higher heat transfer coefficient is due to the following reasons. The first reason is the heat transfer occurs at evaporator section takes place due to nucleate boiling which is the result of bubble formation at the nucleation sites. Second condensation is favored by smoother surface with high contact angle (Brusly Solomon et al. 2012).

From the experimental results it is clear that the parameters at the lower level such as 40W heat input, 0^0angle of inclination and 25% filling ratio shows higher thermal resistance and lower overall heat transfer coefficient where as the effectiveness of the heat pipe is measured by lower thermal resistance and higher overall heat transfer coefficient, hence the above mentioned parameter levels are considered as ineffective.

4.6 Statistical analysis of heat transfer characteristics of heat pipe

Statistical analysis and modeling of the response thermal resistance and overall heat transfer coefficient has been carried out with the help of Box-Behnken design for all the three working fluids. The parameters and levels chosen for analysis and modeling is shown in Table 4.33. The advantage of using Box-Behnken design is that it requires less number of runs for three factors and for four or more factors this advantage disappears (Box 1987).

Table 4.33 Experimental parameter and their levels for statistical analysis

S.No	Parameters	Symbols	Level 1	Level 2	Level 3
1.	Heat input (W)	A	50	60	70
2.	Angle of inclination (deg.)	B	30	60	90
3.	Filling ratio (%)	C	50	75	100

According to Box-Behnken design the experiments are conducted for all the working fluids (DI Water, CuO nanofluid and TiO_2 nanofluid) and the results are tabulated in the Tables from 4.34 to 4.36.

Table 4.34 Experimental design matrix and results for heat pipe using DI Water

Run Order	**A Heat input (W)**	**B Angle of inclination (deg.)**	**C Filling Ratio (%)**	**R Thermal resistance (K/W)**	**U Overall heat transfer coefficient (W/m^2K)**
1	50	30	75	1.32	2234.7
2	70	30	75	1.01	2920.6
3	50	90	75	1.14	2587.5
4	70	90	75	0.86	3430.0
5	50	60	50	1.46	2056.8
6	70	60	50	1.04	2887.5
7	50	60	100	1.38	2137.5
8	70	60	100	1.00	2949.8
9	60	30	50	1.37	2191.9
10	60	90	50	1.22	2461.4
11	60	30	100	1.28	2304.5
12	60	90	100	1.10	2681.6
13	60	60	75	1.15	2565.0
14	60	60	75	1.12	2633.0
15	60	60	75	1.15	2565.0

Table 4.35 Experimental design matrix and results for heat pipe using TiO_2 nanofluid

Run Order	A Heat input (W)	B Angle of inclination (deg.)	C Filling Ratio (%)	R Thermal resistance (K/W)	U Overall heat transfer coefficient (W/m^2K)
1	50	30	75	1.13	2610.4
2	70	30	75	0.68	4338.0
3	50	90	75	0.95	3105.1
4	70	90	75	0.54	5462.6
5	50	60	50	1.18	2499.8
6	70	60	50	0.72	4170.8
7	50	60	100	1.12	2633.7
8	70	60	100	0.65	4538.2
9	60	30	50	1.17	2566.6
10	60	90	50	1.02	2944.7
11	60	30	100	1.08	2731.3
12	60	90	100	0.92	3266.3
13	60	60	75	0.90	3277.6
14	60	60	75	0.89	3314.4
15	60	60	75	0.88	3352.1

Table 4.36 Experimental design matrix and results for heat pipe using CuO nanofluid

Run Order	A Heat input (W)	B Angle of inclination (deg.)	C Filling Ratio (%)	R Thermal resistance (K/W)	U Overall heat transfer coefficient (W/m^2K)
1	50	30	75	0.81	3641.7
2	70	30	75	0.48	6145.5
3	50	90	75	0.64	4609.1
4	70	90	75	0.33	8938.9
5	50	60	50	0.87	3451.7
6	70	60	50	0.45	6673.3
7	50	60	100	0.81	3641.7
8	70	60	100	0.42	7023.4
9	60	30	50	0.77	3900.0
10	60	90	50	0.63	4766.6
11	60	30	100	0.69	4275.2
12	60	90	100	0.53	5565.7
13	60	60	75	0.58	5085.9
14	60	60	75	0.56	5267.5
15	60	60	75	0.59	4999.7

4.7 Modeling of heat transfer characteristics of heat pipe

Modeling of heat transfer characteristics of heat pipe is carried out with the help of response surface methodology. Response surface methodology is a collection of mathematical and statistical technique used for analyzing problems in which several independent variables influence a dependent variable as indicated by Cochran and Cox (1962).In the present work RSM has been applied for developing a mathematical model in the form of multiple regression equation for the quality characteristics of thermal resistance and overall heat transfer coefficient.

The second order polynomial (regression) equation used to represent the response surface Y is shown in equation 4.1 by Balasubramanian et. al. (2008).

$$Y = b_0 + \Sigma b_i x_i + \Sigma b_{ii} x_i^2 + \Sigma b_{ij} x_i x_j + e_r \quad \text{Eq.4.1}$$

Where Y is the response, b_0 is the constant coefficient, b_is are the linear coefficients, b_{ii} s are the quadratic coefficients, b_{ij} s are the interaction coefficients, x_i and x_j are the coded values of the independent variables.

To estimate the regression coefficients of thermal resistance and overall heat transfer coefficients, Box-Behnken design techniques was used for all the three working fluids such as DI Water, TiO_2 nanofluid and CuO nanofluid. All the coefficients for thermal resistance and overall heat transfer coefficient were obtained by using the Minitab 16 statistical software.

4.7.1 Development of mathematical modeling for thermal resistance and overall heat transfer coefficient for the heat pipe using DI Water

Table 4.34 shows the experimental design matrix and their results for DI Water heat pipe. The mathematical model to estimate thermal resistance for the DI Water heat pipe is given in equation 4.2 and for overall heat transfer coefficient is given in equation 4.3.An analysis of variance (ANOVA) procedure was used to analyze the model for significance, test for lack of fit and suitability. A statistical summary for thermal resistance and for overall heat transfer coefficient is given in Table 4.37 and Table 4.38 respectively.

Thermal resistance for heat pipe using DI Water

$$R = 1.15-0.185A-0.08375B-0.04125C-0.03375A^2-0.01125B^2-0.10375C^2+0.05AB+0.01AC-0.0075BC. \quad \text{Eq.4.2}$$

Overall heat transfer coefficient for heat pipe using DI Water

$$U = 2574.43+399.138A+180.813B+59.4750C+176.946A^2+78.8958B^2-243.479C^2+97.2250AB-4.6AC+26.9BC. \quad \text{Eq.4.3}$$

Table 4.37 Analysis of variance for response thermal resistance for heat pipe using DI Water

Source of variation	DF	Sum of Squares	Mean Sum of Squares	F-value	P-value
Regression	9	0.401348	0.044594	73.71	0.000
Linear	3	0.343525	0.114508	189.27	0.000
Square	3	0.047198	0.015733	26.00	0.002
Interaction	3	0.010625	0.003542	5.85	0.043
Residual Error	5	0.003025	0.000605		
Lack-of-Fit	3	0.002825	0.000942	9.42	0.098
Pure Error	2	0.000200	0.000100		
Total	14	0.404373			
R- Squared = 99.25%		R- Squared (adj)= 97.91%			

Table 4.38 Analysis of variance for response overall heat transfer coefficient for the heat pipe using DI Water

Source of variation	DF	Sum of Squares	Mean Sum of Squares	F-value	P-value
Regression	9	1992345	221372	120.33	0.000
Linear	3	1564329	521443	283.45	0.000
Square	3	387225	129075	70.16	0.001
Interaction	3	40790	13597	7.39	0.028
Residual Error	5	9198	1840		
Lack-of-Fit	3	8519	2840	8.37	0.109
Pure Error	2	679	339		
Total	14	2001543			
R-Squared = 99.54%		R-Squared (adj) = 98.71%			

4.7.1.1 Checking the adequacy of the model for thermal resistance for the heat pipe using DI Water

The determination coefficient R^2 indicates the goodness of fit for the model. For the heat pipe using DI Water as working fluid, the value of R^2 = 0.9925 from Table 4.37 and for equation 4.2 indicates relatively high degree of accuracy between the observed and predicted values. The value of determination coefficient R^2 (adj) = 0.9791 is also high, which indicates a high significance of the model. The value of probability from the Table 4.37 for the model is less than 0.05, which indicates that the model is significant. The model also showed that lack of fit F value of 9.42 implies the lack of fit is not significant relative to the pure error even at 0.05 levels. Normal probability of residuals for thermal resistance of DI Water heat pipe is shown in Figure 4.57 reveals that the residuals are falling on the straight line which means the errors are distributed normally. All the above consideration indicates an excellent adequacy of the regression model.

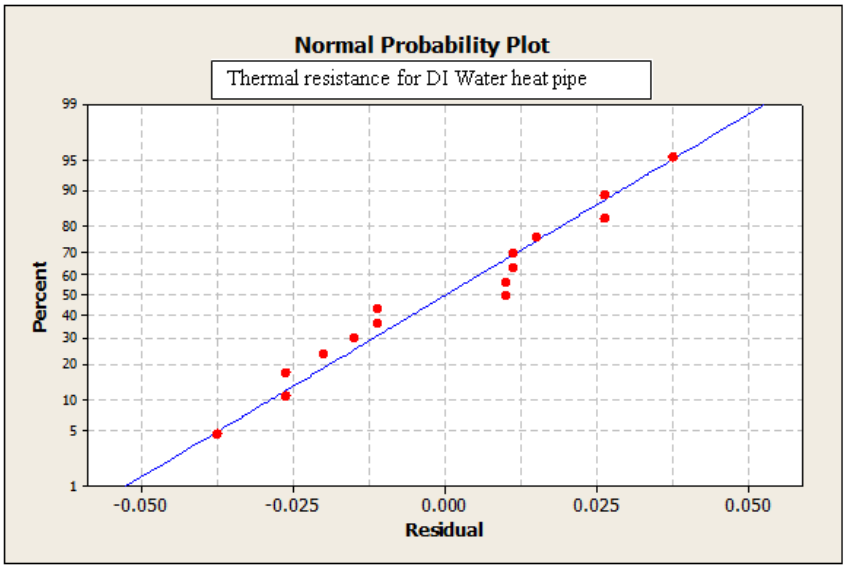

Figure 4.57 Normal probability of residuals for thermal resistance of DI Water heat pipe

4.7.1.2 Checking the adequacy of the model for overall heat transfer coefficient for the heat pipe using DI Water

The goodness of fit of a model is evaluated by determination coefficient R^2. From Table 4.38 the value of R^2 = 0.9954 for equation 4.3 indicates relatively high degree of accuracy between the observed and predicted values for the DI Water working fluid heat pipe. The value of determination coefficient R^2 (adj) = 0. 9871 is also high, which indicates a high significance of the model. The probability value for the model from the Table 4.38 is less than 0.05, which indicates that the model is significant. The model also showed that lack of fit F value of 8.37 implies the lack of fit is not significant relative to the pure error even at 0.05 levels. Figure 4.58 shows the normal probability of residuals for overall heat transfer coefficient of DI Water heat pipe and shows that the residuals are falling on the straight line which means the errors are distributed normally and all the above consideration indicates an excellent adequacy of the regression model.

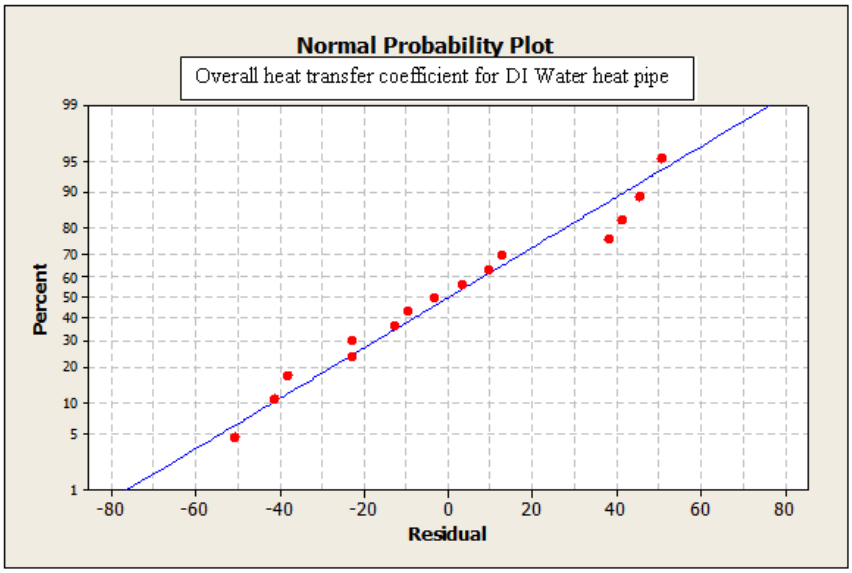

Figure 4.58 Normal probability of residuals for overall heat transfer coefficient of DI Water heat pipe

4.7.2 Development of mathematical modeling for thermal resistance and overall heat transfer coefficient for heat pipe using TiO_2 nanofluid

Table 4.35 shows the experimental design matrix and their results for heat pipe using TiO_2 nanofluid. The mathematical model to estimate thermal resistance for the heat pipe using TiO_2 nanofluid is given in equation 4.4 and for overall heat transfer coefficient is given in equation 4.5. An analysis of variance (ANOVA) procedure is used to analyze the model for significance, test for lack of fit and suitability. A statistical summary for thermal resistance is given in Table 4.39 and for overall heat transfer coefficient in Table 4.40.

Thermal resistance for the heat pipe using TiO_2 nanofluid

$$R = 0.893333-0.22625A-0.08125B-0.04C-0.0966667A^2+0.0333333B^2-0.120833C^2+0.015AB-0.0025AC-0.0025BC. \quad \text{Eq.4.4}$$

Overall heat transfer coefficient for the heat pipe using TiO_2 nanofluid

$$U = 2548.33+393.925A+186.1B+59.4750C+173.958A^2+75.908B^2-214.392C^2+44.15AB-4.6AC+26.9BC. \quad \text{Eq.4.5}$$

Table 4.39 Analysis of variance for the response thermal resistance for the heat pipe using TiO_2 nanofluid

Source of variation	DF	Sum of Squares	Mean Sum of Squares	F-value	P-value
Regression	9	0.575418	0.063935	339.48	0.000
Linear	3	0.475125	0.158375	840.93	0.000
Square	3	0.099343	0.033114	175.83	0.000
Interaction	3	0.000950	0.000317	1.68	0.039
Residual Error	5	0.000942	0.000188		
Lack-of-Fit	3	0.000875	0.000292	8.75	0.104
Pure Error	2	0.000067	0.000033		
Total	14	0.576360			
R- Squared = 99.35%		R- Squared (adj)= 98.17%			

Table 4.40 Analysis of variance for the response overall heat transfer coefficient for the heat pipe using TiO_2 nanofluid

Source of variation	DF	Sum of Squares	Mean Sum of Squares	F-value	P-value
Regression	9	10420895	1157877	53.49	0.000
Linear	3	8156432	2718811	125.6	0.000
Square	3	2142860	714287	33.00	0.001
Interaction	3	121603	40534	1.87	0.025
Residual Error	5	108230	21646		
Lack-of-Fit	3	100238	33413	8.36	0.109
Pure Error	2	7993	3996		
Total	14	10529125			
R-Squared = 98.98%		R-Squared (adj) = 97.14%			

4.7.2.1 Checking the adequacy of the model for thermal resistance for the heat pipe using TiO_2 nanofluid

The determination coefficient R^2 indicates the goodness of fit for the model. For the heat pipe using TiO_2 nanofluid, the value of R^2 = 0.9935 from Table 4.39 for equation 4.4 indicates relatively high degree of accuracy between the observed and predicted values. The value of determination coefficient R^2 (adj) = 0. 9817 is also high, which indicates higher significance of the model. The value of probability from the Table 4.39 for the model is less than 0.05, which indicates that the model is significant. The model also showed that lack of fit F value of 8.75 implies the lack of fit is not significant, relative to the pure error even at 0.05 levels. Normal probability of residuals for thermal resistance of TiO_2 nanofluid heat pipe is shown in Figure 4.59 reveals that the residuals are falling on the straight line which means the errors are distributed normally. All the above consideration indicates an excellent adequacy of the regression model.

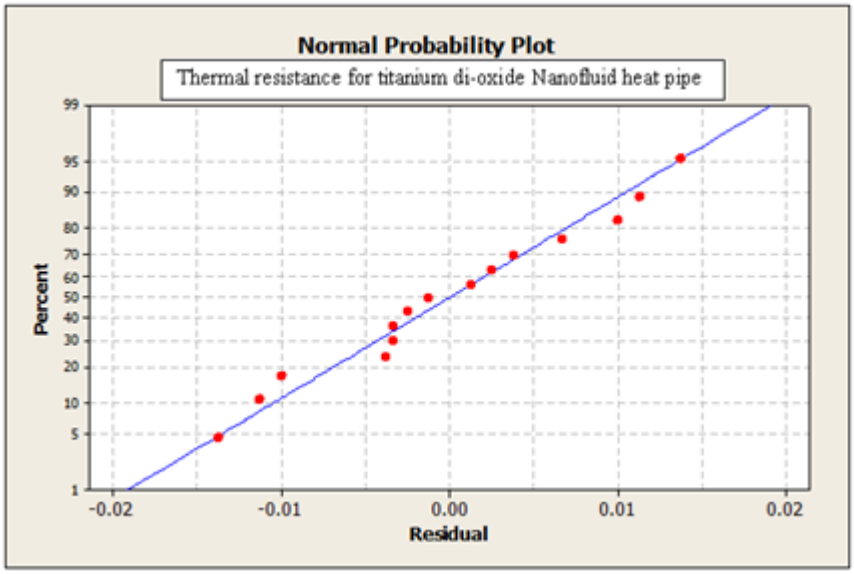

Figure 4.59 Normal probability of residuals for thermal resistance of TiO_2 nanofluid heat pipe

4.7.2.2 Checking the adequacy of the model for overall heat transfer coefficient for the heat pipes using TiO_2 nanofluid

The goodness of fit of a model is evaluated by determination coefficient R^2. From Table 4.40 the value of R^2 = 0.9898 for equation 4.5 indicates relatively high degree of accuracy between the observed and predicted values for the heat pipe using TiO_2 nanofluid. The value of determination coefficient R^2 (adj) = 0. 9714 is also high, which indicates a high significance of the model. The probability value for the model from the Table 4.40 is less than 0.05, which indicates that the model is significant. The model also showed that lack of fit F value of 8.36 implies the lack of fit is not significant relative to the pure error even at 0.05 levels. Figure 4.60 shows the normal probability of residuals for overall heat transfer coefficient of TiO_2 nanofluid heat pipe and shows that the residuals are falling on the straight line which means the errors are distributed normally and all the above consideration indicates an excellent adequacy of the regression model.

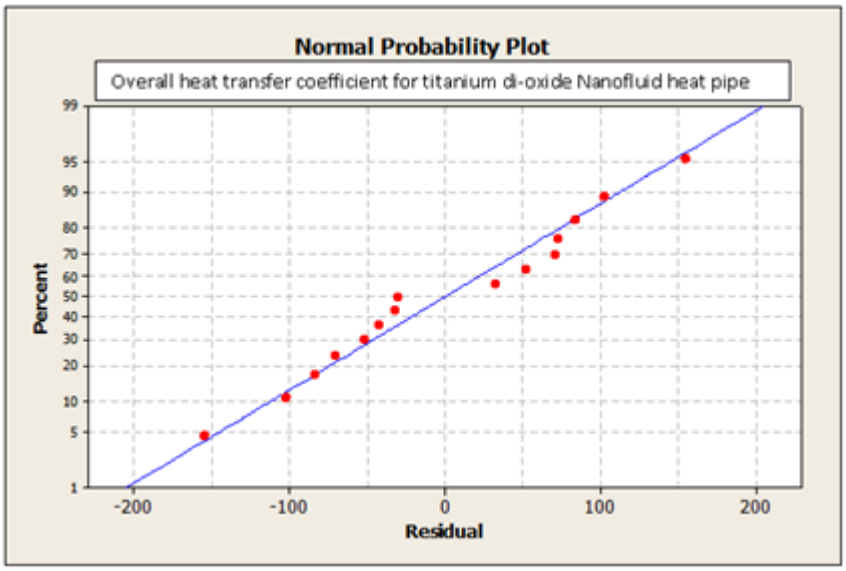

Figure 4.60 Normal probability of residuals for overall heat transfer coefficient of TiO_2 nanofluid heat pipe

4.7.3 Development of mathematical modeling for thermal resistance and overall heat transfer coefficient for heat pipe using CuO nanofluid

Table 4.36 shows the experimental design matrix and their results for heat pipe using CuO nanofluid. A mathematical model to estimate thermal resistance for heat pipe using CuO nanofluid is given in equation 4.6 and for overall heat transfer coefficient is given in equation 4.7.An analysis of variance (ANOVA) procedure is used to analyze the model for significance and suitability. A statistical summary for thermal resistance is given in Table 4.41 and for overall heat transfer coefficient in Table 4.42.

Thermal resistance for heat pipe using CuO nanofluid

$$R = 0.576667-0.18375A-0.0775B-0.03125C-0.0120833A^2+0.0004166B^2-0.0779167C^2+0.005AB-0.0025AC-0.005BC. \quad \text{Eq.4.6}$$

Overall heat transfer coefficient for heat pipe using CuO nanofluid

$$U = 5405+1688.45A+736.075B+201.8C+490.887A^2-54.7625B^2-723.362C^2+463.825AB+65.02AC+105.975BC. \quad \text{Eq.4.7}$$

Table 4.41 Analysis of variance for the response thermal resistance for heat pipe using CuO nanofluid

Source of variation	DF	Sum of Squares	Mean Sum of Squares	F-value	P-value
Regression	9	0.349898	0.038878	29.72	0.001
Linear	3	0.325975	0.108658	83.05	0.000
Square	3	0.023698	0.007899	6.04	0.041
Interaction	3	0.000225	0.000075	0.06	0.036
Residual Error	5	0.006542	0.001308		
Lack-of-Fit	3	0.006075	0.002025	8.68	0.105
Pure Error	2	0.000467	0.000233		
Total	14	0.356440			
R- Squared = 98.16%		R- Squared (adj)= 94.86%			

Table 4.42 Analysis of variance for the response overall heat transfer coefficient for the heat pipe using CuO nanofluid

Source of variation	DF	Sum of Squares	Mean Sum of Squares	F-value	P-value
Regression	9	31436404	3492934	17.42	0.003
Linear	3	27467144	9155715	45.66	0.000
Square	3	3046890	1015630	5.07	0.042
Interaction	3	922370	307457	1.53	0.024
Residual Error	5	1002548	200510		
Lack-of-Fit	3	378498	126160	0.40	0.168
Pure Error	2	624050	312025		
Total	14	32438953			
R-Squared = 96.91%		R-Squared (adj) = 91.36%			

4.7.3.1 Checking the adequacy of the model for thermal resistance for the heat pipe using CuO nanofluid

The determination coefficient R^2 indicates the goodness of fit for the model. For the heat pipe using CuO nanofluid, the value of R^2 = 0.9816 from Table 4.41 for equation 4.6 indicates relatively high degree of accuracy between the observed and predicted values. The value of determination coefficient R^2 (adj) = 0. 9486 is also high, which indicates a high significance of the model. The value of probability from the Table 4.41 for the model is less than 0.05, which indicates that the model is significant. The model also showed that lack of fit F value of 8.68 implies the lack of fit is not significant relative to the pure error even at 0.05 levels. Figure 4.61 shows the normal probability of residuals for thermal resistance of CuO nanofluid heat pipe and shows that the residuals are falling on the straight line which means the errors are

distributed normally and all the above consideration indicates an excellent adequacy of the regression model.

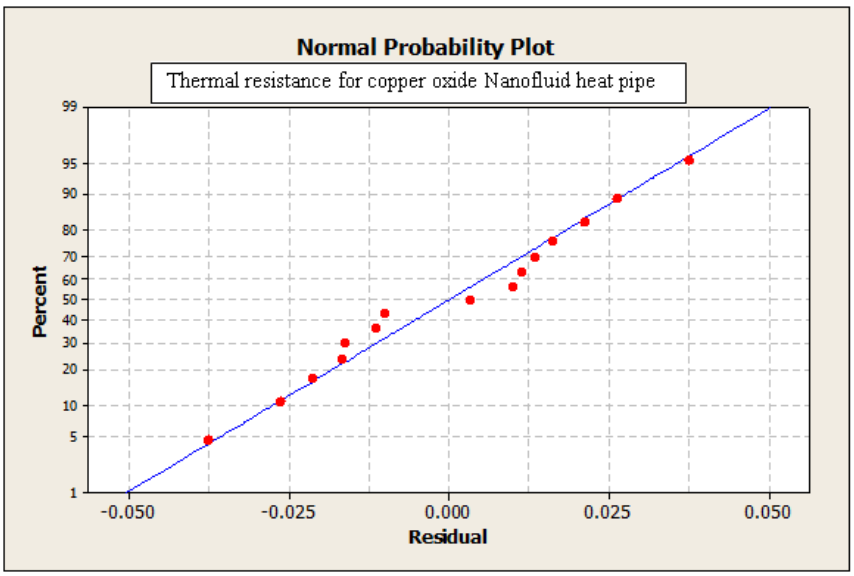

Figure 4.61 Normal probability of residuals for thermal resistance of CuO nanofluid heat pipe

4.7.3.2 Checking the adequacy of the model for overall heat transfer coefficient for the heat pipe CuO nanofluid

The goodness of fit of a model is evaluated by determination coefficient R^2. From Table 4.42 the value of R^2 = 0.9691 for equation 4.7 indicates relatively high degree of accuracy between the observed and predicted values of the heat pipe using CuO nanofluid. The value of determination coefficient R^2 (adj) = 0.9136 are also high, which indicates a high significance of the model. The probability value for the model from the Table 4.42 is less than 0.05, which indicates that the model is significant. The model also shows that lack of fit F value of 0.40 implies the lack of fit is not significant relative to the pure error even at 0.05 levels. Normal probability of residuals for overall heat transfer coefficient of CuO nanofluid heat pipe is shown in Figure 4.62 reveals that the residuals are falling on the straight line which means the errors are distributed normally. All the above consideration indicates an excellent adequacy of the regression model.

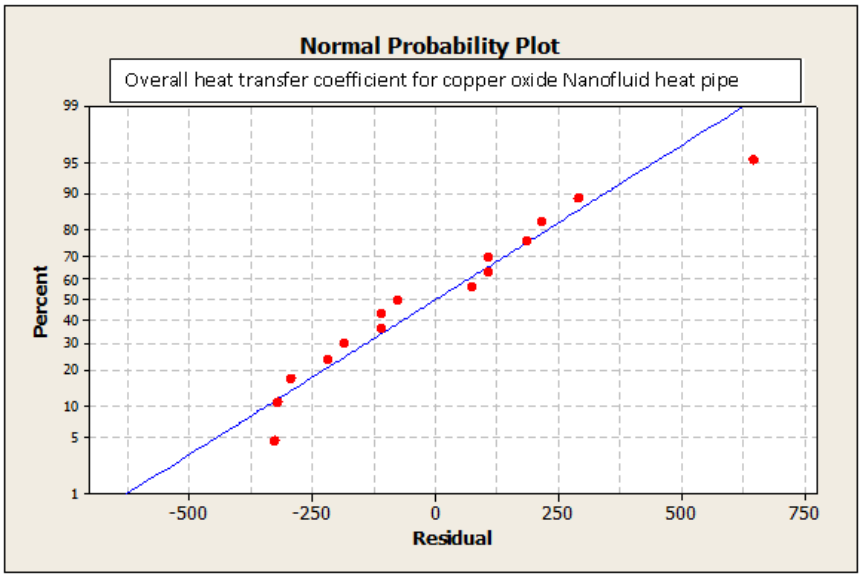

Figure 4.62 Normal probability of residuals for overall heat transfer coefficient of CuO nanofluid heat pipe

CHAPTER- 5

OPTIMIZATION OF HEAT TRANSFER CHARACTERISTICS OF HEAT PIPE

The performance of heat pipe is often affected by different working parameters and also the range of parameters. The effectiveness is measured by its lower thermal resistance and higher overall heat transfer coefficient. Since the number of variables and the parameters ranges are more, optimal response is rarely achieved. It is necessary to identify the optimum level of input parameters so as to achieve the optimum level of output.

5.1 Optimization of heat transfer characteristics of DI Water heat pipe

The heat transfer characteristics of DI Water heat pipe such as thermal resistance and overall heat transfer coefficient are correlated using the second order polynomial response surface equations 4.2 and 4.3.The optimum process parameters are obtained using the response surface method. In this method the objective is to identify the response over the entire factor space and also to obtain its optimum or near optimal value. An optimal search for the response thermal resistance and overall heat transfer coefficient can be obtained using the second order response surface equation for different input parameters such as heat input, angle of inclination and filling ratio. Desirability for the whole process optimization has been calculated to show the feasibility of optimization and to explore whether all the parameters are within their working range or not. The objective is to minimize the thermal resistance and to maximize the overall heat transfer coefficient. Since the composite desirability is close to one it can be concluded that the parameters are within the working range. Optimization plot for both the response is shown in Figure 5.1.From the plot the optimal values are thermal resistance = 0.8316 K/W and overall heat transfer coefficient = 3422.1 W/m^2K. The relevant parameters are heat input = 70W, angle of inclination = 90^0 and filling ratio = 76.82%. A validation test has been conducted for the above input parameters and a good agreement is observed between the predicted and actual values. It can be observed that the calculated errors are within the permissible limits and the values are tabulated in Table 5.1.

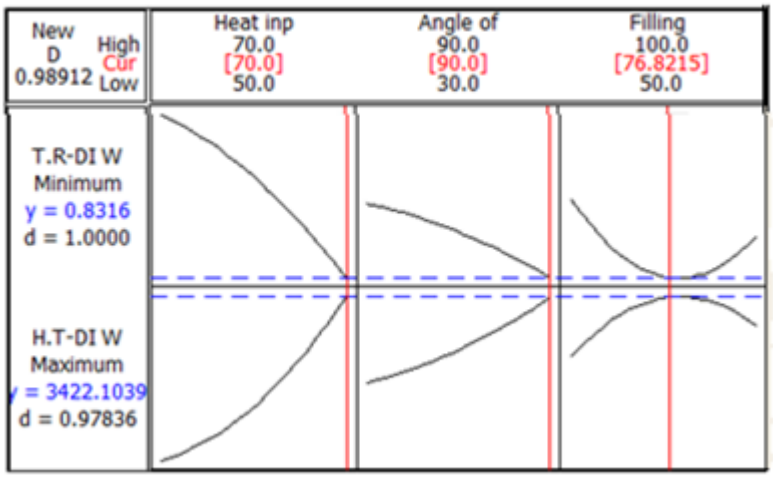

Figure 5.1 Optimal chart obtained from RSM for DI Water heat pipe

Table 5.1 Validation test results for heat transfer characteristics of DI Water heat pipe

Heat input (W)	Angle of inclination (deg.)	Filling ratio (%)	Thermal resistance (K/W)			Overall heat transfer coefficient (W/m^2K)		
			Predicted	Actual	Error %	Predicted	Actual	Error %
70	90	76.82	0.831	0.865	3.9	3422.10	3381	1.2

5.2 Optimization of heat transfer characteristics of TiO_2 nanofluid heat pipe

The heat transfer characteristics of TiO_2 nanofluid heat pipe such as thermal resistance and overall heat transfer coefficient are correlated using the second order polynomial response surface equations 4.4 and 4.5.Since the composite desirability is close to one it can be concluded that the parameters are within the working range. Optimization plot for both the response is shown in Figure 5.2.From the plot the optimal values are thermal resistance = 0.534 K/W and overall heat transfer coefficient = 5324.8 W/m^2K. The relevant parameters are heat input = 70W, angle of inclination = 90^0 and filling ratio = 77.73%. A validation test has been conducted for the above input parameters and a good agreement is observed between the predicted and actual values. It can be observed that the calculated errors are within the permissible limits and the values are tabulated in Table 5.2.

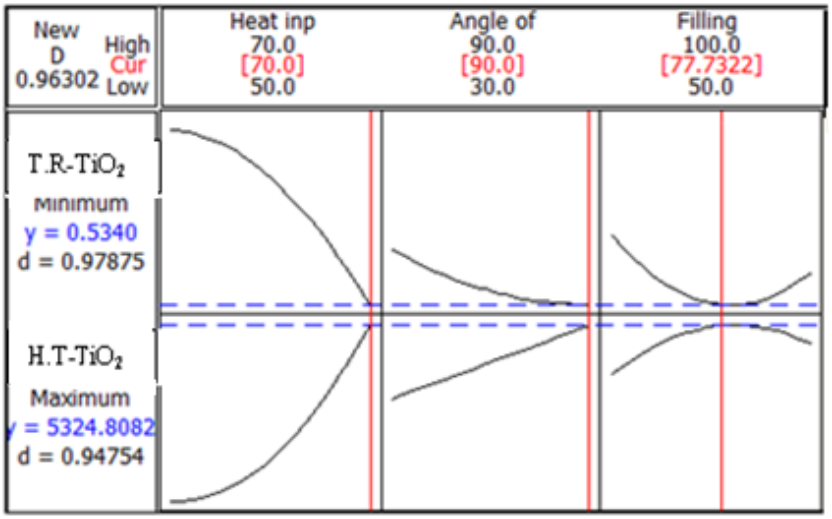

Figure 5.2 Optimal chart obtained from RSM for TiO_2 nanofluid heat pipe

Table 5.2 Validation test results for heat transfer characteristics of TiO_2 nanofluid heat pipe

Heat input (W)	**Angle of inclination (deg.)**	**Filling ratio (%)**	**Thermal resistance (K/W)**			**Overall heat transfer coefficient (W/m^2K)**		
			Predicted	**Actual**	**Error %**	**Predicted**	**Actual**	**Error %**
70	90	77.73	0.534	0.542	2	5324.80	5459	2.4

5.3 Optimization of heat transfer characteristics of CuO nanofluid heat pipe

The heat transfer characteristics of CuO nanofluid heat pipe such as thermal resistance and overall heat transfer coefficient are correlated using the second order polynomial response surface equations 4.6 and 4.7.Since the composite desirability is close to one it can be concluded that the parameters are within the working range. Optimization plot for both the response is shown in Figure 5.3.From the plot the optimal values are thermal resistance = 0.3071 K/W and overall heat transfer coefficient = 8740.37 W/m^2K. The relevant parameters are heat input = 70W, angle of inclination = 90^0 and filling ratio = 76.36%. A validation test has been conducted for the above input parameters and a good agreement is observed between the predicted and actual values. It can be observed that the calculated errors are within the permissible limits and the values are tabulated in Table 5.3.

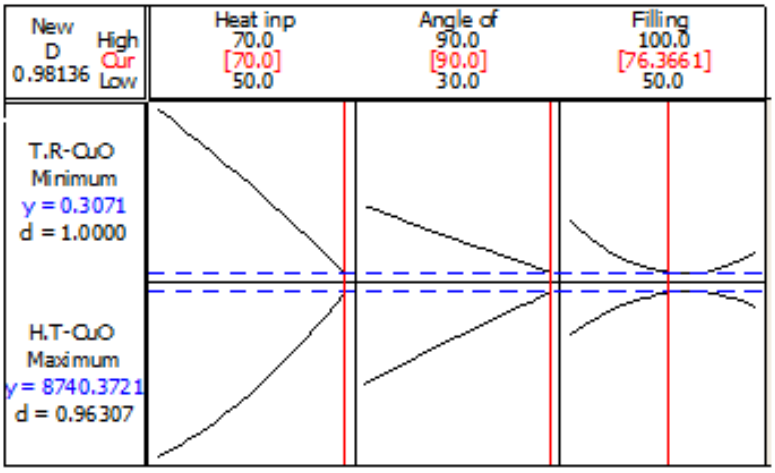

Figure 5.3 Optimal chart obtained from RSM for CuO nanofluid heat pipe

Table 5.3 Validation test results for heat transfer characteristics of CuO nanofluid heat pipe

Heat input (W)	**Angle of inclination (deg.)**	**Filling ratio (%)**	**Thermal resistance (K/W)**			**Overall heat transfer coefficient (W/m^{2}K)**		
			Predicted	**Actual**	**Error %**	**Predicted**	**Actual**	**Error %**
70	90	76.36	0.307	0.326	5.8	8740.37	8914	2

CHAPTER 6

CONCLUSIONS AND SCOPE FOR FUTURE WORK

6.1 Conclusions

The present study investigated the heat transfer characteristics of conventional screen mesh wick heat pipe using three different working fluids such as DI Water, TiO_2 nanofluid and CuO nanofluid.The parameters considered in this study are heat input, angle of inclination and filling ratio. A full factorial design has been applied to carry out the experimental work for all the working fluids. The experimental result reveals that heat input, angle of inclination, filling ratio and working fluid have important effect on the thermal resistance and overall heat transfer coefficient.

Different nanofluids causes different heat transfer characteristics of the heat pipe. The thermal performance of the heat pipe is improved when charged with TiO_2 nanofluid and CuO nanofluid. At higher inclination angle the heat pipe shows better thermal performance than in horizontal position. CuO nanofluid system shows lower thermal resistance when compared to TiO_2 nanofluid system and DI Water system. In general when the heat input is increased the thermal resistance decreases for all the working fluids and an optimum solution is obtained when the heat pipe is operated at 70 W heat input for all the working fluids.

The optimum filling ratio of charged working fluid in the tested heat pipe is about 75% for all the working fluids. The lowest thermal resistance is obtained for all the working fluids when the heat pipe is operated at 70 W heat input, 90^0 angle of inclination and 75% filling ratio. On comparing the thermal resistance of the CuO nanofluid heat pipe with DI Water heat pipe and TiO_2 nanofluid heat pipe the decrease in percentage is about 62% and 37.2% respectively.

The overall heat transfer coefficient is found to increase when the angle of inclination increases from horizontal position to vertical position and highest value is obtained when the heat pipe is operated at vertical position (i.e.90^0 angle of inclination) for all the working fluids. At 75% filling ratio the heat pipe shows highest overall heat transfer coefficient and its value found to decrease when the filling ratio is increased beyond 75%.

When the heat input is increased the overall heat transfer coefficient also increases for all the working fluids. The highest overall heat transfer coefficient is obtained for all the working fluids when the heat pipe is operated at 70 W heat input, 90^0 angle of inclination and 75% filling ratio. On comparing the overall heat transfer coefficient of the CuO nanofluid heat pipe with DI Water heat pipe and TiO_2 nanofluid heat pipe the increase in percentage is about 160.6% and 63.6% respectively.

Response surface methodology involving an experimental design was used to optimize the operating parameters such as heat input, angle of inclination and filling ratio for thermal resistance and overall heat transfer coefficient of the heat pipe which uses DI Water, TiO_2 nanofluid and CuO nanofluid. A mathematical model has been developed between response and the independent parameters and the response surface model was tested with analysis of variance.

From ANOVA tables the models developed for heat transfer characteristics of DI Water heat pipe, TiO_2 nanofluid heat pipe and CuO nanofluid heat pipe are found to be significant and also the value of R^2 indicates high degree of accuracy between the observed and predicted values. The normal probability plot indicates an excellent adequacy of the regression model for the heat pipe using all the three working fluids.

Optimization of heat transfer characteristics of heat pipe has been carried out to minimize the thermal resistance and to maximize the overall heat transfer coefficient using response surface methodology technique. The validation test results are conducted for DI Water heat pipe, TiO_2 nanofluid heat pipe and CuO nanofluid heat pipe. The predicted thermal resistance and overall heat transfer coefficient of heat pipes are compared with actual experimental values. It can be observed that the calculated errors are within the permissible limits and a good agreement was observed between the predicted and actual values.

In this investigation the heat transfer characteristics of heat pipe indicates nanofluid as substitute for DI Water in conventional screen mesh wick heat pipe. This finding makes nanofluid more attractive as a cooling fluid for devices with high energy density.

6.2 Scope for future work

Although the heat transfer characteristics of heat pipe is analyzed for DI Water heat pipe, TiO_2 nanofluid heat pipe and CuO nanofluid heat pipe, still there is a scope for further investigation. The following suggestions may prove useful for future work:

1. The surface morphology of screen mesh wick used in the heat pipe can be analyzed under two conditions i.e. before and after experiments for all the three working fluids.
2. The performance of the heat pipe can be analyzed by using nanoparticle coated wick structure and the results can be compared with uncoated wick heat pipe using nanofluids.
3. By increasing the percentage concentration of nanoparticles and by varying the size of the nanoparticles the thermal performance of the heat pipe can be evaluated.
4. The surface morphology of evaporator and condenser section can be analyzed for all the three working fluids after experimentation and can be compared.

REFERENCES

[1] Abhang, L.B., Hameedullah, M. (2010), "Power Prediction Model for Turning EN-31 Steel Using Response Surface Methodology", Journal of Engineering Science and Technology Review, Vol. 3 (1), pp. 116-122.

[2] Ahamed, H.H., Rajab, R.H. (2010), "An Experimental Study of Parameters Affecting a Heat Pipe Performance", Al-Rafidain Engineering, Vol.18 (3), pp.97-116.

[3] Anwarul Hasan,M.D., Feroz, C.M.D., Sadrul Islam,A.K.M. (2003), "Performance of a gravity assisted heat pipe", Proceedings of the International Conference on Mechanical Engineering, Dhaka, Bangladesh.

[4] Aruna, M., Dhanalaksmi, V. (2012), "Design Optimization of Cutting Parameters when Turning Inconel 718 with Cermet Inserts", International Journal of Mechanical and Aerospace Engineering, Vol. 6l, pp.952-955.

[5] Azad, E. (2008), "Theoretical and experimental investigation of heat pipe solar collector Heat pipes in modern heat exchangers", Experimental Thermal and Fluid Science, Vol. 32, pp. 1666-1672.

[6] Azad, E. (2009), "Performance analysis of wick-assisted heat pipe solar collector and comparison with experimental results", Heat Mass Transfer, Vol.45, pp.645-649.

[7] Balasubramanian, S., Paridhi, G., Bosco, J. D., Kadam, D. M. (2012), "Optimization of Process Conditions for the Development of Tomato Foam by Box-Behnken Design", Food and Nutrition Sciences, Vol.3, pp. 925-930.

[8] Box, G.E., Draper, N.R. (1987), "Empirical model building and response surfaces", Wiley, New York.

[9] Brusly Solomon, A. Ramachandran, K., Pillai, B.C. (2012),"Thermal performance of a heat pipe with nanoparticles coated wick", Applied Thermal Engineering, Vol. 36, pp. 106-112.

[10] Charoensawan, P., Terdtoon, P. (2008), "Thermal performance of horizontal closed-loop oscillating heat pipes", Applied Thermal Engineering, Vol. 28, pp. 460-466.

[11] Chen, Y.T., Wei, W.C., Kang, S.W., Sheng, C. (2008), "Effect of Nanofluid on Flat Heat Pipe Thermal Performance", Annual IEEE Semiconductor Thermal and Management Symposium, DOI: 10.1109/STHERM.

[12] Chi, S. W. (1976), "Heat Pipe Theory and Practice", McGraw-Hill, Washington D.C.

[13] Chiang, K.T., Chang, F.P. (2007), "Analysis of shrinkage and warpage in an injection-molded part with a thin shell feature using the response surface methodology", International Journal of Advanced Manufacturing Technology, Vol. 35, pp.468-479.

[14] Chien, H.T., Tsai, C.Y., Chen, P.H., Chen, P.Y. (2003), "Improvement on thermal performance of a disk-shaped miniature heat pipe with nanofluid", in: Proceedings of the Fifth International Conference on Electronic Packaging Technology, Institute of Electrical and Electronics Engineers, Shanghai, China, pp. 389–391.

[15] Choi, S.U.S., (1995), "Enhancing thermal conductivity of fluids with nanoparticles, Developments and Applications of Non-Newtonian Flows", FED-Vol.231/MD-Vol. 66, pp. 99-105.

[16] Cochran, Cox, G. M. (1962), "Experimental design [M]", New Delhi, Asia Publishing House.

[17] Collier, J.G., Thome, J.R. (1996), "Convective Boiling and Condensation", Clarendon, Press, Oxford.

[18] Dhara, S.K., Kuar, A.S., Mitra, S. (2006), "Optimization of Nd:YAG laser micro-machining using response surface methodology", In proceedings of the 22nd All India manufacturing technology design and research conference, pp. 337-382.

[19] Do, K. H., Ha, H. J., Jang, S.P. (2010), "T'hermal resistance of screen mesh wick heat pipes using the water-based Al_2O_3 nanofluids", International Journal of Heat and Mass Transfer, Vol. 53,pp.5888-5894.

[20] Do, K. H., Jang, S.P. (2010), "Effect of nanofluids on the thermal performance of a flat micro heat pipe with a rectangular grooved wick", International Journal of Heat and Mass Transfer, Vol. 53, pp.2183-2192.

[21] Eastman, J.A., Choi, S.U.S. (2001), "Anomalously increased effective thermal conductivities of ethylene glycol-based nanofluids containing copper nanoparticles", Applied Physics Letters, Vol. 78, pp. 718-720.

[22] Faghri, A. (1995), Heat Pipe Science and Technology, Taylor & Francis, Washington D. C.

[23] Fang, Q., Shen, B. (2010), "Optimization of polyethylenimine-mediated transient transfection using response surface methodology design", Electronic Journal of Biotechnology, Vol. 13(5), pp.2-11.

[24] Fisher, R.A. (1926),"The arrangement of field experiments", Journal of Ministry Agriculture, Vol.33, pp.503-513.

[25] Fisher, R.A. (1935), "*The Design of Experiments",* Oliver and Boyd, Edinburgh.

[26] Fu, J.F., Zhao, Y.Q., Wu, Qiuli. (2006), "Optimising photoelectrocatalytic oxidation of fulvic acid using response surface methodology", Journal of Hazardous Materials, Vol.144 (1-2), pp. 499-505.

[27] George Box, Donald Behnken, (1960), "Some new three level designs for the study of quantitative variables", Technometrics, Vol. 2, pp. 455–475.

[28] Giunta, A.A., Dudley, J.M., Narducci, R., Grossman, B., Haftka. R.T., Mason, W.H., Watson, L.T. (1994), "Noisy Aerodynamic Response and Smooth Approximations in HSCT Design," paper AIAA-94-4376, 5th AIAA Multidisciplinary Analysis and Optimization Symposium, Panama City, Fla.

[29] Groll, M., Schneider, M., Sartre, V., Zaghdoudi, M. C., Monique, L. (1998), "Thermal control of electronic equipment by heat pipes", Revue Generale de Thermique, Vol. 37, pp. 323-352.

[30] Gurses, A.C., Cannistraro, C. (1991), "The inclination effect on the performance of water filled heat pipes", Renewable Energy, Vol.1, pp.667-674.

[31] Hagen, K.D. (1999), "Heat Transfer with Applications", Prentice-Hall.

[32] Hajian, R., Layeghi, M., Sani, K. A., (2012), "Experimental study of nanofluid effects on the thermal performance with response time of heat pipe", Energy Conversion and Management, Vol.56, pp. 63-68.

[33] Han, K., Yee, S.S., Park, S.H., Lee.S.H. (2002), "A study on improvement of heat transfer performance in low temperature closed thermosyphon", KSME International Journal, Vol.16 No, 9, pp.1102-1111.

[34] Hong, T.K., Yang, H.S., Choi, C. J. (2005), "Study of the enhanced thermal conductivity of Fe nanofluids", Journal of Applied Physics, Vol.97, (064311), pp.1-4.

[35] Hopkins, R., Faghri, A., Khrustalev, D. (1999), "Flat miniature heat pipes with micro capillary grooves, Journal of Heat Transfer, Vol.121, pp. 102-109.

[36] Hossain, R.A., Chowdhuri, M.A.K., Feroz, C.M., (2010), "Design, Fabrication and Experimental Study of Heat Transfer Characteristics of a Micro Heat Pipe", Jordan Journal of Mechanical and Industrial Engineering, Vol.4 (5), pp. 531-542.

[37] Hung, Y.H., Teng, T.P., Lin, B.G., (2013), "Evaluation of the thermal performance of a heat pipe using alumina nanofluids", Experimental Thermal and Fluid Science, Vol.44, pp. 504-511.

[38] Hwang, G.S., Kaviany. M., Anderson, W.G., Zuo, J. (2007), "Modulated wick heat pipe", International Journal of Heat and Mass Transfer, Vol.50, pp. 1420-1434.

[39] Jen, T.C., Gutierrez, G., Eapen, S., Barber, G., Zhao, H., Szuba, P.S., Labataille, J., Manjunathaiah, J. (2002), "Investigation of heat pipe cooling in drilling applications. Part I: preliminary numerical analysis and verification", International Journal of Machine Tools & Manufacture, Vol. 42, pp. 643–652.

[40] Jon, H.B. (1999), "An Experimental Study of a Slab-wick Heat Pipe for Medium-high Condenser Temperatures," 11th International Heat Pipe Conference –Tokyo, pp. 143-148.

[41] Jouhara, H., Anastasov, V., Khamis, I. (2009), "Potential of heat pipe technology in nuclear seawater desalination", Desalination, Vol. 249, pp.1055–1061.

[42] Kang, S.W., Wei, W.C., Tsai, S.H., Huang, C.C. (2009), "Experimental investigation of nanofluids on sintered heat pipe thermal performance", Applied Thermal Engineering, Vol. 29, pp. 973–979.

[43] Karthikeyan, R., Raju, S., Naagarazan, S. (2001), "Optimization of electrical discharge machining characteristics of SiCp/LM 25 Al composites using goal programming", Journal of material science and technology, Vol.17, pp. 57-60.

[44] Keblinski, P. Phillpot, S.R. Choi,S.U.S., Eastman, J.A.(2002) "Mechanisms of heat flow in suspensions of nano-sized particles (nanofluids)", International Journal of Heat and Mass Transfer,Vol. 45, pp. 855-863.

[45] Kempers, R., Ewing, D., Ching, C.Y., (2006), "Effect of number of mesh layers and fluid loading on the performance of screen mesh wicked heat pipes", Applied Thermal Engineering, Vol. 26, pp.589-595.

[46] Kerrigan, K., Jouhara, H., O'Donnell, G.E., Robinson, A.J. (2011), "Heat pipe-based radiator for low grade geothermal energy conversion in domestic space heating", Simulation Modelling Practice and Theory, Vol.19, pp. 1154-1163.

[47] Khuri, A. I., Cornell J. A. (1987), "Response Surfaces: Design and Analysis", Marcel Dekker, New York.

[48] Kim, K. S. (1999), "Cooling Characteristics of Micro Heat Pipes with Woven Wired Wick". 11th international Heat Pipe Conference – Tokyo, pp. 239-244.

[49] Kim, K.S., Won, M.H., Kim, J.W., Back, B.J. (2003), "Heat pipe cooling technology for desktop PC CPU", Applied Thermal Engineering, Vol.23,pp. 1137-1144.

[50] Kothandaraman, C.P., Subramanyan, S., (2007), "Heat and Mass Transfer Data Book", Sixth edition, New Age International Publishers.

[51] Lee, S., Choi, S.U.S., Li, S., Eastman, J.A. (1999), "Measuring thermal conductivity of fluids containing oxide nanoparticles", Journal of Heat Transfer, Vol.121, pp.280-289.

[52] Lefevre, F., Conrardy, J.B., Raynaud, M., Bonjour, J. (2012), "Experimental investigations of flat plate heat pipes with screen meshes or grooves covered with screen meshes as capillary structure", Applied Thermal Engineering, Vol.37, pp. 95-102.

[53] Liu, M.S., Lin, M.C., Huang, I.T., Wang, C.C. (2005), "Enhancement of thermal conductivity with carbon nanotube for nanofluids", International Communication in Heat and Mass Transfer, Vol. 32, pp.1202-1210.

[54] Liu, M.S., Lin, M.C.C., Tsai, C.Y., Wang, C.C. (2006), "Enhancement of thermal conductivity with cu for nanofluids using chemical reduction method", International Journal of Heat and Mass Transfer, Vol.49, pp. 3028-3033.

[55] Liu, Z.H., Li, Y.Y., Bao, R. (2011) "Compositive effect of nanoparticle parameter on thermal performance of cylindrical micro-grooved heat pipe using nanofluids" ,International Journal of Thermal Sciences, Vol.50,pp. 558-568.

[56] Lo, C.H., Tsung, T.T., Chen, L.C. (2005), "Shape-controlled synthesis of Cu-based Nanofluid using submerged arc nanoparticle synthesis system (SANSS)", Journal of Crystal Growth, Vol. 277, pp. 636-642.

[57] Ma, H. B., Wilson, C., Borgmeyer, B., Park, K., Yu, Q., Choi, S. U. S., Tirumala ,M.(2006), "Effect of nanofluid on the heat transport capability in an oscillating heat pipe", Applied Physics Letters, 88, 143116.

[58] Magesh, A., Preetha, B., Viruthagiri, T. (2011), "Statistical Optimization of Process Variables for Direct Fermentation of 226 White Rose Tapioca Stem to Ethanol by Fusarium oxysporum", World Academy of Science, Engineering and Technology, Vol.51, pp.785-790.

[59] Mason, R.I., Gunst, R.F., Hess, J.L. (1989), "Statistical design and analysis of experiments", Wiley, New York.

[60] Mirshahi, H., Rahimi, M. (2009), "Experimental Study on the Effect of Heat Loads, Fill Ratio and Extra Volume on Performance of a Partial-Vacuumed thermosyphon", Iranian Journal of Chemical Engineering, Vol. 6(4), pp.15-26.

[61] Montgomery, D. C., 1991, "Design and Analysis of experiments", 3rd edn, Wiley, New York.

[62] Moraveji, M. K., Razvarz, S. (2012), "Experimental investigation of aluminum oxide nanofluid on heat pipe thermal performance", International Communications in Heat and Mass Transfer, Vol. 39, pp.1444–1448.

[63] Mousa, M.G. (2011), "Effect of nanofluid concentration on the performance of circular heat pipe", International Journal of Scientific & Engineering Research, Vol.2 (4), pp.1-8.

[64] Mozumder, A. K., Akon, A. F., Chowdhury, M. S. H., Banik S. C. (2010) "Performance of heat pipe for different working fluids and fill ratios", Journal of Mechanical Engineering, Vol. ME 41(2), pp.96-102.

[65] Mozumder, A.K., Chowdhury, M.S. H., Akon, A.F. (2011), "Characteristics of Heat Transfer for Heat Pipe and Its Correlation", International Scholarly Research Network, Vol.2011, 825073, pp.1-7.

[66] Murshed, S.M.S., Leong, K.C., Yang, C., (2005), "Enhanced thermal conductivity of TiO_2-water based nanofluid", International Journal of Thermal Science, Vol.44, pp.367-373.

[67] Naphon, P., Assadamongkol, P., Borirak, T. (2008), "Experimental investigation of titanium nanofluids on the heat pipe thermal efficiency", International Communications in Heat and Mass Transfer, Vol. 35, pp. 1316-1319.

[68] Naphon, P., Thongkum, D., Assadamongkol, P. (2009) "Heat pipe efficiency enhancement with refrigerant–nanoparticles mixtures", Energy Conversion and Management, Vol.50, pp.772-776.

[69] Natarajan, U., Periyanan, P.R., Yang, S.H., (2011), "Multiple-response optimization for micro-end milling process using response surface methodology", International Journal of Advanced Manufacturing Technology, Vol. 56, pp.177-185.

[70] Nemec, P., Caja, A., Malcho, M. (2011), "Thermal performance measurement of heat pipe", Global Journal of Technology and Optimization, Vol.2, pp.104-110.

[71] Noie-Baghban, S.H., Majideian, G.R. (2000), "Waste heat recovery using heat pipe heat exchanger (HPHE) for surgery rooms in hospitals", Applied Thermal Engineering,Vol.20,pp. 1271-1282.

[72] Paramatthanuwat, T., Boothaisong, S., Rittidech, S., Booddachan, K., (2010), "Heat transfer characteristics of a two-phase closed thermosyphon using de ionized water mixed with silver nano", Heat Mass Transfer, Vol.46, pp 281-285.

[73] Park, J.H. (1997), "A study on thermal performance of heat pipe for optimum placement of satellite equipment", ETRI Journal, Vol.19, (2).pp.59-70.

[74] Patel, H.E., Das, S.K., Sundararagan, T., Nair, A.S., Geoge, B., Pradeep, T. (2003), "Thermal conductivities of naked and monolayer protected metal nanoparticle based nanofluids: manifestation of anomalous enhancement and chemical effects", Applied Physics Letter, Vol. 83, pp. 2931-2933.

[75] Possamai, F.C., Setter, I., Vasiliev, L.L. (2009), "Miniature heat pipes as compressor cooling devices", Applied Thermal Engineering, Vol. 29, pp. 3218-3223.

[76] Putnam, S.A., Cahill, D.G., Braun, P.V. (2006), "Thermal conductivity of nanoparticle suspensions", Journal of Applied Physics, Vol. 99, (084308), pp.1-6.

[77] Reay, D.A., Kew P.A. (2006), "Heat pipes: Theory, Design and Applications", Elsevier Science & Technology Books.

[78] Rosenfeld, J. (2006), "Ultra-Lightweight Magnesium Heat Pipes for Spacecraft Thermal Management", Internal Documentation, Thermacore Inc.

[79] Saedon, J.B., Soo, S.L., Spinwall, D.K A., Barnacle, A., Saad, N.H., (1683), "Prediction and Optimization of Tool Life in Micromilling AISI D2 (~62 HRC) Hardened Steel", Procedia Engineering, Vol.41, pp. 1674-1683.

[80] Saleh, R., Putra,N., Prakoso, S.P., Septiadi, W.N. (2013), "Experimental investigation of thermal conductivity and heat pipe thermal performance of ZnO nanofluids", International Journal of Thermal Sciences, Vol.63, pp. 125-132.

[81] Sarmasti Emami, M. R., Noie, S. H., Khoshnoodi, M. (2008) " Effect of aspect ratio and filling ratio on thermal performance of an inclined two-phase closed thermosyphon", Iranian Journal of Science & Technology, Transaction B, Engineering, Vol. 32(B1), pp 39-51.

[82] Savino, R., Piccolo, C., Fortezza, R., Abe, Y. (2007), "Heat Pipes with Self-Rewetting Fluids under Low-Gravity Conditions", Second International Topical Team Workshop on two-phase systems for ground and space applications October 26-28, Kyoto, Japan.pp.75-77.

[83] Senthilkumar, R., Vaidyanathan, S., Sivaraman, B. (2011), "Performance investigation of heat pipe using aqueous solution of n-Pentanol with different inclinations" Journal of Mechanical Science and Technology, Vol.25 (4), pp. 923-929.

[84] Shafahi, M., Bianco, V., Vafai, K., Manca, O. (2010), "An investigation of the thermal performance of cylindrical heat pipes using nanofluids", International Journal of Heat and Mass Transfer, Vol. 53, pp.376-383.

[85] Shafahi, M., Bianco, V., Vafai, K., Manca, O.(2010), "Thermal performance of flat-shaped heat pipes using nanofluids" International Journal of Heat and Mass Transfer,Vol.53,pp. 1438-1445.

[86] Shukla, K.N., Brusly Solomon, A., Pillai, B.C., Ibrahim. (2010), "Thermal performance of cylindrical heat pipe using nanofluids", Journal of Thermophysics and Heat transfer, Vol.24 (4), pp.796-802.

[87] Shukla, K. N., Brusly Solomon, A., Pillai, B.C., Jacob Ruba Singh, B., Saravana Kumar, S.(2012) "Thermal performance of heat pipe with suspended nano-particles" DOI 10.1007/s00231-012-1028-4.

[88] Silva, G. F., Camargo, F. L., Ferreira, A. L.O. (2011), "Application of response surface methodology for optimization of biodiesel production by transesterification of soybean oil with ethanol", Fuel Processing Technology, Vol.92(3), pp. 407-413.

[89] Teng, T.P., Hsu, H.G., Mo, H.E., Chen, C.C. (2010), "Thermal efficiency of heat pipe with alumina nanofluid", Journal of Alloys and Compounds, Vol.504S, pp. S380-S384.

[90] Tsaia, C.Y., Chien, H.T., Ding, P.P., Chan, B., Luh, T.Y., Chen, P.H., (2004), "Effect of structural character of gold nanoparticles in nanofluid on heat pipe thermal performance", Materials Letters, Vol.58, pp.1461-1465.

[91] Vargaftik, N.B. (1975), "Tables of the Thermophysical Properties of Liquids and Gases", Second edition, John Wiley and Sons.

[92] Vikas Kumar., Gangacharyulu, D., Tathgir, R. G., (2007), "Heat Transfer Studies of a Heat Pipe", Heat Transfer Engineering, Vol. 28(11), pp.954–965.

[93] Wang, S., Chen, J., Hu, Y., Zhang, W. (2011), "Effect of evaporation section and condensation section length on thermal Performance of flat plate heat pipe", Vol.31, Issues14-15, pp.2367-2373.

[94] Wang, X., Xu, X., Choi, S.U.S. (1999), "Thermal conductivity of nanoparticle-fluid mixture", Journal of Thermo physics and Heat Transfer, Vol.13, pp.474-480.

[95] Wang, Y.H., Park, H.S., Lee, J.K., Jung, W.H. (2006), "Thermal conductivity and lubrication characteristics of nanofluids", Current Applied Physics, 6SI, pp.67-71.

[96] Wani, T. A., Ahmad, A., Zargar, S., Khalil, N.Y., Darwish, I.A. (2012), "Use of response surface methodology for development of new microwell-based spectrophotometric method for determination of atrovastatin calcium in tablets", Chemistry Central Journal, Vol. 6 (134). pp.1-9.

[97] Wong, S.C., Kao, Y.H. (2008), "Visualization and performance measurement of operating mesh-wicked heat pipes", International Journal of Heat and Mass Transfer ,Vol.51,pp. 4249-4259.

[98] Wong, S.C., Lin, Y.C. (2011), "Effect of copper surface wettability on the evaporation performance: Tests in a flat-plate heat pipe with visualization", International Journal of Heat and Mass Transfer, Vol.54, pp.3921-3926.

[99] Xuan, Y., Li, Q. (2000), "Heat transfer enhancement of nanofluids", International Journal of Heat and Fluid Flow, Vol. 21, pp.58–64.

[100] Yu, C.J., Richter, A.G., Datta, A., Durbin, M.K., Dutta P. (2007) "Molecular layering in a liquid on a solid substrate: an X-ray reflectivity study", Physica B, Vol. 283, pp. 27-31.

[101] Zhu, H., Lin, Y., Yin, Y., (2004), "A novel one-step chemical method for preparation of copper nanofluids", Journal of Colloid Interface Science, Vol.227, pp. 100-103.

[102] Zhang, M., Liu, Z., Ma, G. (2008), "The experimental investigation on thermal performance of a flat two-phase thermosyphon", International Journal of Thermal Sciences, Vol.47, pp.1195-1203.

[103] Zhang, N. (2001), "Innovative heat pipe systems using a new working fluid", International Communications in Heat and Mass Transfer, Vol.28 (8), pp.1025-1033.

LIST OF PUBLICATIONS

PUBLICATIONS IN JOURNALS

[1] Manimaran, R., Palaniradja, K., Alagumurthi, N. (2012), "Factors Affecting the Thermal Performance of Heat Pipe-A Review". Journal of Engineering Research and Studies, Vol. III/ Issue II/April-June, pp. 20-24.

[2] Manimaran, R., Palaniradja, K., Alagumurthi, N. (2012), "An Investigation of Thermal Performance of Heat Pipe Using DI-water", Science and Technology, 2(4), pp. 77-80.

[3] Manimaran, R., Palaniradja, K., Alagumurthi, N.(2012),"Effect of Filling Ratio on Thermal Characteristics of Wire-mesh Heat Pipe using Copper oxide nanofluid", Frontiers in Heat Pipes (FHP).3: 023004.

[4] Manimaran, R., Palaniradja, K., Alagumurthi, N. (2013), "Preparation and characterization of copper oxide nanofluid for heat transfer applications". Applied Nanoscience-Springer, January, DOI 10.1007/s13204-012-0184-7.

[5] Manimaran, R., Palaniradja, K., Alagumurthi, N. (2013), "Experimental comparative study of heat pipe performance using CuO and TiO_2 nanofluids", International Journal of Energy Research. DOI: 10.1002/er.3058

[6] Manimaran, R., Palaniradja, K., Alagumurthi, N. (2013), "Synthesis and characterization of titanium di-oxide nanofluid", Chinese Physics letters.

..... Communicated

PUBLICATIONS IN CONFERENCES

[1] Manimaran, R., Palaniradja, K., Alagumurthi, N. (2012), "Experimental investigation of heat pipe using DI water as working fluid held', second international conference on advances in engineering and technology", held at E.G.S Pillay College of Engineering, Nagapattinam.March 28-29.

[2] Manimaran, R., Palaniradja, K., Alagumurthi, N. (2012), "Heat transfer performance of heat pipe using nanofluid", International conference on Advances in Construction, Manufacturing and automation Research, held at kongu Engineering College, Perundurai, Erode. March 30-31.

VITAE

Mr.R.Manimaran received his Bachelor of Engineering in the year of 2003, from Madras University, Chennai and Master of Engineering in the year of 2008 from Annamalai University, Chidambaram. He has nearly five and half years of teaching experience. He is also a life member in Indian Society for Technical Education (ISTE).He has five publications in international journal and presented number of papers in National and International Conferences. His research interest includes Heat and Mass transfer and Thermal Engineering.